Spring 5-16-2014

# Hydrodynamics and Salinity of Pontchartrain Estuary During Hurricanes

Sina Amini
*University of New Orleans*, samini1@uno.edu

# Hydrodynamics and Salinity of Pontchartrain Estuary during Hurricanes

A Thesis

Submitted to the Graduate Faculty of the
University of New Orleans
In partial fulfillment of the
Requirements for the degree of

Master of Science
in
Civil and Environmental Engineering
Coastal and River Modeling
By

Sina Amini

B.S. Hormozgan University, 2011

May, 2014

## ACKNOWLEDGMENTS

I would like to express my sincere gratitude to my professor Dr. Alex McCorquodale for offering me a position in his research lab without which I wouldn't be finishing graduate school successfully; for training me under his unique system which has led me to be able to write this thesis and for patiently supervising my work.

My mother deserves limitless amount of gratefulness for financially and morally supporting me during my entire life. I wish to thank my siblings, Ali and Mitra, for their help and support. My wife Nina must be indefinitely thanked for her patience and love. I am truly grateful to my uncle Hadi, for his gracious support and encouragement.

Dr. Joao Pereira, Dr. Ioannis Georgiou and Dr. Ehab Meselhe are thanked for sharing their modeling experience with me.

I must thank my friends and colleagues, Grecia, Jed, Tatiana, Chris and Luis for being with me while I was doing this research.

I would like to say thank you to Dr. Jian Tao, Dr. Jim Chen and the other people in SIMULOCEAN group for setting up the SIMULOCEAN interface.

Furthermore, I would like to thank Dr. Bhaskar Kura for his guidance and assistance in the admission process.

Funding Louisiana Board of Regents and the Mississippi River Hydrostudy group is acknowledged.

The Deltares Academy is acknowledged for making the Delft3D code freely available to non-commercial researchers. Dr. Chanshang Chen and the FVCOM group are thanked for providing the FVCOM code.

This research was funded in part by National Science Foundation (NSF) as a part of the Northern Gulf Coastal Hazards Collaboratory (NG-CHC; http:\\ngchc.org).

# Table of Contents

## List of Figures

## List of Tables

## Nomenclature

| Symbol | Description | Unit |
|---|---|---|
| c | Chézy coefficient | $m^{1/2}/s$ |
| c | courant number | non-dimensional |
| c | mass concentration | $kg/m^3$ |
| d | water depth | m |
| E | evaporation | m/s |
| $F_\eta$ | | $m/s^2$ |
| $\sqrt{G_{\xi\xi}}$ | coefficient used to transform curvilinear to rectangular coordinates | m |
| $\sqrt{G_{\eta\eta}}$ | coefficient used to transform curvilinear to rectangular coordinates | m |
| g | gravity acceleration | $m/s^2$ |
| H | total water depth ($h= d + \zeta$) | m |
| $M_\xi$ | source or sink of momentum in the ξ-direction | $m/s^2$ |
| $M_\eta$ | source or sink of momentum in the η-direction | $m/s^2$ |
| n | Manning's roughness coefficient | $m^{-1/3}/s$ |
| P | hydrostatic water pressure | $kg/m.s^2$ |
| $P_\xi$ | gradient hydrostatic pressure in ξ-direction | $kg/m^2.s^2$ |
| $P_\eta$ | gradient hydrostatic pressure in η-direction | $kg/m^2.s^2$ |
| $P_{atm}$ | atmospheric pressure | $kg/m.s^2$ |
| P | precipitation | m/s |
| Q | global source or sink per unit area | m/s |
| $q_{in}$ | local source per unit volume | $s^{-1}$ |
| $q_{out}$ | local sink per unit volume | $s^{-1}$ |
| R | earth radius | m |

| Symbol | Description | Unit |
|---|---|---|
| S | salinity | ppt |
| t | time | s |
| T | temperature | °C |
| U | depth-averaged velocity x- in ξ-direction | m/s |
| u | velocity in x- or ξ-direction | m/s |
| V | depth-averaged velocity y- in η-direction | m/s |
| v | velocity y- in η-direction | m/s |
| ω | velocity in σ-direction | m/s |
| φ | latitude co-ordinate in spherical co-ordinates | deg |
| λ | longitude co-ordinate in spherical co-ordinates | deg |
| σ | scaled vertical co-ordinate (surface, σ = 0; bed level, σ = −1) | non-dimensional |
| ρ | density of water | $kg/m^3$ |
| $\rho_0$ | reverence density of water | $kg/m^3$ |
| ζ | water level above datum | m |

## Abstract

A hurricane is a combination of sustained winds, low atmospheric pressures and precipitation. Over the past decades, Louisiana has experienced several devastating hurricanes.

The east bank of the City of New Orleans is bounded by Lake Pontchartrain to the North and the Mississippi River to the South. Lake Pontchartrain is a brackish system connected to the Gulf of Mexico through Lake Borgne to the East. As a Hurricane enters the Estuary from the Gulf of Mexico, it imposes a sustained surge of a few meters which may lead to flooding in areas which are not protected by levees. These flood water may be saline.

Saltwater flooding is an environmental issue in flooded marshlands since saltwater can be fatal to some plants. The response of salinity and storm surge to hurricane duration which represents the forward speed of the storm is numerically modeled. The maximum gage height certainly agrees with $\zeta = \zeta_{max}(1 - e^{-k/VF})$.



Keywords: 3-Dimensional numerical modeling, Storm surge, Salinity, Hurricane duration, Delft3D, FVCOM, Lake Pontchartrain, Flooding

# 1. INTRODUCTION

## 1.1.Background

The Pontchartrain Estuary is a combination of three connected Lakes leading to the Gulf of Mexico located on Southeast Louisiana. The estuary consists of Lakes Maurepas, Pontchartrain and Borgne. Lake Pontchartrain is connected to Lake Borgne by two narrow passes, Rigolets and Chef Menteur pass. Figure 1.1 shows a map of Southeastern USA. Figure 1.2 is a map of the Pontchartrain Estuary.

The Estuary is bounded by levees, beaches, marshes and swamps depending on the location. The objective of levees is to protect sensitive urban locations from flooding. The marshlands and swamps are habitat of several plant and animal species that are native to Louisiana. Figure 1.3 shows shoreline type around the estuary (Williams, 2006).


**Figure 1.1- Southeast U.S.A.**

**Source: National Atlas of the United States of America**

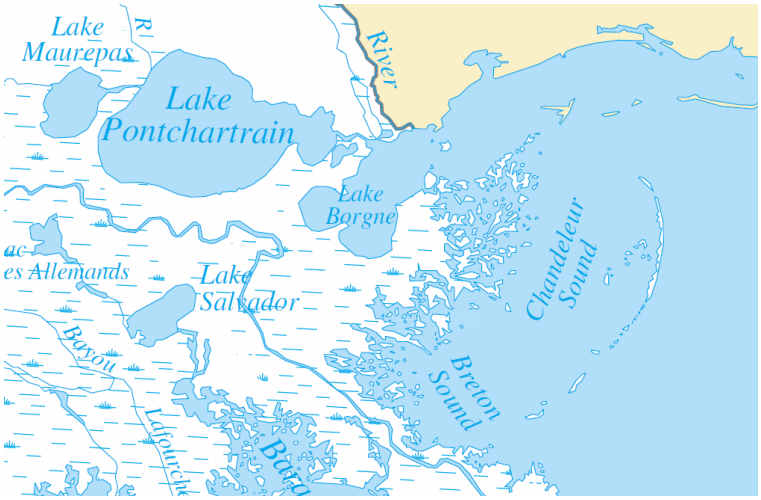


**Figure 1.2- The Pontchartrain Estuary**
**Source: National Atlas of the United States of America**

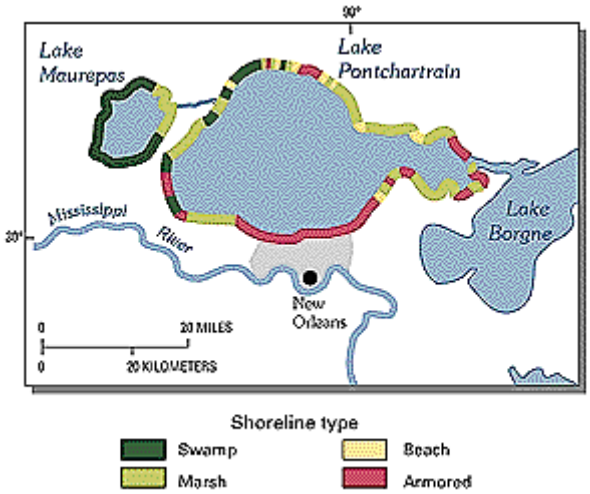


**Figure 1.3- Shoreline types around Pontchartrain Estuary**
**Source: United States Geological Survey**

During the hurricane season, which is typically from early June to late November, there is a chance of hurricanes and tropical storms. A hurricane is a combination of sustained winds circulating over the center (eye) of the storm and rainfall. Saffir and Simpson provided a classification of hurricanes by wind speed in 1971. There are five categories of Hurricanes in their classification with Category 5 being the strongest, most devastating and Category 1 being the weakest. Table 1.1 shows hurricane categories and their corresponding sustained wind speeds (NOAA 2013)

| Category | Sustained Wind speed (mph) | Types of Damage Due to Hurricane Winds |
|---|---|---|
| 1 | 74-95 | "*Very dangerous winds will produce some damage: Well-constructed frame homes could have damage to roof, shingles, and vinyl siding and gutters. Large branches of trees will snap and shallowly rooted trees may be toppled. Extensive damage to power lines and poles likely will result in power outages that could last a few to several days*." (NOAA, 2013) |
| 2 | 96-110 | "*Extremely dangerous winds will cause extensive damage: Well-constructed frame homes could sustain major roof and siding damage. Many shallowly rooted trees will be snapped or uprooted and block numerous roads. Near-total power loss is expected with outages that could last from several days to weeks*." (NOAA, 2013) |
| 3 | 111-129 | "*Devastating damage will occur: Well-built framed homes may incur major damage or removal of roof decking and gable ends. Many trees will be snapped or uprooted, blocking numerous roads. Electricity and water will be unavailable for several days to weeks after the storm passes*" (NOAA, 2013) |
| 4 | 130-156 | "*Catastrophic damage will occur: Well-built framed homes can sustain severe damage with loss of most of the roof structure and/or some exterior walls. Most trees will be snapped or uprooted and power poles downed. Fallen trees and power poles will isolate residential areas. Power outages will last weeks to possibly months. Most of the area will be uninhabitable for weeks or months*." (NOAA, 2013) |
| 5 | >157 | "*Catastrophic damage will occur: A high percentage of framed homes will be destroyed, with total roof failure and wall collapse. Fallen trees and power poles will isolate residential areas. Power outages will last for weeks to possibly months. Most of the area will be uninhabitable for weeks or months*." (NOAA, 2013) |

**Table 1.1-Saffir- Simpson wind scale (NOAA, 2013)**

Rainfall tends to vary directly with the storm duration over an area, i.e. the forward speed of the storm. Typically, Category 5 has the least and tropical storms have the most precipitation (Needham, 2006).

When a hurricane approaches land, there will be a storm surge propagated by winds over the open water areas. For example, the maximum surge in Lake Pontchartrain was about 2 meters during

Hurricane Isaac; some of this surge is due to high surge at the Gulf which is transported into the estuary and some of the surge is due to local wind effects.

The City of New Orleans is bounded between the Mississippi River to the south and Lake Pontchartrain to the North. Overall, the most of the City is below sea level especially in some new neighborhoods. However both the Mississippi River and Lake Pontchartrain water surface elevations are above sea level. The City is protected by man-made levees which protect the City in times of flooding. The early French settled on natural levees built by the sedimentation during overflows of the River. The City's runoff is collected in a drainage canals and pumped out to the Lake Pontchartrain since there is no hydraulic gradient from New Orleans to either the Lake or the Mississippi River. Figure 1.4 shows a LIDAR image of New Orleans topography versus the water levels in the River and the Lake. Mississippi river has a water level of between 2 and 17 feet in New Orleans.

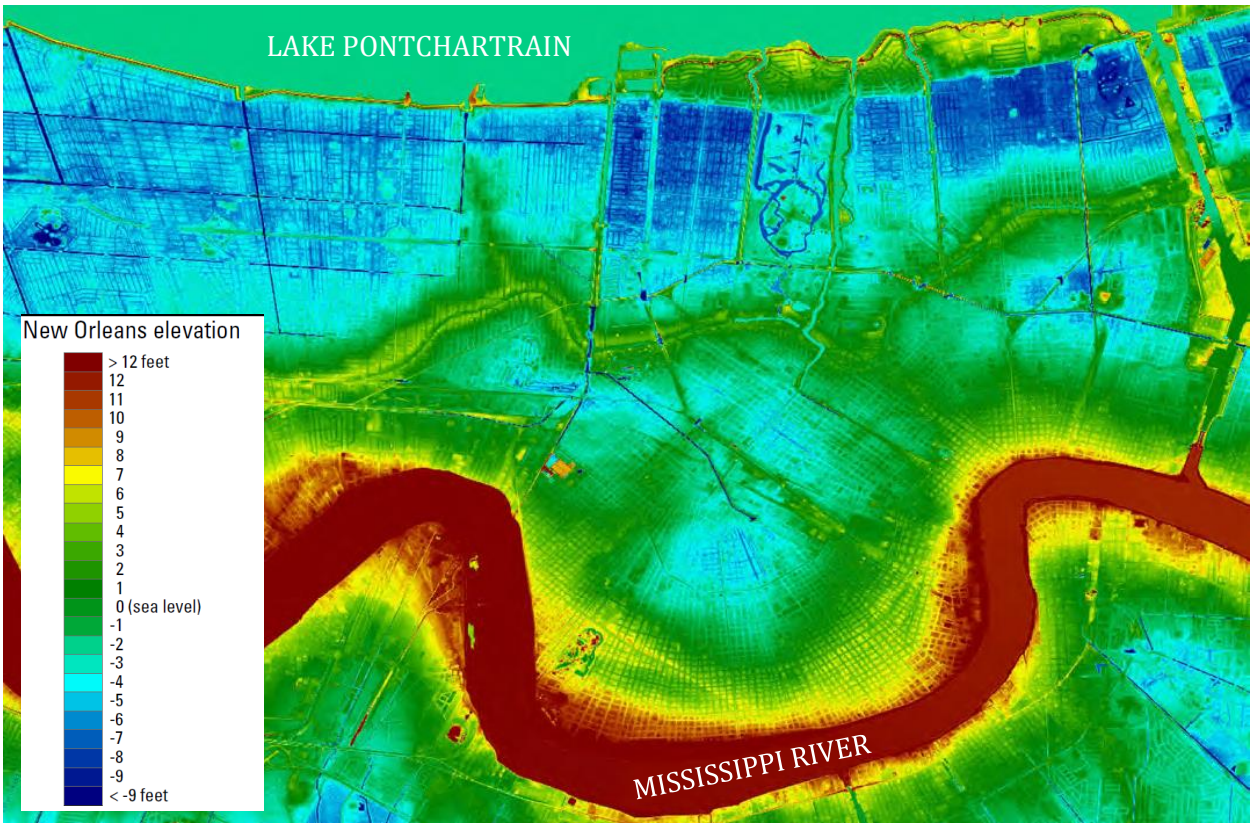


**Figure 1.4- LIDAR topography of New Orleans Area**

**Source: United States Geological Survey**

To understand what happens to a system under a certain event, one could do a field trip and measure what is happening. This is generally called monitoring. Monitoring is not always practical since it is expensive, the researcher does not have control and the event or circumstance (for example a hurricane) might have a return period of several years. The researcher cannot control the direction or the magnitude of the boundary conditions. For these reasons scientists have switched to modeling. There are two methods of modeling: 1) Physical and, 2) Numerical.

Physical modeling is when a scaled model is built in the laboratory to represent the prototype. The same or different scales can be applied to the horizontal and vertical directions depending on whether the model is non-distorted or distorted. When the physical model is built, the modeler imposes the boundary conditions and records the model response, e.g. water level. Unlike prototype monitoring, the circumstances are under control in physical modeling and what-if experiments can be conducted and concluded. Some advantages of physical modeling are:

a) Good visualization and self-explaining capability
b) Freedom from instability issues (instabilities occur in numerical modeling.)
c) Faster simulation time in some cases such as sediment transport runs

Disadvantages of physical modeling include:

a) High setup and operating cost
b) Scale effects, accuracy, precision and user error issues
c) Inability to make simultaneous runs
d) Physical space issues

Numerical modeling is numerical simulation of the governing phenomena based on the solution of mathematical equations that approximate the physical conservation laws. Computational Fluid Dynamics, CFD for short, started in the 1940s and has improved each year. A typical CFD application includes three major steps: pre-processing, processing, and post processing (Versteeg & Malalasekera, 2007). Pre-processing includes procedures modelers take to set up a model, such as grid generation and gathering boundary conditions. Processing covers the act of running the simulation. Post processing includes visualization of results plus calculating other parameters of interest (for example flow can be calculated by integrating velocity over a cross section). It is important to note that numerical models solve the governing partial differential equations as algebraic equations with values at discrete points; therefore the results are not continuous. Some advantages of numerical modeling include:

a) Low setup and operation costs
b) Convenience in modifying the geometry,
c) Ability to make simultaneous runs
d) Freedom from physical space issues

Whereas disadvantages of numerical modeling include:

a) Consistency, boundedness and stability issues
b) Poor visualization capability especially for non-professional audience
c) Slow simulation time in some cases such as sediment
d) Computational limitations, e.g. truncation errors in the mathematical formulation
e) Imperfect mathematical representation of the physical phenomenon being modeled.

Numerical models can be one, two, or three dimensional depending on which variations in dependent variable is more important. For instance, in the case of modeling flow in a river, the water level along the channel is more important than across the channel. Of course the gauge height might not be constant across a cross-section especially on a bend, but the 1-D information is enough to answer many questions. Two dimensional models are capable of solving the governing equations in both x and y directions. For example in case of modeling a lake, a 1-D model cannot show the spatial variability in the flow while 2-D models work for many parameters of interest. Three dimensional models have the capability to solve equations in x, y, and z direction. For instance, if vertical salinity distribution through the water column in a lake is of interest then a 3-D model has to be used.

## 1.2.Overview of CFD modeling

As mentioned, Computational Fluid Dynamics numerically solves the governing differential equations. The results are not continuous over the domain, yet dense enough to give sufficient representation of the system.

### 1.2.1. Properties of numerical solution methods

Any numerical solution has to satisfy some required properties. According to Guillot (2013), it is safe to first assume CFD outputs are incorrect, until enough reason are found to convince oneself

that they are correct. Some required properties that a numerical model has to satisfy are consistency, stability and boundedness.

#### 1.2.1.1. Consistency

The term “Truncation error” is defined as the difference between discretized equation and the exact one. To satisfy consistency the truncation error has to approach zero while time step and grid size are approaching zero.

#### 1.2.1.2. Stability

Stability is an important issue in modeling. A model is stable if it does not magnify errors associated with discretization. There are several types of instabilities. Instability might appear as sharp changes in results. For instance water level or velocity at a point may change too much per time step which may lead to having so called NaN (Not a Number). The term NaN might appear in a model results making the simulation useless. To save computational effort, some models such as Delft3D automatically kill the simulation if a parameter’s change is too high per time step at a certain node. For instance Delft3D stops processing if water level change is greater than 25 meters per half time step at a certain node. However, some models such as FVCOM keep on running with instabilities and even using NaNs in further time steps which may lead to useless results.

Instability may also appear as noise in results. This type of instability does not necessarily lead to unrealistic high or low values. However; it is highly recommended to fix the situation.

There are several steps a modeler can take to fix instability issues, including:

1) Gradually applying (ramping) boundary conditions in the beginning of simulation
2) Taking a shorter time step, especially in explicit models
3) Improving the geometry of cells. Slender cells tend to bring instability
4) Increase upwinding; however this may lead to artificial diffusion.

#### 1.2.1.3. Boundedness

The certain results of a numerical model may be bounded between the values of boundary conditions. For example, if temperature variation in a rod with one end in ice and the other end in steam is modeled, the results are expected to vary between 0 °C and 100 °C. Numerical solutions containing unbounded values are not accepted.

### 1.2.2. Grid

In all CFD models, a mesh must be generated to cover the domain. The solution is calculated in each grid point or cell center. Coarse grid sizes are faster to solve while a fine grid makes it slower to process. A dimensionless value called the Courant number is defined as:

$$C = \frac{\Delta t \sqrt{g D_m}}{\Delta x} \tag{1.1}$$

where:

| | |
|---|---|
| C | Courant Number [dimensionless] |
| Δx | Grid spacing [meters or feet] |
| Δt | Time step [seconds] |
| g | Gravitational acceleration [$m/s^2$ or $ft/s^2$] |

The Courant number gives the ratio of the distance gravity waves travel during a time step to distance between two nodes. Implicit mode models are able to handle Courant numbers > 1; on the contrary, explicit models require Courant numbers of less than one.

While a fine mesh might seem to give more accurate results; due to computational costs and truncation errors, the best mesh is not necessarily the finest. To keep the Courant number in a reasonable range, one has to reduce the time step if the grid size is decreased. Small time step with having small grid sizes make the simulation computationally costly. A coarse mesh on the other hand may fail to provide enough information in the areas of interest or where variables have sharp gradients.

An experienced modeler will use a high resolution on the areas of interest or where high gradients of values are expected and a low resolution in locations where are far from areas of interest or have low variable gradients.

### 1.2.3. Grid Structure

There are two different types of grids: structured and unstructured. Each one has its own advantages and disadvantages. Structured grid cells are easy to locate and suitable for finite difference discretization while unstructured grids are capable of covering complex geometries.

#### 1.2.3.1. Structured Grid System

In a structured mesh, the grid is built so that one can use "i" and "j" notations to address each node. This is believed to be the simplest method since it is corresponds to a Cartesian grid (Ferziger, 2002). The main advantage of using structured grid is its simplicity to annotate the grid and calculate the fluxes through each edge. It also leads to narrow banded coefficient matrices, i.e. tri-diagonal or penta-diagonal matrices which make the use of the Crank-Nicholson and Alternating Direction Implicit Methods more convenient (Ferziger, 2002).

A structured grid system is not as convenient as unstructured grid for capturing complex geometries; furthermore if one does local refinements of the grid in a specific location, these refinements will be extended into unwanted areas. This results in a waste of computation time. Figure 1.5 shows the unwanted refinement applied to two lakes since high resolution was required to capture a pass.

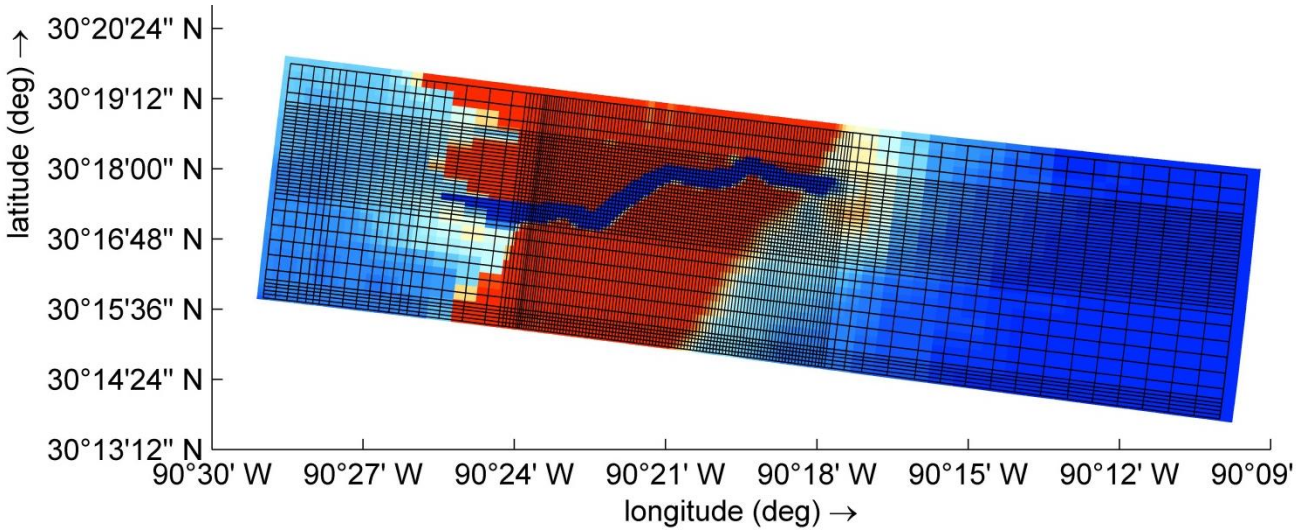


**Figure 1.5-Unwanted grid refinement going to two lakes from a pass**

The other issue that structured grids may have is called stair stepping. This usually happens while the modeler tries to cover some area where the boundary does to follow the Orthogonality of the grid. This may cause wet-drying problems as well as creating artificial roughness. Figure 1.6 demonstrates stair stepping in a channel.

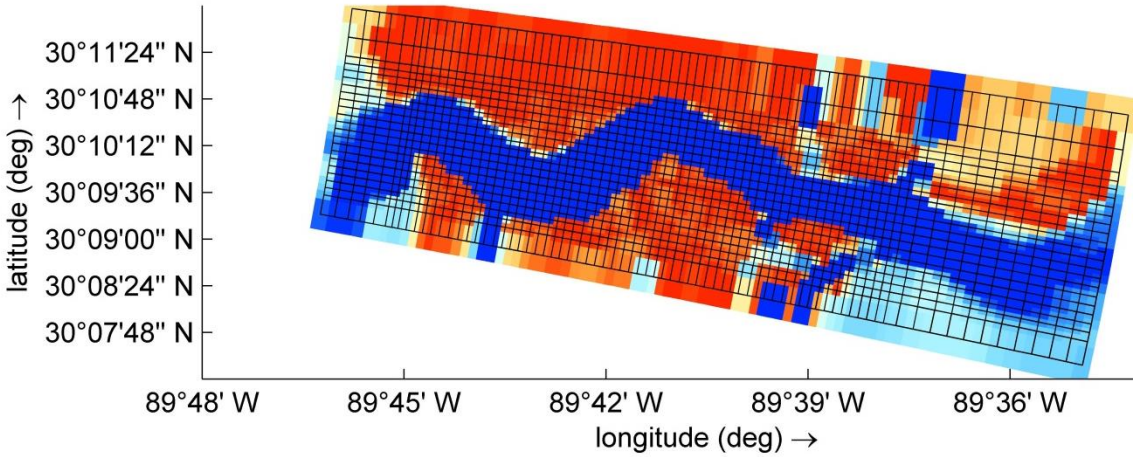


**Figure 1.6- Stair stepping in a narrow channel which does not follow the orthogonality**

Typically the boundaries of rivers and estuaries are curved hence not smoothly representable on a rectangular grid. Therefore, Stair stepping is likely to occur. Stair stepping can be avoided to some extend by using a curvilinear grid, e.g. in modeling a single meandering channel if Orthogonality follows the meander. The modeler simply follows the curvature of the channel while developing the curvilinear mesh. Figure 1.7 shows how curvilinear grid system has perfectly fit the geometry of Southport bend (RM 104.5 Mississippi River).

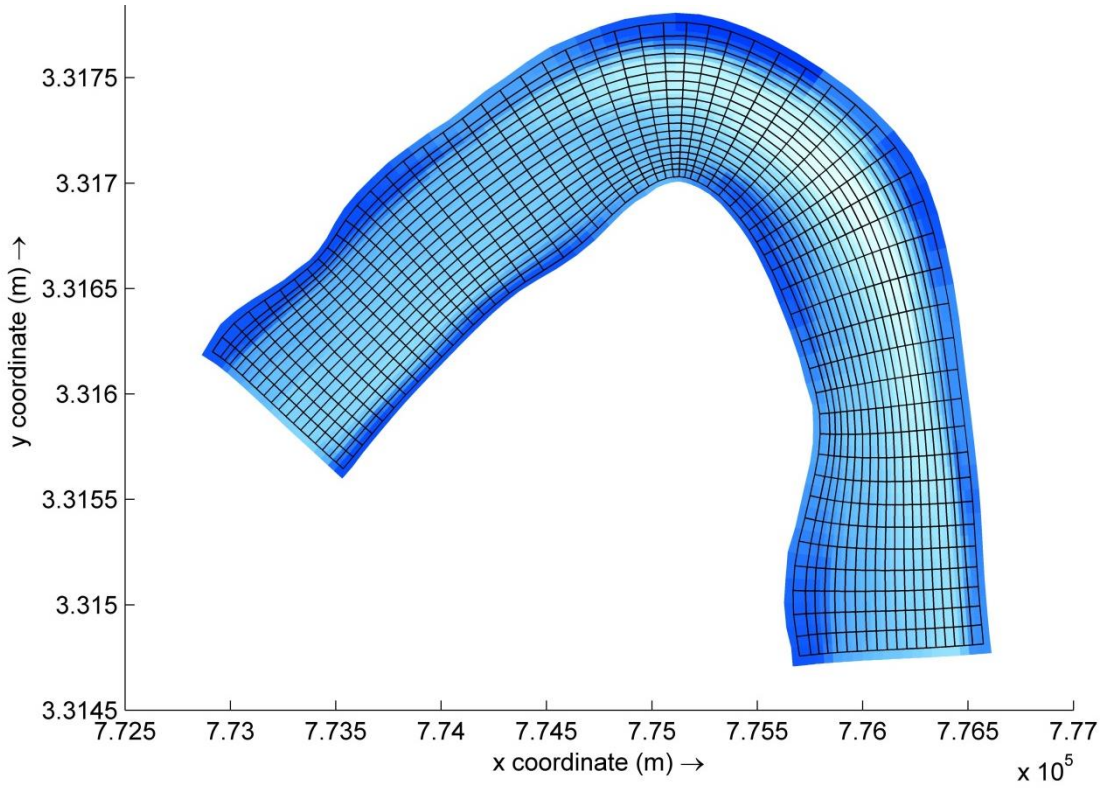


**Figure 1.7-Curvilinear grid successfully covering Mississippi River at Southport, Louisiana**

#### 1.2.3.2. Unstructured Grid System

When nodes are not locatable using i and j notations, the grid is unstructured. Usually unstructured grid cells are triangles or quadrilaterals. Mathematically, unstructured grids can be used for any type of discretization method, however use of unstructured grids for Finite Element and Finite Volume methods are more practical hence more common.

Using unstructured grid system makes it effective to cover complex geometries. The grid is free from local refinement issues. However cell numbering and addressing might difficult. For instance, the grid form in FVCOM is an ASCII file with having x and y coordinates of each node, then followed by cell number and connectivity list.

### 1.2.4. Vertical Boundary Fitting

In the vertical direction there are two common boundary fitting methods: the σ coordinate system and the Z coordinate system.

#### 1.2.4.1. The σ co-ordinate system

The σ co-ordinate system was initially created by Phillips (1957) for atmospheric models. The σ grid contains layers bordered by two sigma planes, which follow the bottom bathymetry and the free surface. Since the σ-grid is boundary fitted to the bottom and the free surface, a soft illustration of the bathymetry is obtained.

The number of layers over the entire horizontal computational area remains constant, regardless of the local water depth. Allocation of each layer's thickness is typically non-uniform in order to have more accuracy in the zones of interest such as the near surface area for wind-driven flows and the near bed area for sediment transport. The σ co-ordinate system is defined as:

$$\sigma = \frac{z - \zeta}{d + \zeta} = \frac{z - \zeta}{H}, \tag{1.2}$$

in which

| | |
|---|---|
| z | vertical co-ordinate in physical space |
| ζ | water surface elevation above reference plane |
| d | water depth below reference plane |
| H | total water depth which is given by is given by H= d + ζ |

At the bottom σ = 1 while at the free surface σ= 0. The partial derivatives in the original Cartesian co-ordinate system are expressed in σ co-ordinates by the chain rule introducing additional terms (Stelling & van Kester, 1994).The flow domain of a 3D shallow water model consists in the horizontal plane of a restricted (limited) area composed of open and closed (land) boundaries and in the vertical of a number of layers. In the σ co-ordinate system, the number of layers is the same at every location in the horizontal plane, i.e. the layer interfaces are chosen following planes of constant σ (figure 1.8). For each layer a set of coupled conservation equations is solved.

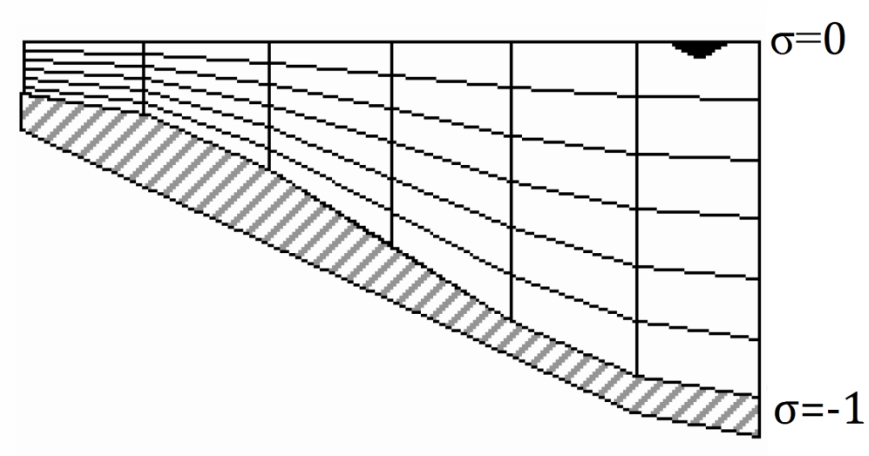


**Figure 1.8- The σ co-ordinate system. Source: Delft3D FLOW manual**

#### 1.2.4.2. The Z co-ordinate system

Unlike the σ model, in this type of co-ordinate system the layers lie almost parallel to the water surface. The z-model makes a significant improvement in coastal areas with steep slopes. If the σ-model is used in such areas, the co-ordinate lines might intersect the density interfaces which may lead to significant errors in the calculation of purely horizontal density gradients. On the other hand, according to Ayres (2013) , the current z-version of Delft3D has several bugs.

It is important to keep in mind that unlike the σ-model, in the z-model, the number of layers does not necessarily remain constant everywhere in the system, while in fact; it depends on the water depth. In the sigma model the percent share of each layer from the water column is prescribed, whereas in the z model the thickness of each layer is prescribed (figure 1.9).

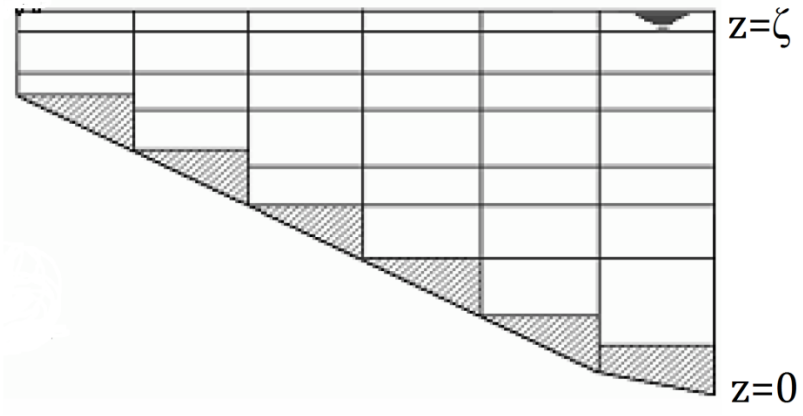


**Figure 1.9- The Z co-ordinate system. Source: Delft3D FLOW manual**

### 1.2.5. Discretization Methods

There are three typical discretization methods: 1) The finite difference method, 2) The finite volume method, and 3) The finite element method. The FDM appears to be the oldest method of discretization. The FEM is more suitable to solid mechanics and the FVM appears to be the most suitable in case of fluids.

#### 1.2.5.1. The Finite Difference Method

Believed to have been developed by Euler in the 18th century, the finite difference method is the oldest and easiest method to solve partial differential equations. The method starts with defining the governing differential equations, then replacing the derivatives by Taylor series approximations. Each node will have one algebraic equation in which the unknown value in each cell is unknown (Ferziger, 2002).

Mathematically, the finite difference method can be applied to all kinds of grid systems. Nevertheless, application of the method to unstructured grid systems is difficult. The main disadvantage of this method is lack of satisfying the conservation

#### 1.2.5.2. The Finite Volume Method

In The finite volume method original form of the conservation equations are used as the starting point (Ferziger, 2002). The computational domain is divided into a finite number of control volumes. Conservation equations are written for centroid each control volume. The values at CV surfaces are expressed by interpolation. Then, surface and volume integrations are done. This leads

to some number of equations and same number of unknowns which can be solved by several methods.

The finite volume method, which is very reliable, widely used method of discretization, uses the above principle. This method carries the concept of conservation by itself, bringing it a significant improvement over the FDM and FEM.

#### 1.2.5.3. Finite Element Method

In this method the domain is subdivided into several finite elements that are typically unstructured. The elements could be triangles or quadrilaterals in 2D, whereas in 3D they can be tetrahedrons or hexahedrons. A weighting function is multiplied by the equations, before integration. In a simple case the solution is estimated by a linear function inside each element in a way continuity guaranteed way. The function can be formed from its corner values.

The approximation is then substituted and the equations are derived by forcing the derivative of the integral with regard to each nodal value to zero. The result is a set of non-linear algebraic equations. (Ferziger, 2002)

## 1.3.Problem Statement

The background section indicated how important flooding issue is to the City and the habitants. Billions of dollars have been spent on improving the levee system to protect the City from floods. However, since salt flood exposure is not fatal to human beings, less attention has been taken of this issue. In general, fish, shells, and clams in are considered somewhat sensitive to saline patterns if these patterns persist (Retana, 2008). On the other hand, there is another important impact which occurs during hurricanes where there is saltwater flooding in marshlands. This is important in two ways: 1) The marshland and swamps around Lakes Maurepas and Pontchartrain are mostly freshwater marsh and can be damaged by ponded saltwater, and 2) There are cypress swamps that typically cannot handle salinity concentrations over 6 ppt, especially if they are young (Doyle, Conner , Day, Ken, & Swarzenski, 2005).

Initially, hurricane category might seem as a determinant of surge height. However, less consideration is taken to account for hurricane duration. The experience of category one hurricane Isaac raised this question whether or not the hurricane duration might have a role to play in surge height (USACE, 2012).

Salinity variation in the Pontchartrain estuary is balanced by freshwater discharges from rivers, tributaries, canals, rainfall, Mississippi river diversions, and evaporation (Georgiou, 2002). The estuary is fresh to brackish with an average salinity of around 0 ppt in Lake Maurepas, 5 ppt in Lake Pontchartrain, 10 ppt in Lake Borgne, 20 ppt in the Gulf of Mexico West of Chandelier Islands and greater than 30 ppt South and East of Chandelier Islands.

Although there have been several 2-d and 3-d numerical models for the Pontchartrain estuary, there has been not enough focus on salinity and saltwater flooding. Furthermore, some of the previous models do not extend into the marshlands. Thousands of simulations have been run to model storm surges for various hurricane categories and tracks, but less attention has taken place to determine the dependence of maximum surge height to hurricane duration.

## 1.4.Objective

The overall objective of this study is to develop a three dimensional numerical model for Pontchartrain estuary that is capable of modeling storm surges and salinity distribution throughout the system. It should also contain the coastal areas that are subject to flooding. The selected model should be able to take winds and rainfall into account.

The grid should be fine enough in the areas of interest to capture Pass Manchac, Rigolets and Chef Menteur Pass; however, coarse enough in the offshore areas to save computational time.

The model should be able to determine the salinity variation as well as response of maximum surge height to hurricane duration. The model should be able to provide the answer to questions about the role of hurricane duration in surge height and salinity.

## 1.5.Methodology

The following methodology is taken to solve the proposed objective:

1) A literature review was conducted.
2) Possible models were carefully reviewed in order to select the most suitable numerical model.
3) Bathymetry and Topography data of the area was obtained from NOAA.
4) A grid was made to represent the system into several finite size cells.
5) Conservativeness, Boundedness, and consistency tests were ran to check the model.
6) Field data boundary conditions were obtained from USGS, NOAA and USACE.
7) The model was calibrated and validated for normal conditions as well as hurricanes.

The model was applied to answer selected questions about the estuary hydrodynamics such as storm duration and salinity flooding impacts.

# 2. LITERATURE REVIEW OF PREVIOUS STUDIES

A brief review on earlier studies on was important in two ways. First, it was essential to have an understanding of the estuary's behavior in previous numerical models and compare with this study model to verify typical behaviors. Second, it was important to find recommendations in previous literatures and follow them if interested.

Most of the previous studies reviewed in this section were done at the University of New Orleans. Over the past decades, students and professors have done several studies on the Estuary. Dozens of theses and dissertations were focused on the estuary's hydrodynamics, water quality, fish, salinity, nutrient etc.

## 2.1.Haralampides (2000)

As a PhD dissertation funded by Freeport-McMoRan Inc., Haralapides (2000) used a finite element model named RMA2 to look at Hydrodynamic and salinity regimes in Lake Pontchartrain. Figure 2.1 shows a snapshot of Haralampides's computational grid. She successfully modeled tide and surge responses in lakes Maurepas, Pontchartrain and Borgne. As a test Haralapides simulated the behavior of the system to several constant wind speeds and directions. It was concluded that the model typically develops two gyres for most winds on both Lake Pontchartrain and Maurepas (Figure 2.2). Haralampides also modeled the opening of Bonnet Carré Spillway in 1997.

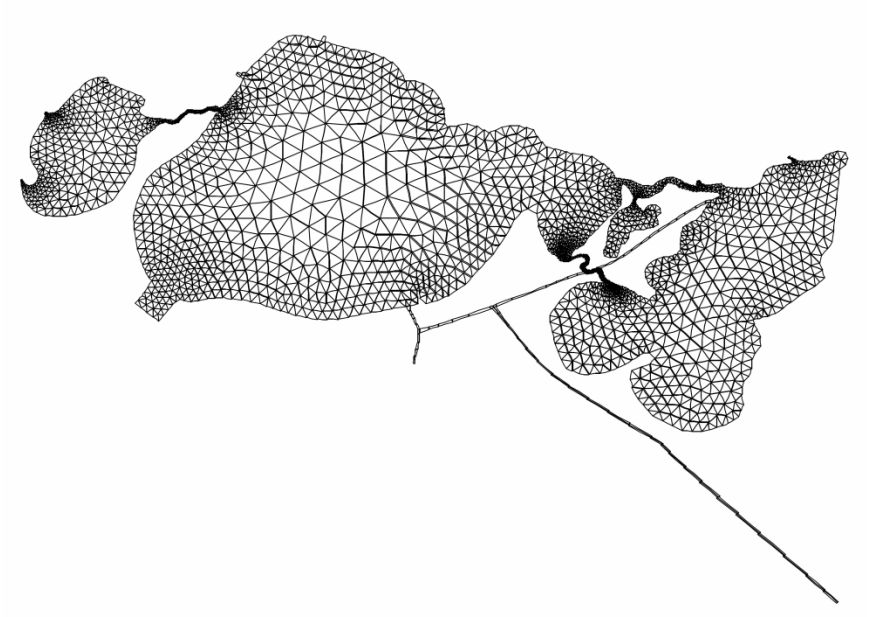

**Figure 2.1 Computation domain used by Haralampides**

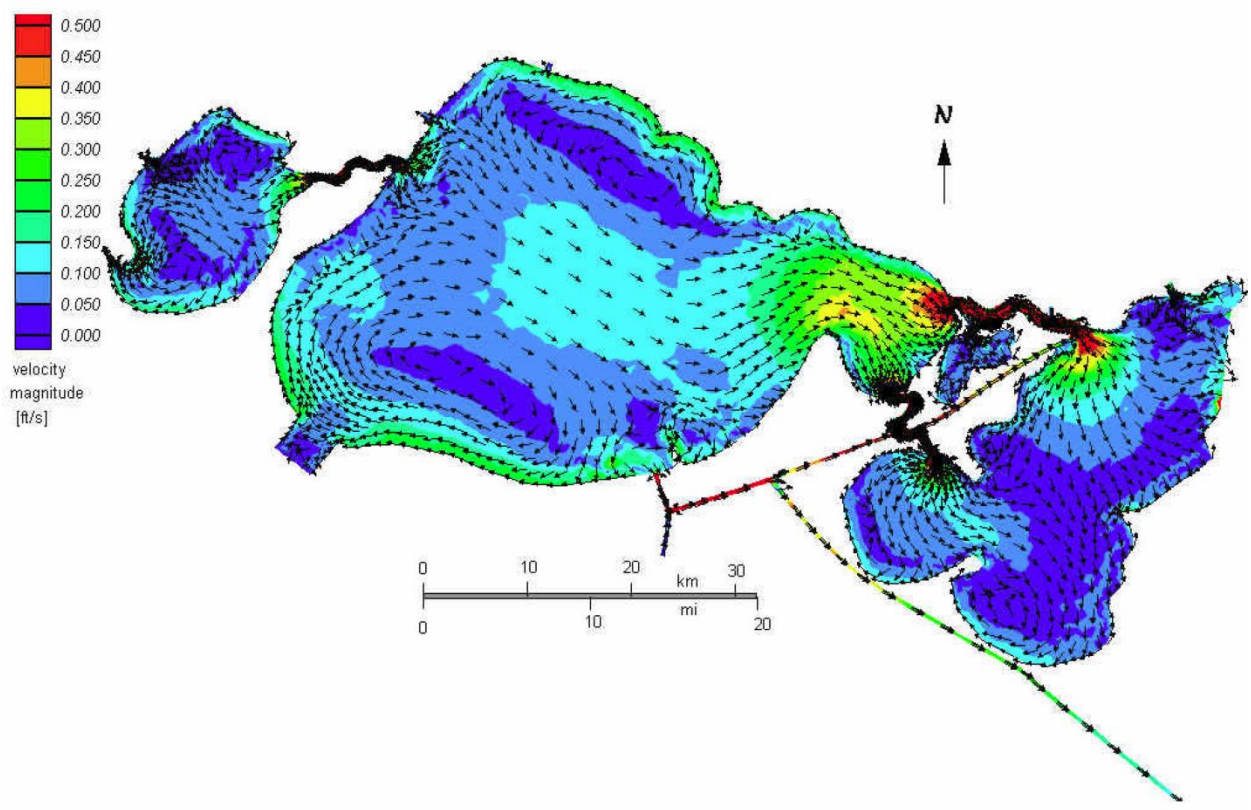


**Figure 2.2- Depth averages velocity vectors. System is exposed to 6m/s southeast winds.**

## 2.2.Georgiou (2002)

In 2002, the Princeton Ocean Model (POM) was used by Georgiou to simulate saltwater intrusion and circulation in Lake Pontchartrain in 3-D. In order to avoid stability issues Georgiou had to smooth wind and open boundary tidal data using a temporal filter. Georgiou's simulations also confirmed development of a two-gyre circulation pattern by wind shear (Figure 2.4). Georgiou also studied salinity stratification in Lake Pontchartrain near the IHNC. The model showed density gradients cause the saltwater wedge to propagate large distances into the lake. Figure 2.3 contains an image of Georgiou's computational grid in POM.

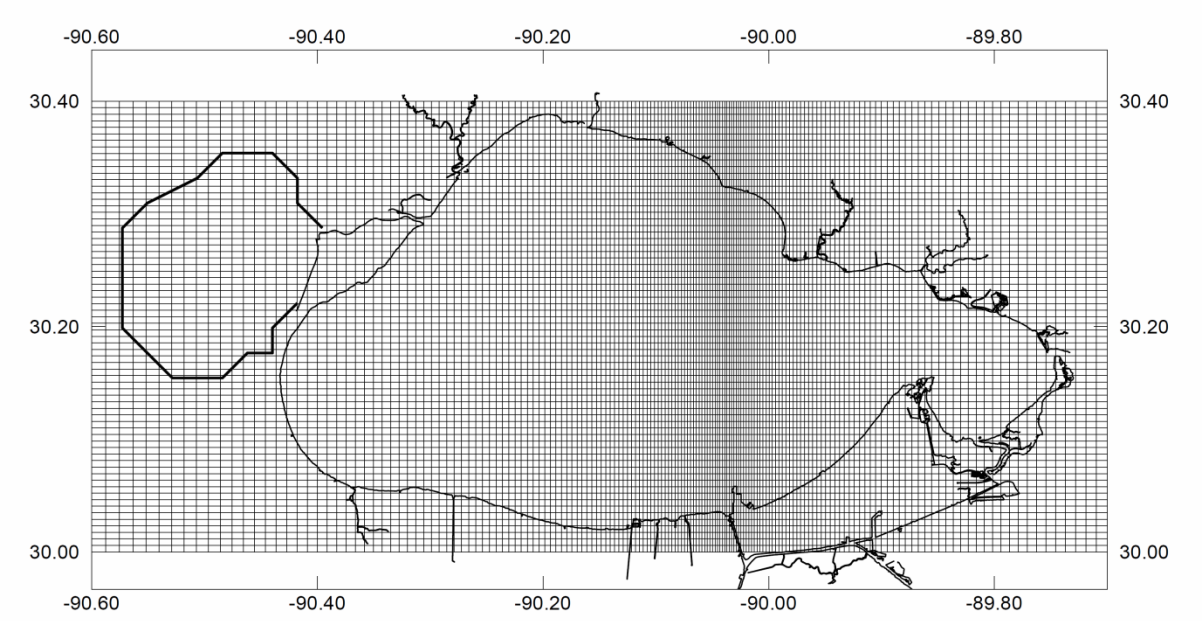


**Figure 2.3- Georgiou's computational domain in POM**

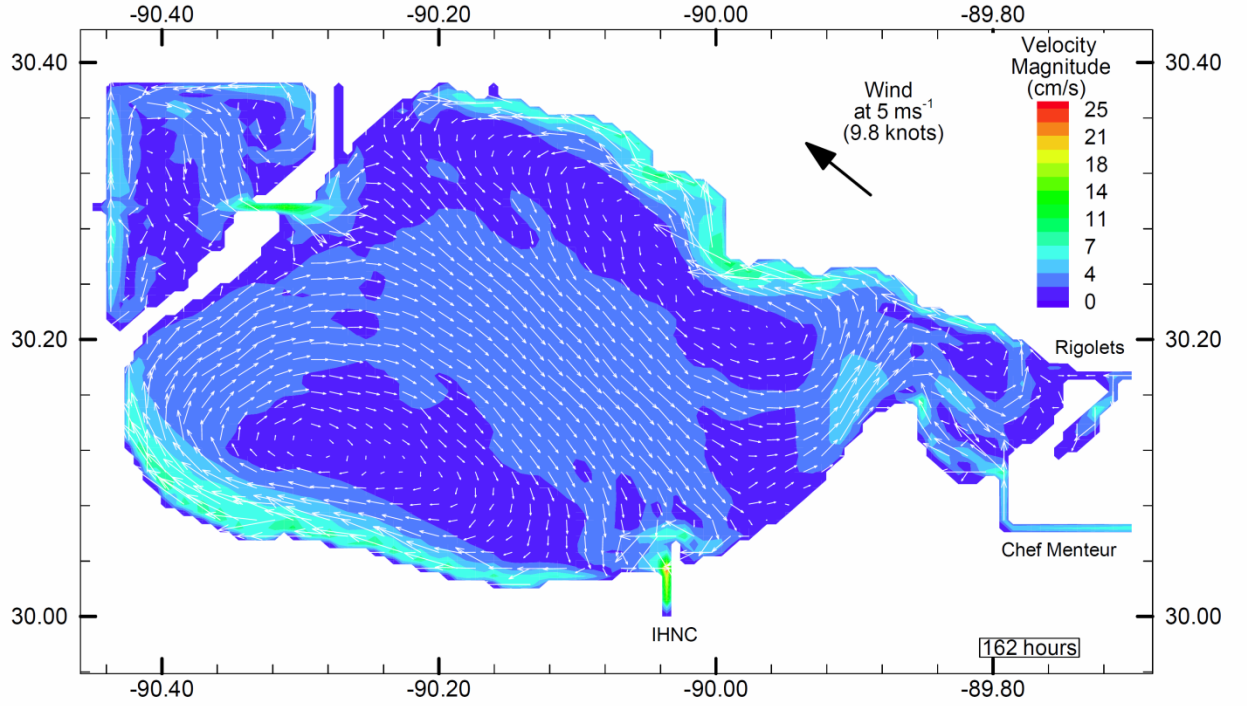


**Figure 2.4- Development of two-gyre pattern in Georgiou's POM model**

## 2.3.Chilmakuri (2005)

Chilmakuri (2005) used the Estuarine, Coastal and Ocean Modeling System with Sediment (ECOMSED) to look at sediment transport and pathogen indicators in Lake Pontchartrain. The two-gyre circulation pattern was also confirmed by Chilmakuri. Furthermore, the system was applied to several wind speeds and directions. During the research, Chilmakuri found out that ECOMSED does not fully support wetting and drying. Since structured grid was used, Chilmakuri had to use equivalent channels to represent Rigolets, Chef Menteur Pass and Inner Harbor Navigation Canal.

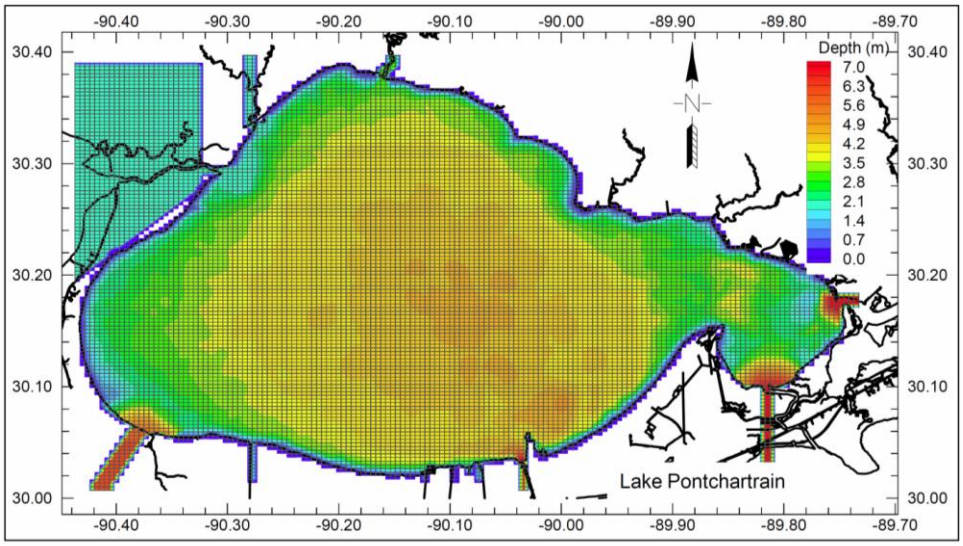


**Figure 2.5- Chilmakuri's grid in ECOMSED**

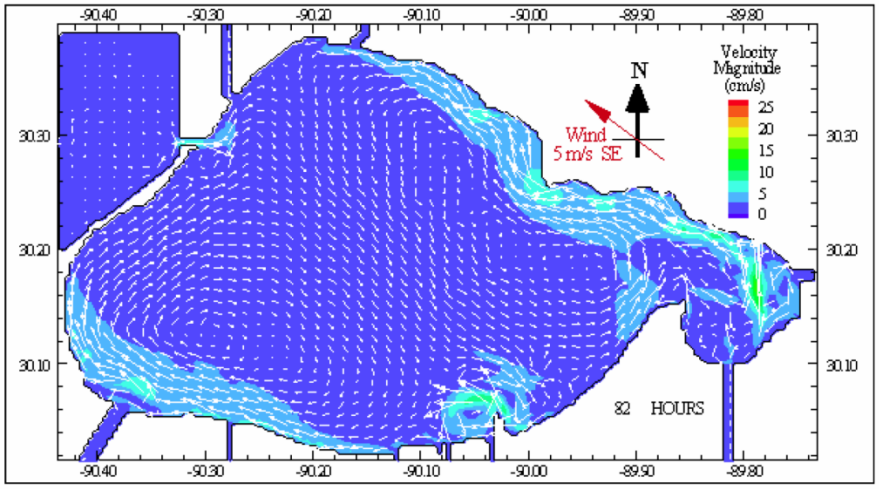


**Figure 2.6- Typical two-gyre response confirmed by Chilmakuri**

## 2.4.Retana (2008)

Retana (2008) used Finite Volume Coastal Ocean Model (FVCOM) and developed a model too look mainly at salinity. By going into the source code, Retana was able to implement spatially variable roughness for the model. Later Pereira (2010) corrected a bug in spatially variable wind ability of the code. Retana introduced 9 sigma layers in his model. Figure 2.7 has a snapshot of Retana's grid in FVCOM.

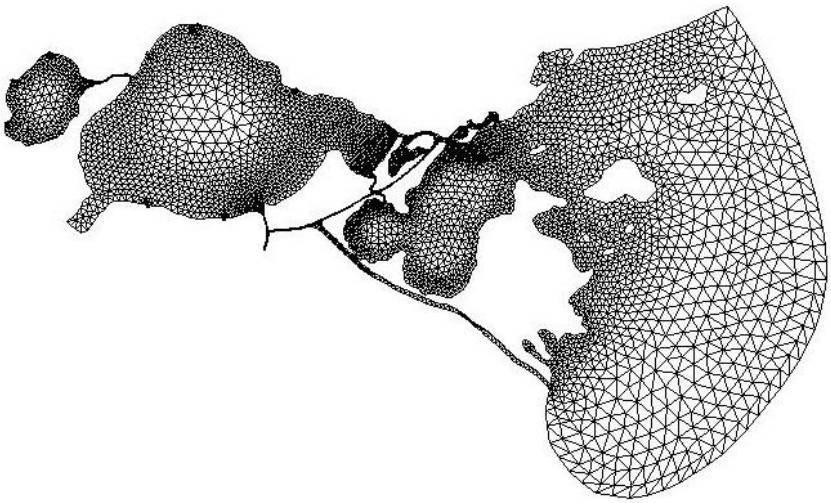

**Figure 2.7- FVCOM grid used by Retana**

Retana's model was then used by Amini and Pereira (2012) to run hydrodynamics in the period of 2010 Deepwater Horizon oil spill. Figure 2.8 indicates a stage validation in Lake Pontchartrain during the Deepwater Horizon oil spill.

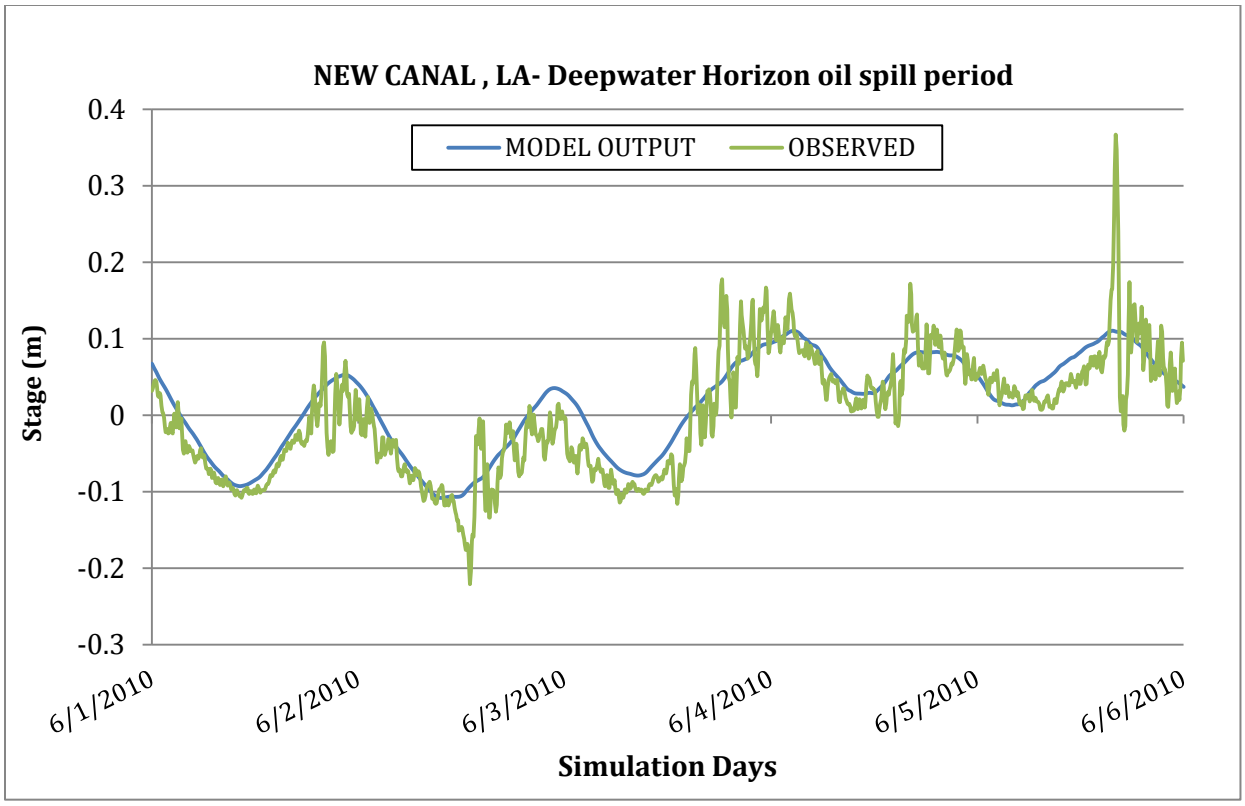


**Figure 2.8- Validation for the 2010 Deepwater Horizon Oil spill period at New Canal, LA**

## 2.5.Schindler (2010)

Finite volume costal Ocean model (FVCOM) was used by Schindler (2010) with the main goal of determining the effect of sea level rise on land loss. Schindler's grid covered parts of the Gulf of Mexico as well as the estuary (see figure 2.9). The model was run for hydraulics as well as salinity.

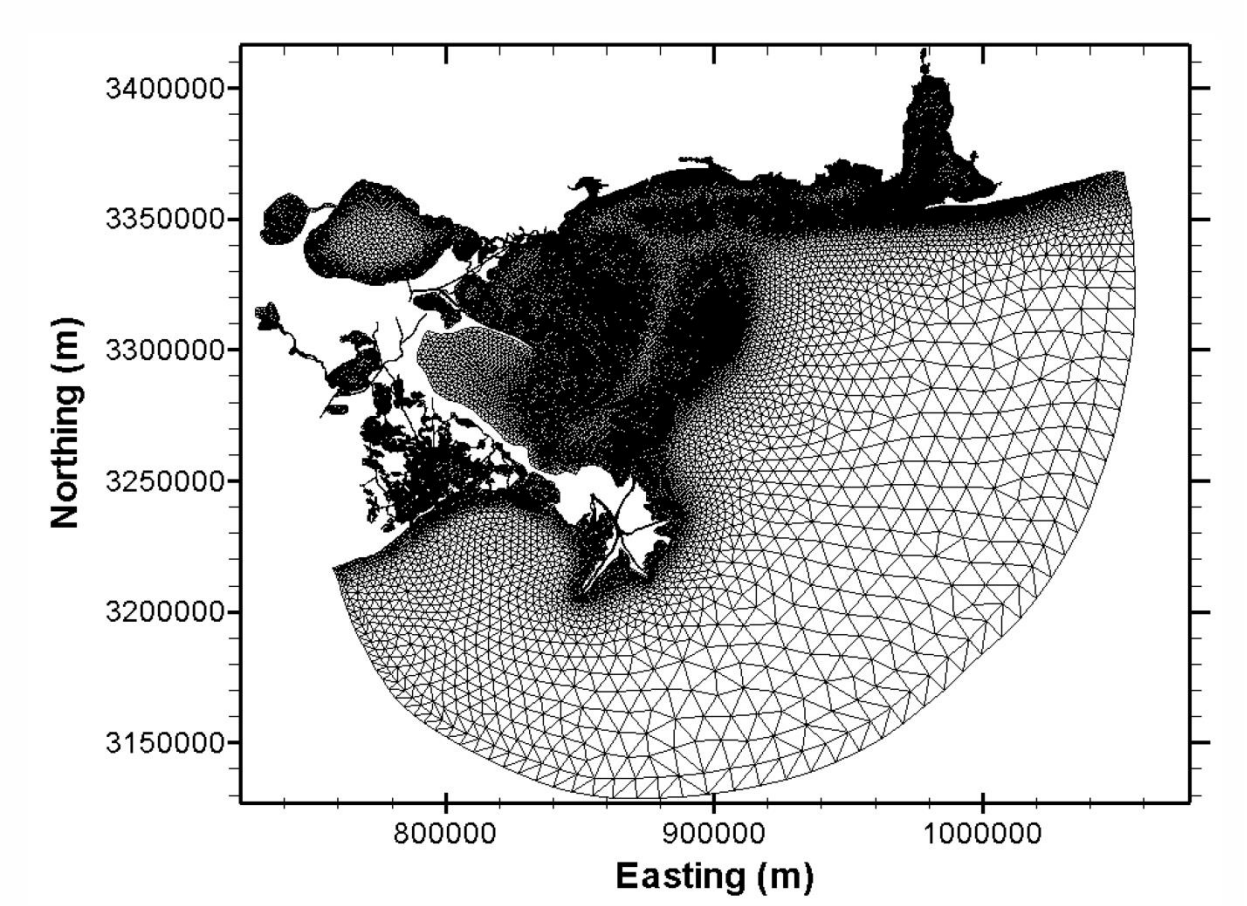


**Figure 2.9- Schindler's Computational grid in FVCOM**

## 2.6.Amini *et al* (2013)

As part of a National Science Foundation study, Amini *et al* (2013) looked at how hurricane duration affects surge height. FVCOM was used to model the period of 08/25/2015 to 09/05/2012 with the estuary exposed to various hurricane durations having same wind field and track as Isaac. It was found that initially surge height increases linearly as hurricane duration increases, but seeking some asymptote in relatively slow moving storms (Amini et al, 2013).

## 2.7.USACE (2012)

The United States Army Corps of Engineers published a detailed report titled "Hurricane Isaac with and without 2012 100-year HSDRRS evaluation". The ADCIRC model was used to determine the surge height with and without the 100 year Hurricane & Storm Damage Risk Reduction System. It was found that wind duration was a major factor in producing higher than usual storm surges compared to a general Category 1 hurricane. Moreover, it was found that every hurricane behaves

uniquely; therefore, the Saffir-Simpson scale could not be used as the only risk predictor (USACE, 2012). Figure 2.11 contains an example of the Modeling results done by the USACE.

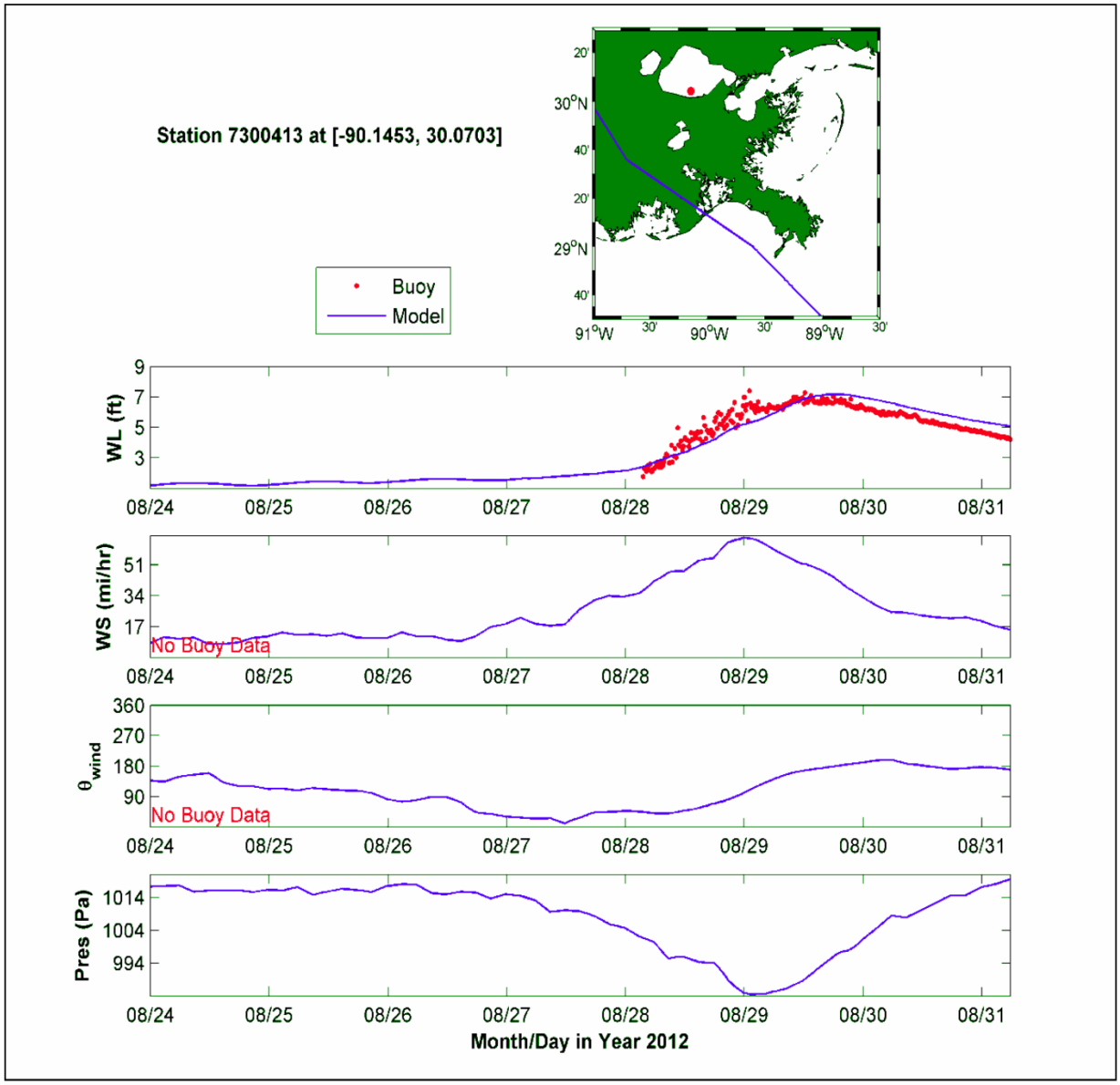


**Figure 2.10- US Army Corps of Engineers ADCIRC modeling results**

## 2.8.Georgiou *et al* (2009)

Georgiou *et al* (2009) published a paper on the impact of freshwater diversions on the salinity distribution in the Pontchartrain Estuary under tidal forcing using FVCOM. A series of scenarios were run to determine the effects of several possible diversions. The model finally showed when other divisions are functioning in the upper portion of the Estuary; the Violet diversion can be operated at significantly reduced flow and still achieve the desired salinity regime. It was also found

that flows through the narrow passes such as, IHNC, Rigolets and Chef Menteur will change as a result of opening or closure of other diversions. Figure 2.11 from Georgiou et al. (2009) provides a basis for setting the salinity gradients in Pontchartrain Estuary models.

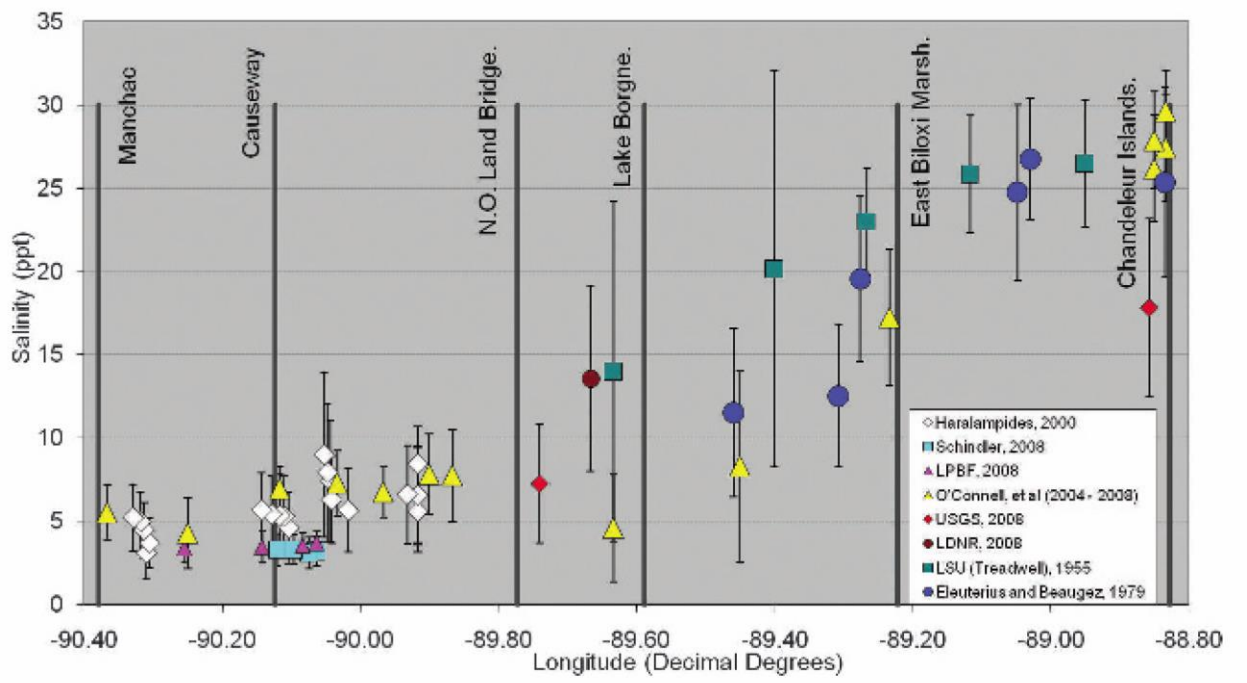


**Figure 2.11- Pontchartrain Estuary salinity gradients as a function of longitude; Georgiou *et al* (2009)**

## 2.9.Rego (2009)

As parts of his PhD dissertation, Rego (2009) used the Finite Volume Coastal Ocean Model to look at various forward speeds of Hurricanes with the same category and track. Rego found out that typically, maximum surge increases as a Hurricane forward speed decreases, but there is a limit on that.

## 2.10. Li *et al* (2010)

Lie *et al* (2010) looked at flux of water at Lake Pontchartrain Tidal Passes during hurricanes Gustav and Ike it was found that Hurricane Gustav passed 963 million cubic meters of water through Rigolets (35%), Chef Pass (55%) and IHNC (10%). While the outward flux was three times the input (3163 million $m^3$), the percentage share of each channel was roughly the same. It is believed that

rainfall and discharges from several tributaries were responsible for the huge difference between influx and out flux. (Lie *et al,* 2010)

The values published by Lie *et al* (2010) are inconsistent with Haralampides's measurements (2000) and values in table 4.3 from Georgiou *et al* (2009).

# 3. MODEL SELECTION

## 3.1.Possible models

After carefully reviewing several available 3 dimensional, finite volume models, three models were selected for further consideration. The Delft3D developed by the Deltares Academy (Deltares, 2011), The Finite Volume Coastal Ocean Model (FVCOM) developed at University of Massachusetts Dartmouth and Estuarine Coastal (Chen et al, 2011) and Ocean Modeling System with Sediment (ECOMSED) developed by HDR-HydroQual (HydroQual, 2004) . One of the above models had to be picked to build the Pontchartrain Estuary Model.

### 3.1.1. FVCOM

Finite Volume Coastal Ocean Model (FVCOM) was first developed by the University of Massachusetts Dartmouth by The Marine Ecosystem Dynamics Modeling Laboratory. It solves momentum, temperature, continuity, salinity and density equations. FVCOM uses unstructured triangular mesh which makes it powerful to cover complex geometries. The code cannot run in Windows environment, therefore the user needs to use a UNIX/LINUX system. FVCOM is only does the processing step. For pre-processing and post-processing purposes, other programs need to be used. The model is able to run in parallel mode as well as serial.

FVCOM has been successfully tested and used at the University of New Orleans by Georgiou (2005-2014), Retana (2008), Pereira (2010), Schindler (2008) and Amini (2012). It uses a split mode procedure for the computations, i.e. an explicit mode to solve the surface wave (continuity) with a very small time step controlled by the Courant Number and a longer time step to solve the vertical distribution of the momentum. The controlling time step is only a fraction of a second in the Pontchartrain Estuary. FVCOM supports wetting and drying.

### 3.1.2. Delft3D

Developed by the Deltares Academy, Delft3D is able to model hydraulics, sediment transport, water quality, waves and morphology. It uses a structured curvilinear orthogonal grid. Delft3D

supports wetting and drying simulation making it a powerful model for flooding simulations. The model has parallelization capability being able to effectively use the CPU. Since it uses implicit mode from one time step to another, longer time steps can be used without disturbing stability. Delft3D has powerful pre-processing and post-processing tools included.

#### 3.1.3. ECOMSED

Standing for Estuarine, Coastal and Ocean Modeling System with Sediments, ECOMSED is a three-dimensional, structured grid, sigma coordinate model with sediment transport module. Chilmakuri (2005) indicated that ECOMSED does not support wet/dry calculations. ECOMSED does not support parallelization, making it computationally ineffective. At the University of New Orleans, ECOMSED was tested an applied to lower Mississippi river by Pereira (2011) and Pontchartrain estuary by Chilmakuri (2005). The model does not run in parallel mode.

## 3.2.Selection Criteria

An approach is taken to find the most suitable model for the study case. This is based on each model capabilities and the study needs. The minimum requirements of the model are:

1) Have 3-D capabilities
2) Have successfully tested salinity, wind and Hydraulics modules
3) Be freely or inexpensively available to non-commercial researchers

A desired model would preferably:

1) Have unstructured grid to be able of capturing complex geometries
2) Have a straight forward and self-explanatory user's manual
3) Have pre-processing and post processing capabilities included
4) Contain good sediment and wave modules for future studies
5) Be able to run in parallel
6) Be able to run fast enough with a relatively long time step
7) Be easy to work with
8) Have the least bugs

There is no model that satisfies all the above criteria. Therefore an evaluation was made to select the most suitable model from three possible choices: Delft3D, ECOMSED, and FVCOM. For essential

requirements scores are out of 10 whereas for desired characteristics scores are given out of 5. Table 3.1 shows the evaluation conducted to select the most suitable model.

| Criteria | Models | | | | | |
|---|---|---|---|---|---|---|
| | Delft3D | | ECOMSED | | FVCOM | |
| | Description | score | Description | score | Description | score |
| Method | Finite Volume | N/A | Finite Volume | N/A | Finite Volume | N/A |
| 3-D Capabilities | ✓ | 10 | ✓ | 10 | ✓ | 10 |
| Availability to non-commercial Researchers | FREE | 10 | FREE | 10 | FREE | 10 |
| Grid system | Structured | 0 | Structured | 0 | Unstructured | 5 |
| Salinity Module | ✓ | 10 | ✓ | 10 | ✓ | 10 |
| Wind Module | ✓ | 10 | ✓ | 10 | ✓ | 10 |
| Precipitation/Evaporation | ✓ | 5 | ✓ | 5 | ✓ | 5 |
| Sediment Module | ✓ | 5 | ✓ | 5 | Poor | 0 |
| Time Step Range Used for UNO models | 0.5-1.0 Minutes | 5 | 0.2-0.5 Seconds | 3 | 0.2-0.5 Seconds | 3 |
| Parallelization Capability | ✓ | 5 | × | 0 | ✓ | 5 |
| Pre-Processing tool | Included | 5 | × | 0 | × | 0 |
| Post-Processing tool | Included | 5 | × | 0 | × | 0 |
| Wet/Dry Capability | ✓ | 10 | Poor | 0 | ✓ | 10 |
| Total Score | 80 | | 53 | | 68 | |

**Table 3.1- Evaluation for model selection**

Since Delft3D gained the highest score in table 3.1, it was selected as the main model for this study. However; FVCOM was also applied to model storm surge and determine surge height dependence on storm duration. Some more information about Delft3D is discussed further.

## 3.3.Overview of Delft3D

Deltares Academy has developed Delft3D, a fully integrated numerical model for a multi-disciplinary approach and 3-Dimensional computations for coastal, river and estuarine

applications. Delft3D is capable of modeling hydraulics, sediment transport, water quality, waves, morphology and ecology. Figure 3.1 shows the Delft3D system architecture.

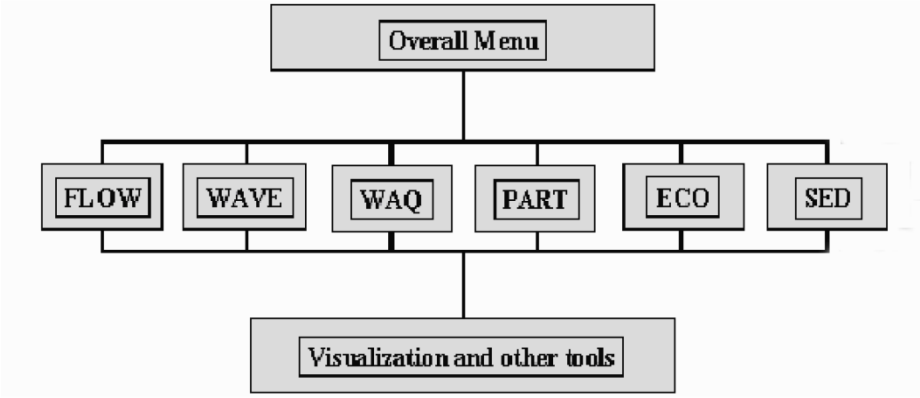


**Figure 3.1- Delft3D sub modules. (Deltares, 2011)**

While in this text the term Delft3D refers to Delft3D-FLOW, there are other sub modules of Delft3D which are able to model other phenomena. Other sub modules of Delft3D are:

| | |
|---|---|
| Delft3D-WAVE | short wave propagation |
| Delft3D-WAQ | far-field water quality |
| Delft3D-PART | mid-field water quality and particle tracking |
| Delft3D-ECO | ecological modelling |
| Delft3D-SED | cohesive and non-cohesive sediment transport |

### 3.4. Governing Equations

As mentioned earlier, CFD is numerical simulation of governing phenomena. It is important to realize what equations each model solves.

Delft3D is able to handle both Cartesian co-ordinates (ξ, η) and spherical co-ordinates (λ, φ). Transfer between Cartesian and spherical co-ordinates is done with

$$\xi = \lambda, \tag{3.1}$$

$$\eta = \phi, \tag{3.2}$$

$$\sqrt{G_{\xi\xi}} = R\cos\phi,$$

$$\sqrt{G_{\eta\eta}} = R,$$

(3.3)

(3.4)

where,

| | |
|---|---|
| λ | longitude |
| φ | latitude |
| R | Earth Radius |

Delft3D solves the Navier-Stokes equations for an incompressible fluid, under the shallow water and the Boussinesq assumptions. Vertical accelerations are neglected in the vertical momentum equation, which leads to the hydrostatic pressure equation. In 3D models the vertical velocities are calculated using continuity equation.

Delft3D uses orthogonal curvilinear co-ordinates. Both Cartesian and spherical coordinates are supported. In the vertical direction the model offers two different vertical boundary fitting systems: the σ-model and the Z-model.

### 3.4.1. Continuity

Continuity equation is written as:

$$\frac{\partial \zeta}{\partial t} + \frac{1}{\sqrt{G_{\xi\xi}}\sqrt{G_{\eta\eta}}} \frac{\partial \left[(d+\zeta)\, U \sqrt{G_{\eta\eta}}\right]}{\partial \xi} + \frac{1}{\sqrt{G_{\xi\xi}}\sqrt{G_{\eta\eta}}} \frac{\partial \left[(d+\zeta)\, V \sqrt{G_{\xi\xi}}\right]}{\partial \eta} = Q, \tag{3.5}$$

with Q representing the contributions per unit area due to the discharge or withdrawal of water, precipitation and evaporation

$$Q = H \int_{-1}^{0} (q_{in} - q_{out})\, d\sigma + P - E \tag{3.6}$$

with,

| | |
|---|---|
| $q_{in}$ | source of water per unit volume |
| $q_{out}$ | sink of water per unit volume |
| P | non-local source term of precipitation |
| E | non-local sink term due to evaporation |

### 3.4.2. Momentum

Equations of Momentum in ξ and η direction are written as:

$$\frac{\partial u}{\partial t}+\frac{u}{\sqrt{G_{\xi\xi}}}\frac{\partial u}{\partial \xi}+\frac{v}{\sqrt{G_{\eta\eta}}}\frac{\partial u}{\partial \eta}+\frac{\omega}{d+\zeta}\frac{\partial u}{\partial \sigma}-\frac{v^2}{\sqrt{G_{\xi\xi}}\sqrt{G_{\eta\eta}}}\frac{\partial \sqrt{G_{\eta\eta}}}{\partial \xi}+$$
$$+\frac{uv}{\sqrt{G_{\xi\xi}}\sqrt{G_{\eta\eta}}}\frac{\partial \sqrt{G_{\xi\xi}}}{\partial \eta}-fv=-\frac{1}{\rho_0\sqrt{G_{\xi\xi}}}P_\xi+F_\xi+$$
$$+\frac{1}{(d+\zeta)^2}\frac{\partial}{\partial \sigma}\left(\nu_V\frac{\partial u}{\partial \sigma}\right)+M_\xi, \tag{3.7}$$

and

$$\frac{\partial v}{\partial t}+\frac{u}{\sqrt{G_{\xi\xi}}}\frac{\partial v}{\partial \xi}+\frac{v}{\sqrt{G_{\eta\eta}}}\frac{\partial v}{\partial \eta}+\frac{\omega}{d+\zeta}\frac{\partial v}{\partial \sigma}+\frac{uv}{\sqrt{G_{\xi\xi}}\sqrt{G_{\eta\eta}}}\frac{\partial \sqrt{G_{\eta\eta}}}{\partial \xi}+$$
$$-\frac{u^2}{\sqrt{G_{\xi\xi}}\sqrt{G_{\eta\eta}}}\frac{\partial \sqrt{G_{\xi\xi}}}{\partial \eta}+fu=-\frac{1}{\rho_0\sqrt{G_{\eta\eta}}}P_\eta+F_\eta+$$
$$+\frac{1}{(d+\zeta)^2}\frac{\partial}{\partial \sigma}\left(\nu_V\frac{\partial v}{\partial \sigma}\right)+M_\eta. \tag{3.8}$$

### 3.4.3. Vertical Velocity

Delft3D calculates the vertical velocity ω from the continuity equation. Vertical velocity is given by

$$w=\omega+\frac{1}{\sqrt{G_{\xi\xi}}\sqrt{G_{\eta\eta}}}\left[u\sqrt{G_{\eta\eta}}\left(\sigma\frac{\partial H}{\partial \xi}+\frac{\partial \zeta}{\partial \xi}\right)+v\sqrt{G_{\xi\xi}}\left(\sigma\frac{\partial H}{\partial \eta}+\frac{\partial \zeta}{\partial \eta}\right)\right]+$$
$$+\left(\sigma\frac{\partial H}{\partial t}+\frac{\partial \zeta}{\partial t}\right). \tag{3.9}$$

### 3.4.4. Pressure

Delft3D takes Hydrostatic Pressure Assumption. Assuming shallow water, the pressure gradient is written as

$$\frac{\partial P}{\partial \sigma}=-g\rho H. \tag{3.10}$$

Therefore, the hydrostatic pressure can be written as

$$P=P_{atm}+gH\int_\sigma^0\rho\left(\xi,\eta,\sigma',t\right)d\sigma'.$$

(3.11)

Assuming Constant density all over the system, the pressure gradients in each direction will be calculated by

$$\frac{1}{\rho_0\sqrt{G_{\xi\xi}}}P_\xi = \frac{g}{\sqrt{G_{\xi\xi}}}\frac{\partial\zeta}{\partial\xi} + \frac{1}{\rho_0\sqrt{G_{\xi\xi}}}\frac{\partial P_{atm}}{\partial\xi}, \tag{3.12}$$

and

$$\frac{1}{\rho_0\sqrt{G_{\eta\eta}}}P_\eta = \frac{g}{\sqrt{G_{\eta\eta}}}\frac{\partial\zeta}{\partial\eta} + \frac{1}{\rho_0\sqrt{G_{\eta\eta}}}\frac{\partial P_{atm}}{\partial\eta}. \tag{3.13}$$

Density changes as salinity, sediment concentration and temperature vary. Therefore, the constant density assumption might not give precise enough results. Delft3D uses Leibniz rule and calculates pressure gradients by

$$\frac{1}{\rho_0\sqrt{G_{\xi\xi}}}P_\xi = \frac{g}{\sqrt{G_{\xi\xi}}}\frac{\partial\zeta}{\partial\xi} + g\frac{d+\zeta}{\rho_0\sqrt{G_{\xi\xi}}}\int_\sigma^0\left(\frac{\partial\rho}{\partial\xi} + \frac{\partial\rho}{\partial\sigma}\frac{\partial\sigma}{\partial\xi}\right)d\sigma' \tag{3.14}$$

and

$$\frac{1}{\rho_0\sqrt{G_{\eta\eta}}}P_\eta = \frac{g}{\sqrt{G_{\eta\eta}}}\frac{\partial\zeta}{\partial\eta} + g\frac{d+\zeta}{\rho_0\sqrt{G_{\eta\eta}}}\int_\sigma^0\left(\frac{\partial\rho}{\partial\eta} + \frac{\partial\rho}{\partial\sigma}\frac{\partial\sigma}{\partial\eta}\right)d\sigma' \tag{3.15}$$

### 3.4.5. Density

The first empirical equation to find water density based on temperature and salinity is developed by Eckart (1958). According to Deltares (2011) Eckart's formulation is only based on few measurements in 1910. Eckart equation is written as

$$\rho = \frac{1,000P_0}{\lambda + \alpha_0 P_0}, \tag{3.16}$$

with

t temperature (°C) [Range: 0 < t < 40 °C]

s salinity (ppt) [Range: 0 < s < 40 ppt]

and

$$\begin{aligned}\lambda &= 1779.5 + 11.25t - 0.0745t^2 - (3.80 + 0.01t)\, s,\\ \alpha_0 &= 0.6980,\\ P_0 &= 5890 + 38t - 0.375t^2 + 3s.\end{aligned}$$

Eckart equation fails to give the maximum density at temperature of 4 °C. Since this temperature is critical in lake modeling Delft3D uses UNESCO formulation as default. The UNESCO formulation (UNESCO, 1981) is written as:

$$\rho = \rho_0 + As + Bs^{3/2} + Cs^2 \tag{3.17}$$

with

t temperature (°C) [Range: 0 < t < 40 °C]

s salinity (ppt) [Range: 0.5 < s < 43 ppt]

and

$$\begin{aligned}\rho_0 &= 999.842594 + 6.793952 \cdot 10^{-2} t - 9.095290 \cdot 10^{-3} t^2 +\\ &\quad + 1.001685 \cdot 10^{-4} t^3 - 1.120083 \cdot 10^{-6} t^4 + 6.536332 \cdot 10^{-9} t^5\\ A &= 8.24493 \cdot 10^{-1} - 4.0899 \cdot 10^{-3} t + 7.6438 \cdot 10^{-5} t^2 +\\ &\quad - 8.2467 \cdot 10^{-7} t^3 + 5.3875 \cdot 10^{-9} t^4\\ B &= -5.72466 \cdot 10^{-3} + 1.0227 \cdot 10^{-4} t - 1.6546 \cdot 10^{-6} t^2\\ C &= 4.8314 \cdot 10^{-4}\end{aligned}$$

Unlike Eckart, UNESCO formulation is more accurate and does give the maximum density at 4 °C. The user can switch between Eckart and UNESCO formulations. However; Deltares recommends use of UNESCO formulation (Deltares 2011).

### 3.4.6. Transport

In Delft3D, Transport is modeled with advection-diffusion equation in three co-ordinate directions which include source and sink terms. Moreover, first-order decay procedures may be taken into account. A first-order decay process exponentially decreases. Delft3D uses the following equation to model transport

$$\frac{\partial (d+\zeta)\, c}{\partial t} + \frac{1}{\sqrt{G_{\xi\xi}}\sqrt{G_{\eta\eta}}} \left\{ \frac{\partial \left[\sqrt{G_{\eta\eta}}\,(d+\zeta)\, uc\right]}{\partial \xi} + \frac{\partial \left[\sqrt{G_{\xi\xi}}\,(d+\zeta)\, vc\right]}{\partial \eta} \right\} + \frac{\partial \omega c}{\partial \sigma} =$$
$$\frac{d+\zeta}{\sqrt{G_{\xi\xi}}\sqrt{G_{\eta\eta}}} \left\{ \frac{\partial}{\partial \xi} \left( D_H \frac{\sqrt{G_{\eta\eta}}}{\sqrt{G_{\xi\xi}}} \frac{\partial c}{\partial \xi} \right) + \frac{\partial}{\partial \eta} \left( D_H \frac{\sqrt{G_{\xi\xi}}}{\sqrt{G_{\eta\eta}}} \frac{\partial c}{\partial \eta} \right) \right\} +$$
$$+ \frac{1}{d+\zeta} \frac{\partial}{\partial \sigma} \left( D_V \frac{\partial c}{\partial \sigma} \right) - \lambda_d\, (d+\zeta)\, c + S, \qquad (3.18)$$

with

| | |
|---|---|
| $D_H$ | Horizontal Diffusion Coefficient |
| $D_V$ | Vertical Diffusion Coefficient |
| $\lambda_d$ | representing first order decay process |
| S | source/sink term per unit area due to discharge/withdrawal |

# 4. MODEL SETUP, TESTING, CALIBRATION AND VALIDATION

## 4.1.Model Setup

After selecting a program to solve governing equations, one has to setup a model for the case of study. First, the area of study has to be chosen. Then, bathymetry and topography data need to be obtained (e.g. from National Geophysics Data Center). Later, a mesh has to be generated to cover the study area and the boundaries have to be declared. This whole procedure is called pre-processing.

### 4.1.1. Study Area

An area of study containing all areas of interest was selected. The domain contains lakes Maurepas, Pontchartrain, St Katherine and Borgne plus parts of the Gulf of Mexico. Figure 4.1 shows the area of study picked to generate the grid on.

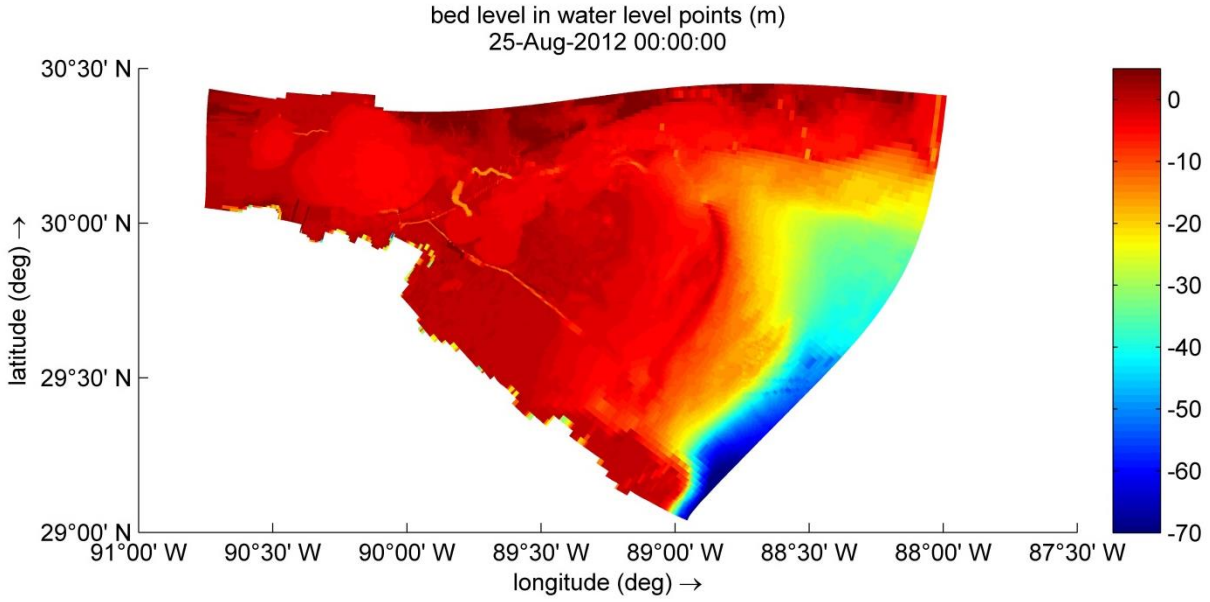


**Figure 4.1- Bathymetry of the computational domain**

### 4.1.2. Mesh Generation

Mesh was generated in RFGRID, Deltares's grid generation tool. As mentioned earlier, Delft3D uses structured orthogonal curvilinear grid system. The mesh was refined in required areas, such as connecting passes to be able to cover such locations. Figure 4.2 shows a view of the computational grid. Delft3D uses *m*, *n* and *k* notations to address each node in ξ, η and σ coordinates respectively.

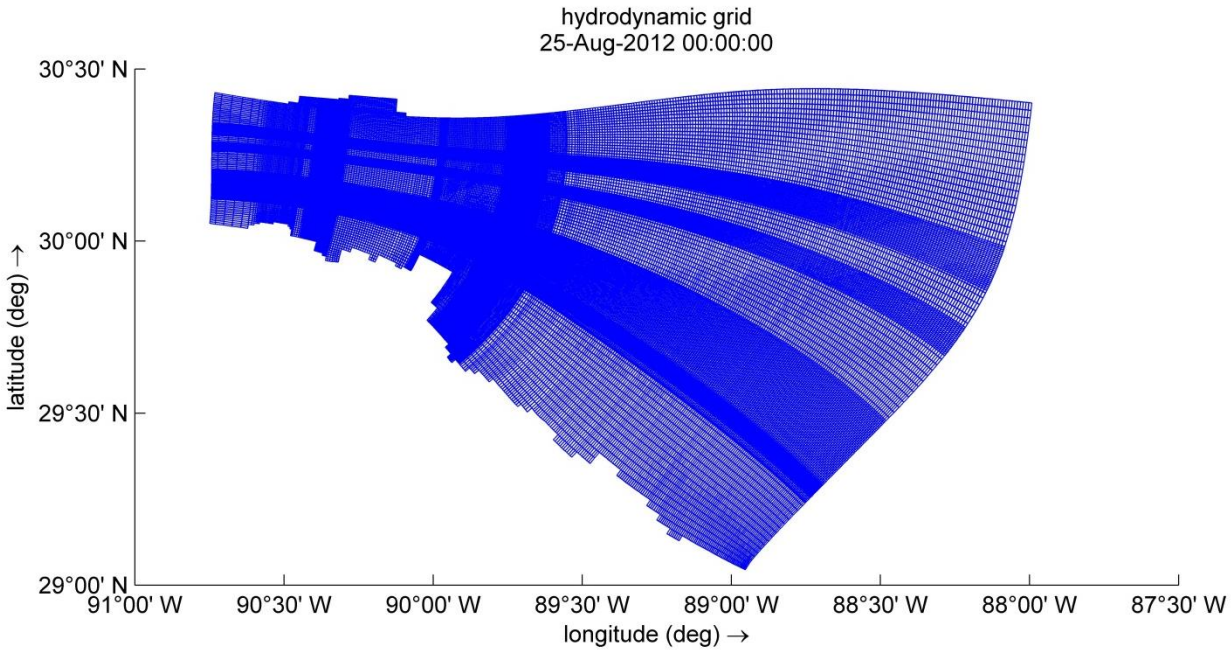


**Figure 4.2- Hydrodynamic grid covering the area**

### 4.1.3. Open Boundary

The eastern edge of the model is defined as open boundary. Time series of Water level is prescribed on the open boundary by the user. The water level data was obtained from United States Geological Survey. As a requirement, salinity concentrations must be defined at the boundary. Open boundary salinity concentrations were obtained from Lake Pontchartrain Basin Foundation weekly maps. For normal conditions, the water level values from USGS Gulfport light station (30°15'16"N, 88°52'08"W) was applied all over the open boundary.

### 4.1.4. Bathymetry

The bathymetry was obtained from National Geophysics Data Center with an original resolution of 30 meters. The original bathymetry was in ESRI grid format. Therefore, a FORTRAN code was written to convert the bathymetry to Longitude, Latitude, and Elevation. In order to ease the bathymetric interpolation to the grid, the data was later thinned. Delft3D Quickin offers 5 different methods for bathymetry interpolation including: Average Value of Near Points, Value of Closest Point, Maximum Value of Near Points, Minimum Value of Near Points and Shepard. The Shepard method is a weighted average method which is defined as:

$$\bar{s} = \frac{\sum_{i=1}^{N} \frac{s_i}{d_i^2}}{\sum_{i=1}^{N} \frac{1}{d_i^2}} \tag{4.1}$$

Where

| | |
|---|---|
| $\bar{s}$ | Averaged value |
| N | number of samples within the polygon |
| $d_i$ | distance between grid point and sample point i |
| $s_i$ | value of sample point i |

The bathymetry from National Geophysics Data Center did not contain the Flood Protection levees. Therefore, they were added manually by drawing polygons and changing the depth. Levee maps were obtained from Corps of Engineers (USACE, 2012).

### 4.1.5. Roughness

Delft3D offers four options of roughness input including Chézy, Manning, Z0 and White-Colebrook. It is up to the modeler which method to select. However, the model calculations are fundamentally based on Chézy. Therefore, the model converts any other friction factor to Chézy C.

According to Delft3D manual, if the input roughness is in Manning's, the Chézy conveyance will be calculated from

$$C = \frac{H^{1/6}}{n} \tag{4.2}$$

With

| | |
|---|---|
| H | water depth [m] |
| n | Manning's n [$s/m^{1/3}$] |

Since using Manning's n is more commonly used in the United States, the roughness was set in Manning's form. Table 4.1 shows Manning's n values used in the model.

| Area | Manning's n [$s/m^{1/3}$] |
|---|---|
| Lakes and the Gulf | 0.02 |
| Marsh | 0.1 |
| Passes | 0.015-0.02 |

**Table 4.1-Manning's n values used for each area**

The values from table 4.1 was interpolated into the grid and exported as depth values in Delft3D Quickin. However, since the model requires 2 roughness values for both η and ξ directions, it was required to duplicate the output file, and then save it under an *"rgh"* extension which is what the model reads.

### 4.1.6. Vertical Grid

Nine vertical sigma layers (10 sigma levels) were used. Since the model had wind module on, the layers distributed double parabolically with high resolution given to surface and bottom. Figure 4.3 shows percentage share of each layer deep inside the water column.

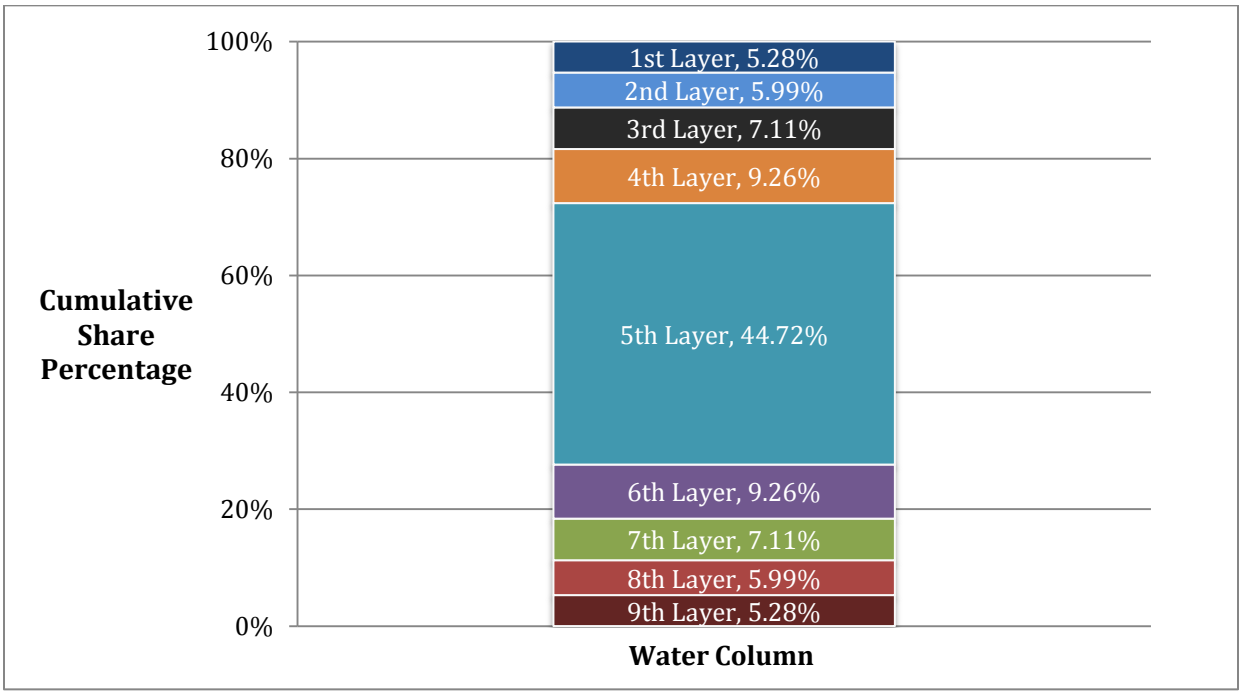


**Figure 4.3- Distribution of layers in the water column**

### 4.1.7. Initial Conditions

In order to get the proper salinity distribution in the model to start with, propagation simulations have to be run. Starting with zero salinity everywhere makes the propagation slow leading it to take months to reach equilibrium; Figure 2.11 from Georgiou et al. can be used to get an initial condition to speed up the response. Delft3D can use both uniform and spatially varied initial conditions as well as reading a restart file. The initial conditions file is a typical ASCII file with an *"ini"* extension containing the required information in a gridded format. The information order is follows:

- water level at all nodes
- u velocity at all nodes in layer 1
- u velocity at all nodes in layer 2

  .

  .
- u velocity at all nodes in layer 9
- v velocity at all nodes in layer 1
- v velocity at all nodes in layer 2

  .

  .
- v velocity at all nodes in layer 9
- salinity at all nodes in layer 1
- salinity at all nodes in layer 2

  .

  .
- salinity at all nodes in layer 9

Table 4.3 contains initial salinities that the model was started with at the first place.

| Area | Salinity (ppt) |
|---|---|
| Lake Maurepas | 0 |
| Lake Pontchartrain | 5 |
| Lake Borgne | 10 |
| Gulf of Mexico | 20 |

**Table 4.2- Initial salinity values used to start the propagation run**

After running a few months with initial salinities of Table 4.2, the salinity was propagated well enough to save a hot start. Unlike the initial conditions file, the restart file is a binary file which is an output of a previous run. The hot start was then used for major salinity runs. Figure 4.4 shows the surface salinity in hot start.

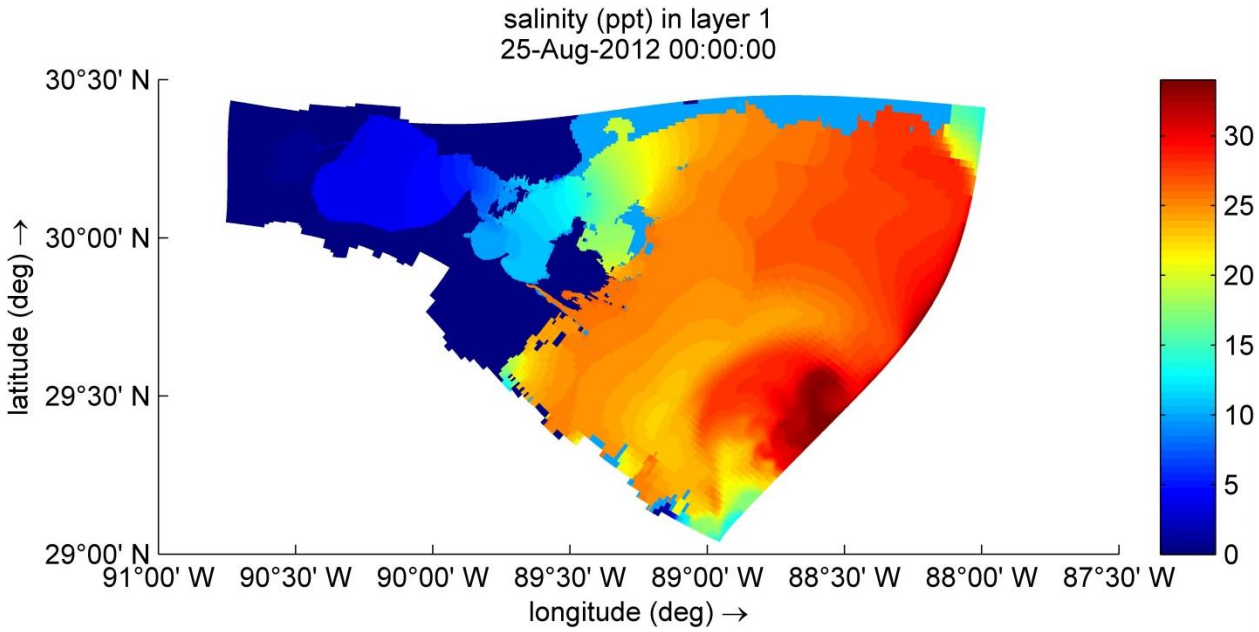


**Figure 4.4- Surface Salinity used from 'hot start'**

### 4.1.8. River Discharges

There are major 12 tributaries discharging to the system. Tributaries discharge freshwater to the systems which play a big role in salinity distribution. The river discharges were obtained from United States Geological Survey (http://waterdata.usgs.gov). It is important to know that during a hurricane surge, there can be no river discharge or even reverse discharge. For salinity calculation purposes, the salinity of 0.2 ppt was assigned to all rivers. The tributaries are listed in Appendix II.

### 4.1.9. Wind data

Wind plays a major role in storm surge modeling. It is essential to consider winds while modeling a hurricane. Delft3D can run with constant winds as well as spatially variable winds. In this research wind data is obtained from New Canal Station of NOAA (http://tidesandcurrents.noaa.gov).

## 4.2.Model testing and Calibration

After the mesh was generated and the model was set up, several tests were made to make sure the model works alright. Most of these tests were run to verify axiomatic facts such as having bounded solutions and development of two-gyre pattern. A set of the tests are given below

### 4.2.1. Step function

There are several tests a modeler can conduct to indicate that the model is working correctly in terms of Conservation and Boundedness. One test is to run a few days with some constant water level prescribed at the open boundary, and then impose a step for a few more days. After a few days, the water level should asymptotically reach the step level everywhere in the model. If this test fails, it indicates that there might be some unwanted flow going out of the system. In this study case, the model was run for 15 days with a water level of zero at the open boundary then imposing a step of 1m for the next 15 days. Water level in Lake Maurepas, New Canal Station in Lake Pontchartrain, Shell beach at Lake Borgne and Bay St Louis are plotted in Figure 4.5. As seen in Figure 4.5, all location asymptotically reach a water level of 1 meter.

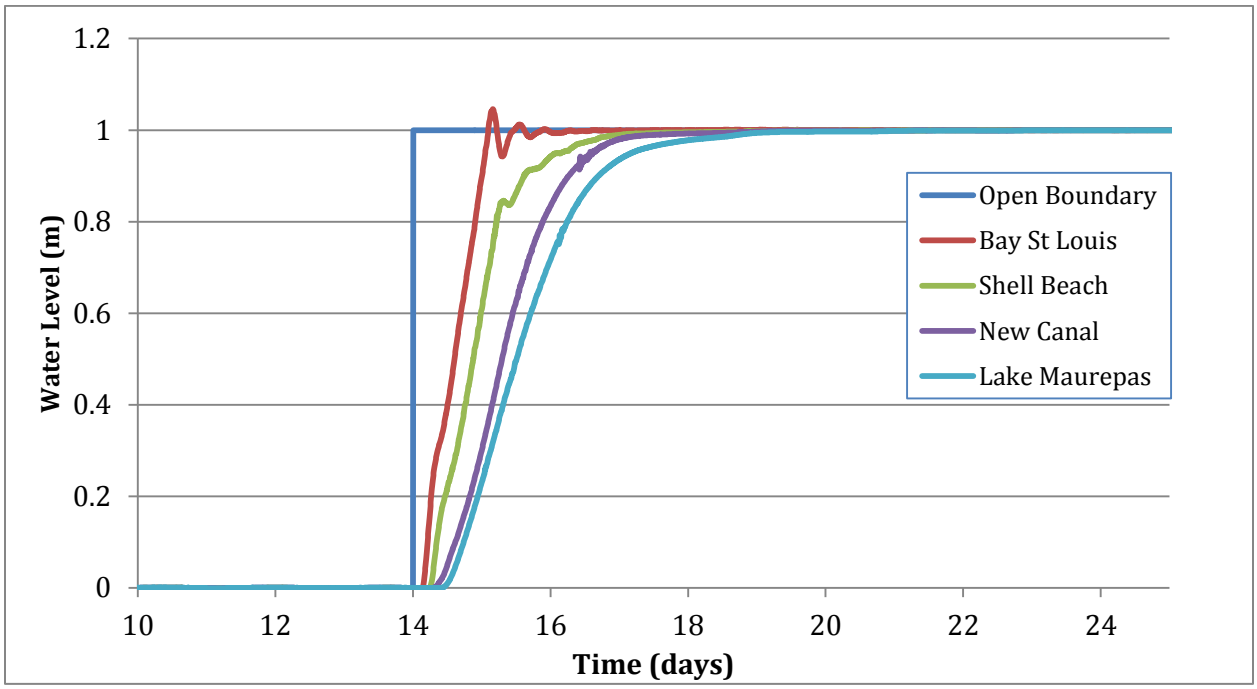


**Figure 4.5- Water level for step test**

### 4.2.2. Flow through the Passes

Another important determining factor to realize whether or not the model is working fine is flow in 3 key passes, Pass Manchac, the Rigolets and Chef Menteur Pass. Since an equivalent channel was used to represent Chef Menteur (to avoid stair-stepping), it was required to make sure it is handling the correct flow.

Several tests were done to finally get the correct amount of flow through the Passes. The flow calibration was done by fine tuning Manning's n. Table 4.3 compares measured and modeled flows at selected passes.

| Channel Name | Pass Manchac | Rigolets | Chef Menteur Pass |
|---|---|---|---|
| Measured Flow ($ft^3/s$) | 35,000 | 180,000 | 85,000 |
| Modeled Flow ($ft^3/s$) | 38,000 | 179,000 | 89,000 |

**Table 4.3- Modeled and Measured flow in Pass Manchach, Rigolets and Chef Menteur Pass. Measured data source: (Georgiou et al,2009)**

### 4.2.3. Circulation Test

Wind is a major factor in a hurricane, in fact it is the only factor to determine hurricane category in Saphir and Simpson classification. A powerful Storm surge model has to successfully pass wind circulation test(s). The test was as follows: 5 m/s constant southeast winds were applied over the estuary for several days. The drag coefficient was adjusted until the circulation patterns became consistent with findings of Haralampides (2002) and Chilmakuri (2005). Figure 4.6 shows normalized depth averaged velocity vectors developed after a few days of 5 m/s southeast winds. As shown in Figure 4.6, the typical anticipated two-gyre pattern is developed in Delft3D as predicted by Haralampides (2000), Georgiou (2002) and Chilmakuri (2005)

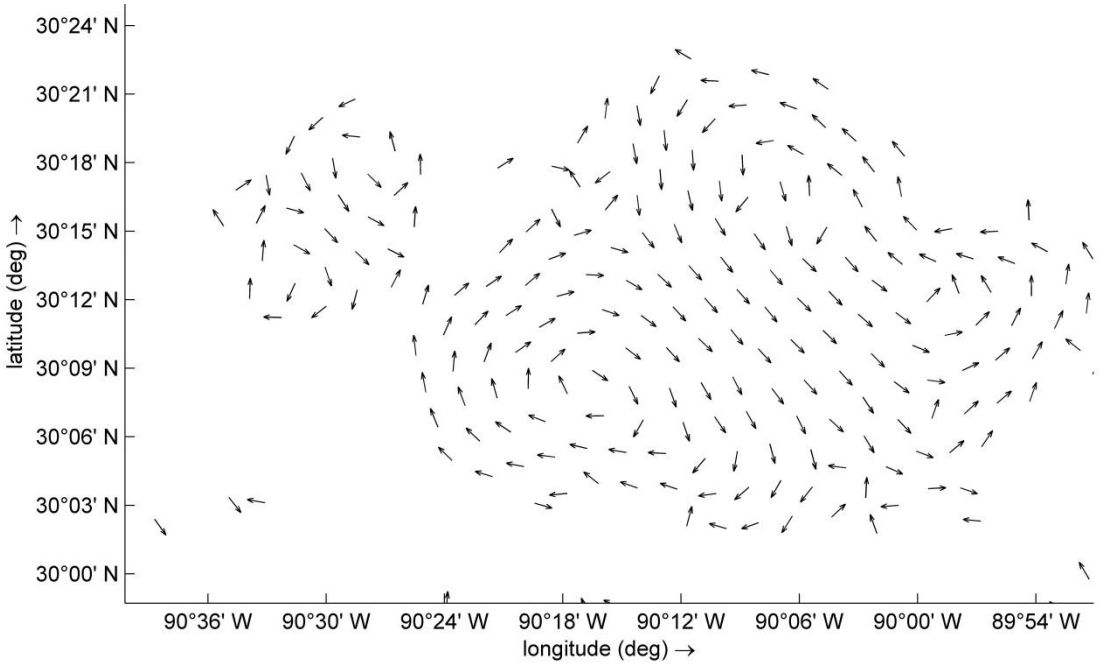


**Figure 4.6- Normalized depth averaged velocity vectors developed by 5m/s Southeast winds**

## 4.3.Calibration and Validation

### 4.3.1. Regular Conditions

The model was calibrated for period of September 4th 2013 to September 18th 2013 and validated for the period of August-September 2012. Figures 4.17-4.15 contain water level plots of the Calibration period.

## Shell Beach

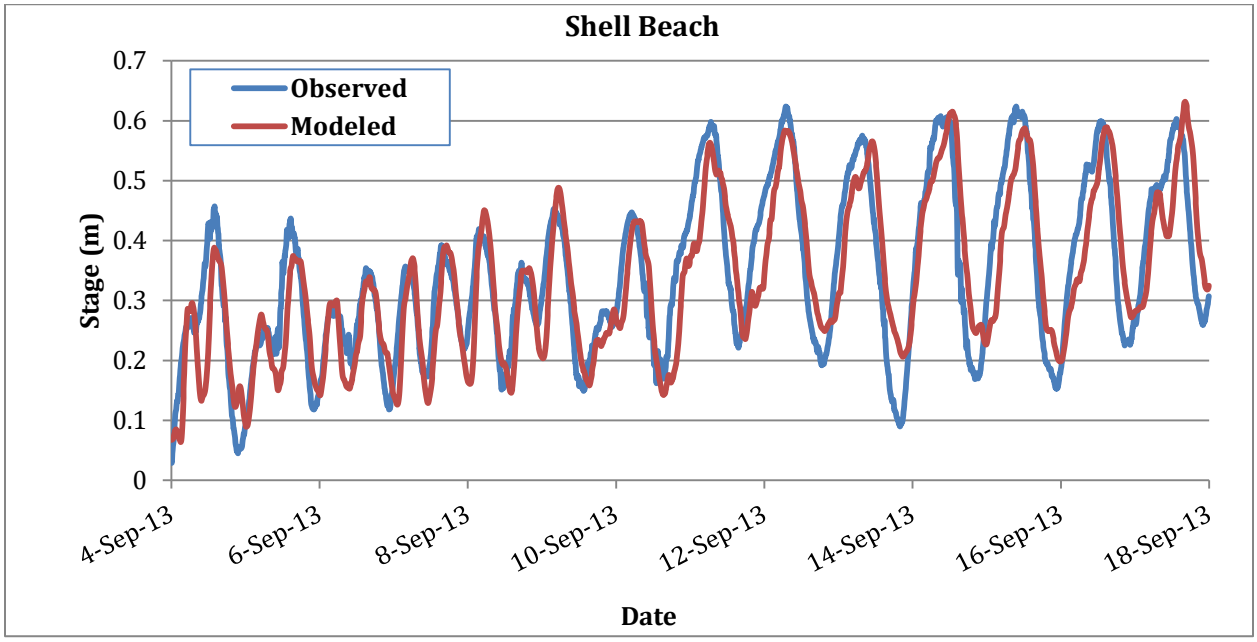


**Figure 4.7- Shell Beach Water Level Calibration 9/4/13-9/18/13 (Observed Source: NOAA, 2013)**

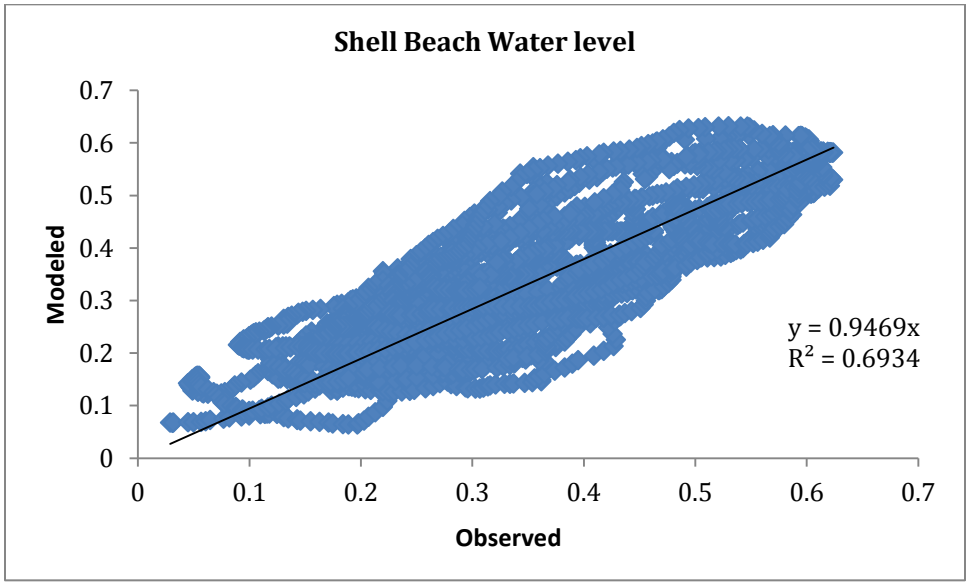


**Figure 4.8- Shell Beach Bias error calculation 9/4/13-9/18/13 (Observed Source: NOAA, 2013)**

| Shell Beach 9/4/2013-9/18/2013 | | |
|---|---|---|
| Bias based on Slope | Surge Bias (m) | $R^2$ |
| 5.3% under predicting | -0.01 | 0.69 |

**Table 4.4- Error Calculation for Shell Beach 9/4/2013-9/18/2013**

## New Canal

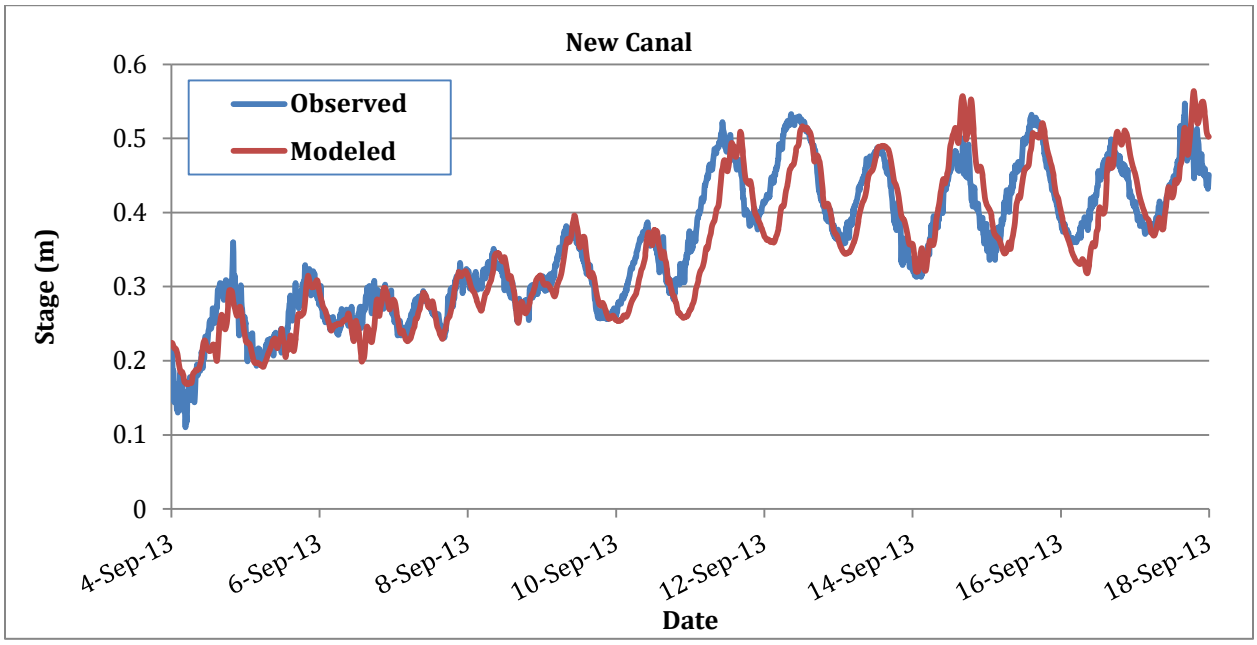


**Figure 4.9- New Canal Water Level Calibration 9/4/13-9/18/13 (Observed Source: NOAA, 2013)**

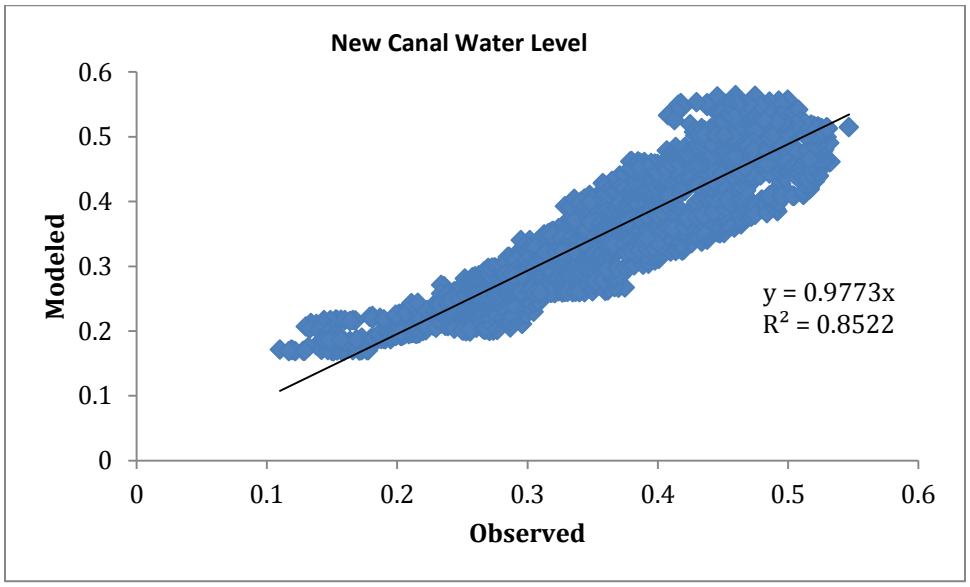


**Figure 4.10- New Canal Bias error calculation 9/4/13-9/18/13 (Observed Source: NOAA, 2013)**

| New Canal 9/4/2013-9/18/2013 | | |
|---|---|---|
| Bias based on Slope | Surge Bias (m) | $R^2$ |
| 2.3% under predicting | -0.008 | 0.85 |

**Table 4.5- Error Calculation for New Canal 9/4/2013-9/18/2013**

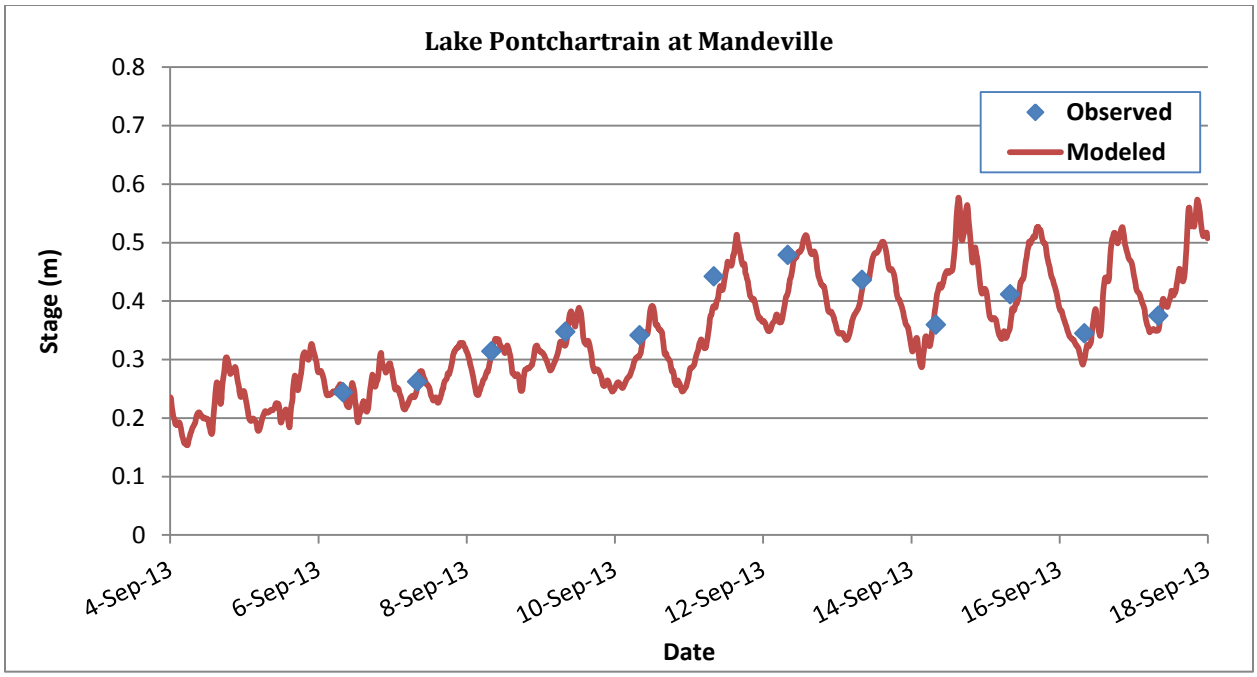


**Figure 4.11-Mandeville Water Level Calibration 9/4/13-9/18/13 (Observed Source: USACE, 2013)**

## Joseph Island

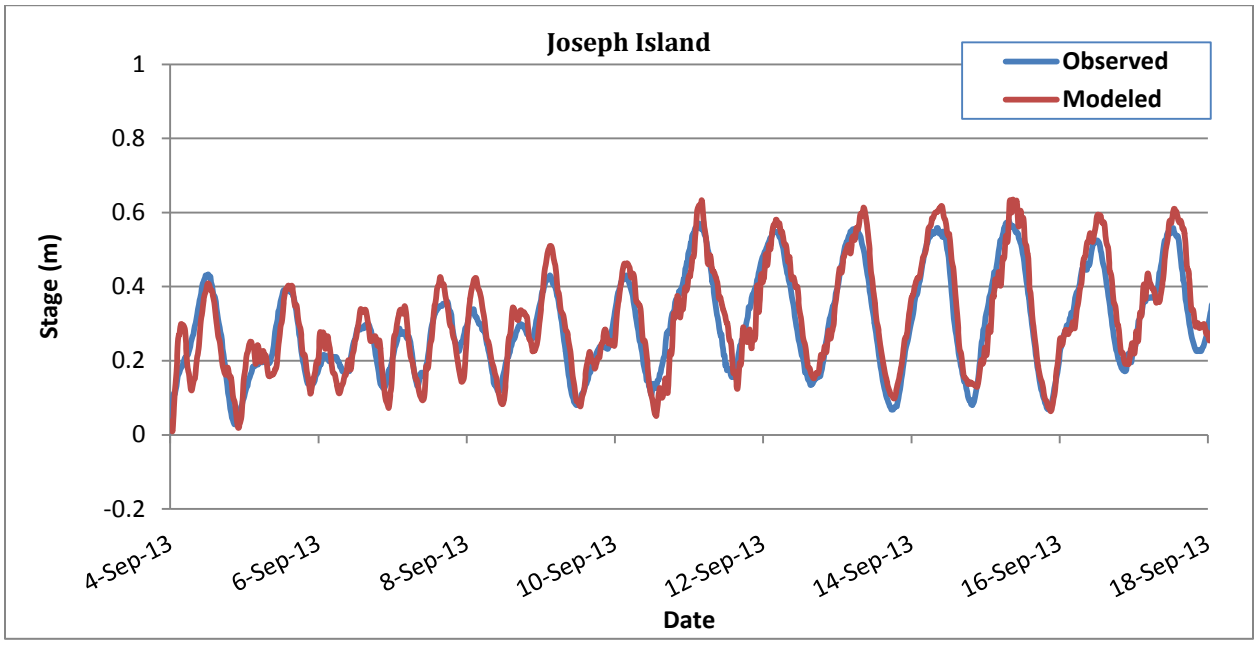


**Figure 4.12- Joseph Island Water Level Calibration 9/4/13-9/18/13 (Observed Source: USGS, 2013)**

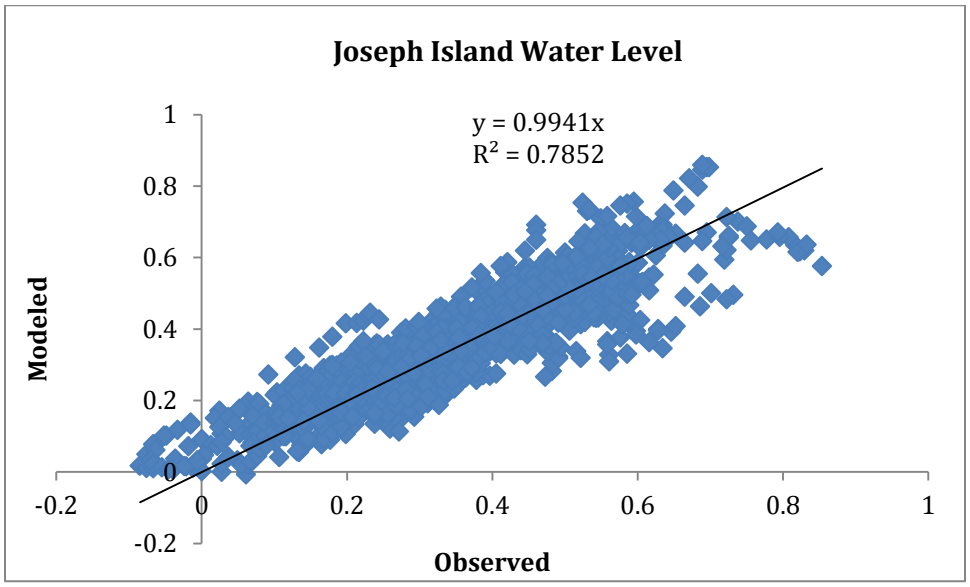


**Figure 4.13- Joseph Island Bias error calculation 9/4/13-9/18/13 (Observed Source: USGS, 2013)**

| Joseph Island 9/4/2013-9/18/2013 | | |
|---|---|---|
| Bias based on Slope | Surge Bias (m) | $R^2$ |
| 0.6% under predicting | 0.008 | 0.79 |

**Table 4.6- Error Calculation for Joseph Island 9/4/2013-9/18/2013**

## Biloxi Bay

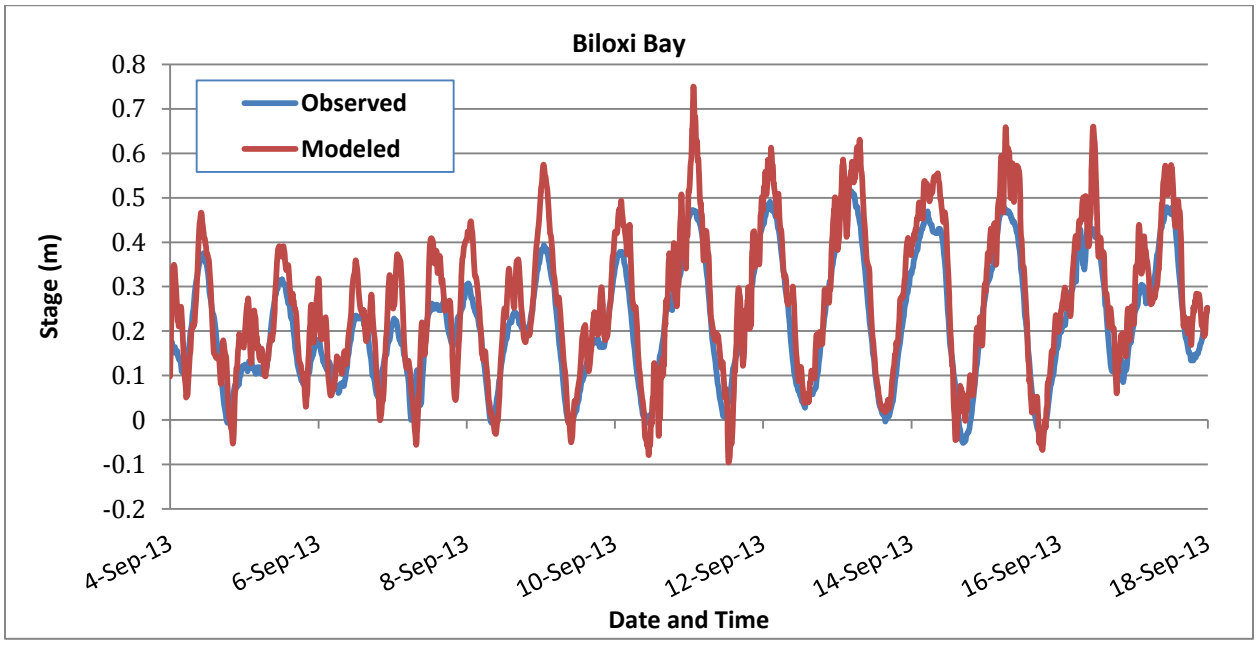


**Figure 4.14- Biloxi Bay Water Level Calibration 9/4/13-9/18/13 (Observed Source: USGS, 2013)**

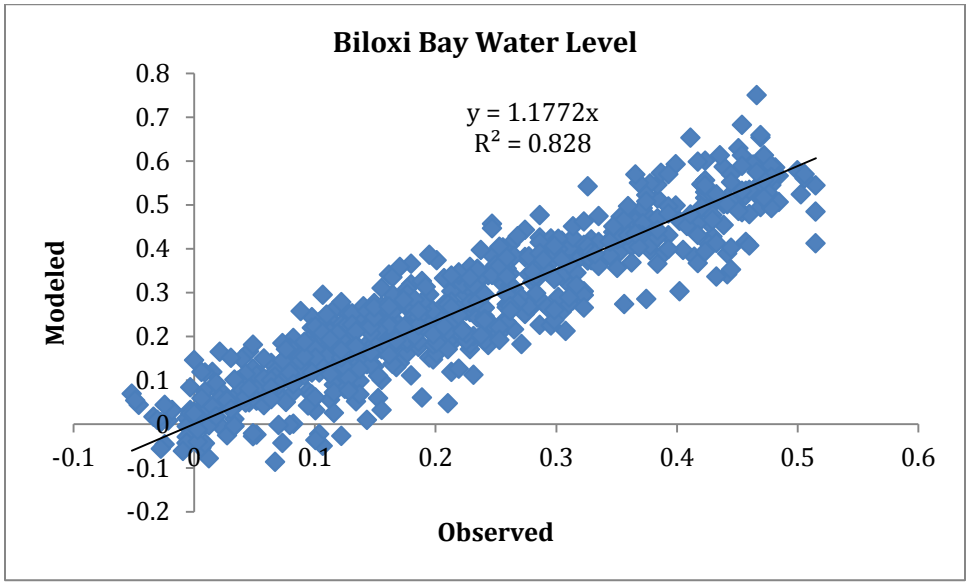


**Figure 4.15- Biloxi Bay Bias error calculation 9/4/13-9/18/13 (Observed Source: USGS, 2013)**

| Biloxi Bay 9/4/2013-9/18/2013 | | |
|---|---|---|
| Bias based on Slope | Surge Bias (m) | $R^2$ |
| 17.7% over predicting | 0.046 | 0.83 |

**Table 4.7- Error Calculation for Biloxi Bay 9/4/2013-9/18/2013**

### 4.3.2. Event of a Hurricane

As a test, the category one hurricane Isaac was chosen. The calibrated model was run for the period of 8/25/2012 to 9/25/2012. Water level and maximum salinity in various locations were plotted against observed data. Observations were obtained from COE, USGS, NOAA and CPRA. In some stations specific conductivity at 25°C was converted to salinity. The conversion can be done using the following empirical formula (Wagner, Boulger, Oblinger, & Smith, 2006):

$$S = K_1 + (K_2 \times R^{1/2}) + (K_3 \times R) + (K_4 \times R^{3/2}) + (K_5 \times R^2) + (K_6 \times R^{5/2}), \quad (4.3)$$

where,

$K_1$=0.0120,
$K_2$=-0.2174,
$K_3$=25.3283,
$K_4$=13.7714,
$K_5$=-6.4788,
$K_4$=2.5842.

The variable R equals to specific conductance at 25 °C divided by 53.087 milli-siemens per centimeter. If water salinity is 35 ppt and temperature is 25 °C the specific conductivity is 53.087 milli-siemens per centimeter.

#### 4.3.2.1. Open Boundary Conditions

Since it is required to provide the boundary condition at the open boundary, water level time series were gained from United States Geological Survey. USGS Gulfport light station at co-ordinates 30°19'07" N and 88°58'20"W is used for near north edge of the open boundary (Boundary **A** in figure 4.16). For the south edge of the open boundary (Boundary **C** in figure 4.16), water level time series were obtained from USGS Bay Gardene station located at 29°35'08.7"N and 89°36'21.5W. Average of water level in **A** and **C** was used for Boundary **B** during hurricane conditions, whereas maximum water level of **A** and **B** was used at **C** before and after storm (see Figure 4.17).

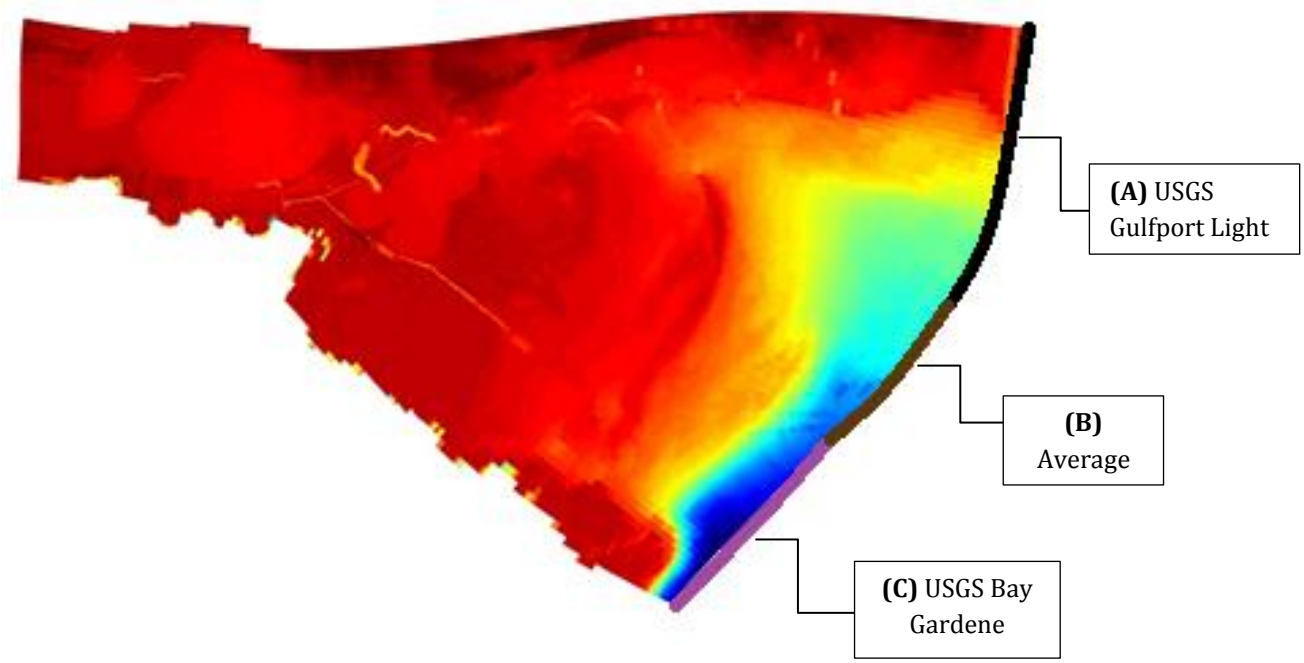


**Figure 4.16- Stations used to obtain water level time series at the open boundary**

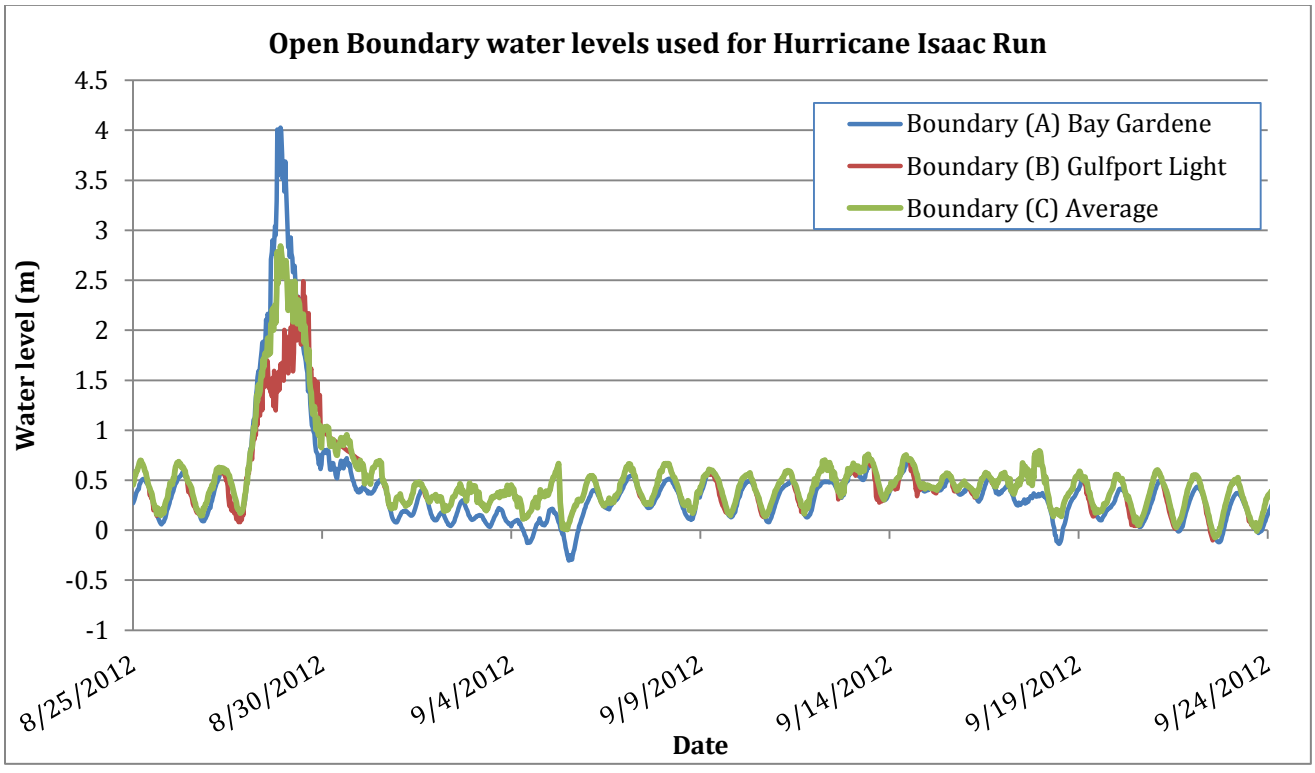


**Figure 4.17- Open Boundary water levels used for Hurricane Isaac run (USGS, 2012)**

#### 4.3.2.2. River flows

Freshwater discharge is a balancing component in salinity distribution over the estuary. Under or overestimated freshwater discharge in the model will results to uncertainties in model results. Furthermore, rivers in the estuary have been found to have no or even reverse flow during hurricane surges.

River discharges were obtained from available USGS stations (http://waterdata.usgs.gov). There was enormous amount of freshwater flow right after the storm in case of Isaac. For rivers with unavailable discharge data, the hydrograph from the most similar river in terms of drainage area was used. Moreover, it is assumed the rivers won't discharge if the water level is above 1 meter in their mouths.

#### 4.3.2.3. Winds

Wind data were obtained from NOAA new canal station (30° 1.6'N, 90° 6.8'W). It is assumed that winds are constant in space. For a more accurate simulation, it is suggested to use spatially varied winds. In case of Isaac however, since the radius of the hurricane was considerably long, spatially constant wind seems like a reasonable assumption. Figure 4.18 Shows wind data used in the model (NOAA, 2013).

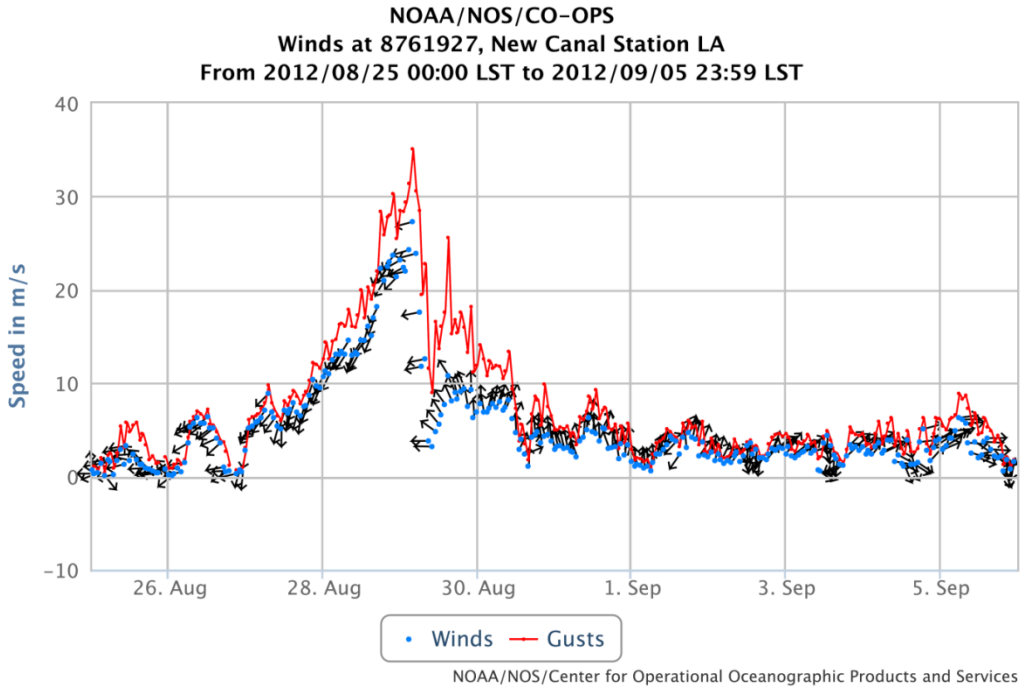


**Figure 4.18- Wind data used for hurricane Isaac Run (NOAA, 2013)**

#### 4.3.2.4. Model results

There are several locations of interest. Water level and salinity results have to be compared to field data. Figures 4.20 to 4.26 contain some water level validation of the model results. Water level validation and error calculation were done in the following Stations

- Bay St. Louis, MS (NOAA, 30° 19.5' N, 89° 19.5' W)
- Shell Beach, LA (NOAA, 29° 52.0' N, 89° 40.3' W)
- New Canal, LA (NOAA, 30° 1.6' N, 90° 6.8' W)
- Joseph Island, MS (USGS, 30°11'27" N, 89°25'20" W)

Water level map at August 30th 2012 9:00 AM is shown in Figure 4.19

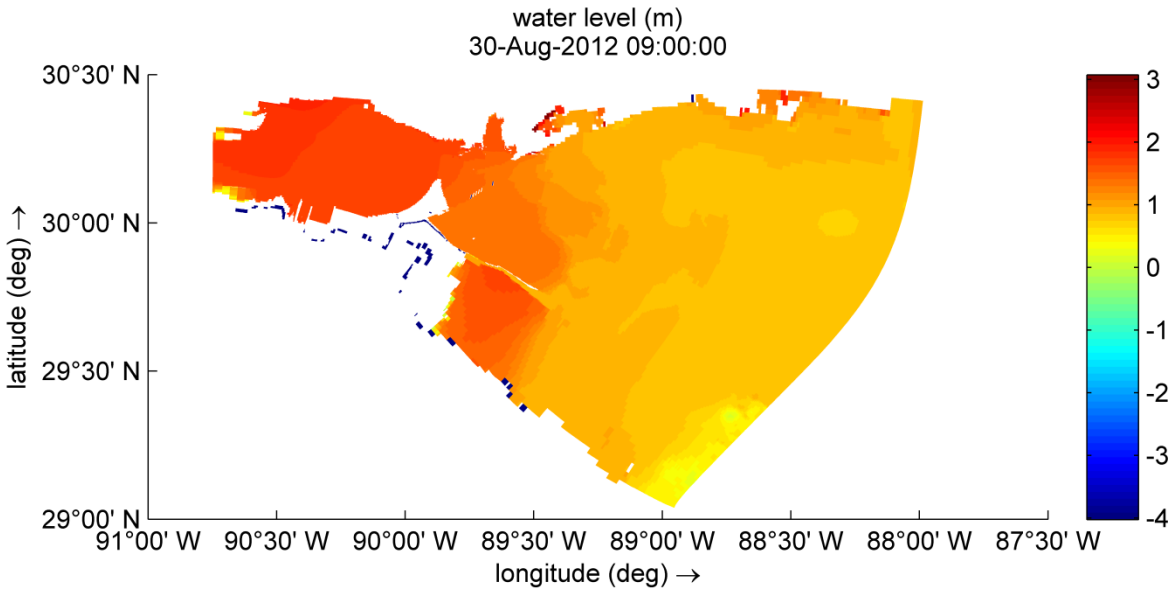


**Figure 4.19- Water level as of 8/25/2012 9:00AM**

**Bay St Louis**

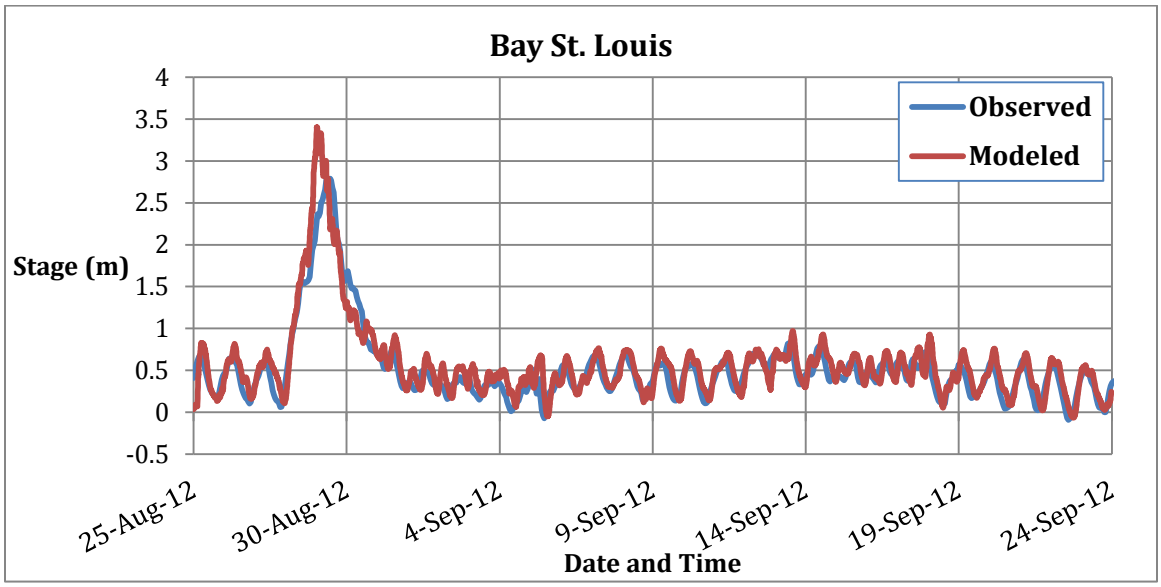


**Figure 4.20- Hurricane Isaac water level validation for Bay St Louis (Observed Source: NOAA, 2012)**

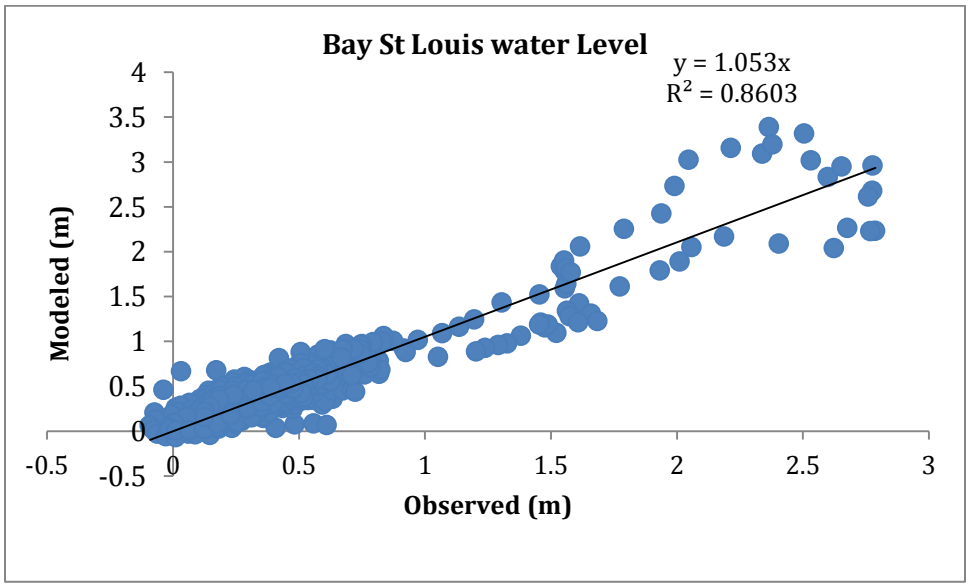


**Figure 4.21- Bias error calculation for Bay St. Louis water level during Isaac (Observed Source: NOAA, 2012)**

| Bay St Louis 8/25/2012-9/25/2011 | | |
|---|---|---|
| Bias based on Slope | Surge Bias (m) | $R^2$ |
| 5.3% over predicting | 0.055 | 0.86 |

**Table 4.8- Calculated errors for Bay St. Louis water level during Isaac**

**Shell Beach**

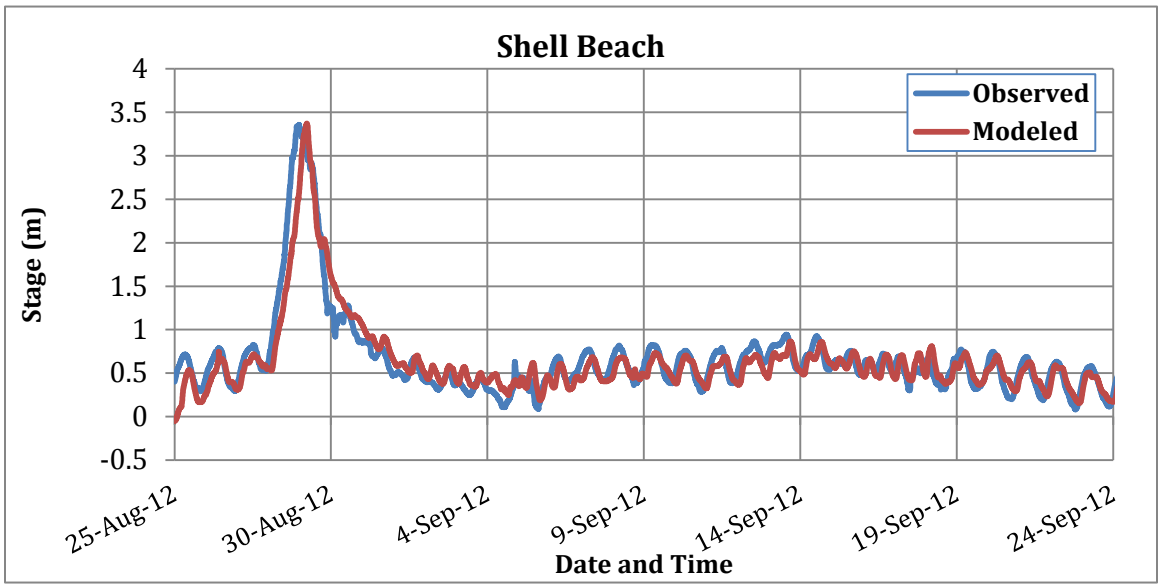


**Figure 4.22-Hurricane Isaac water level validation for Shell Beach (Observed Source: NOAA, 2012)**

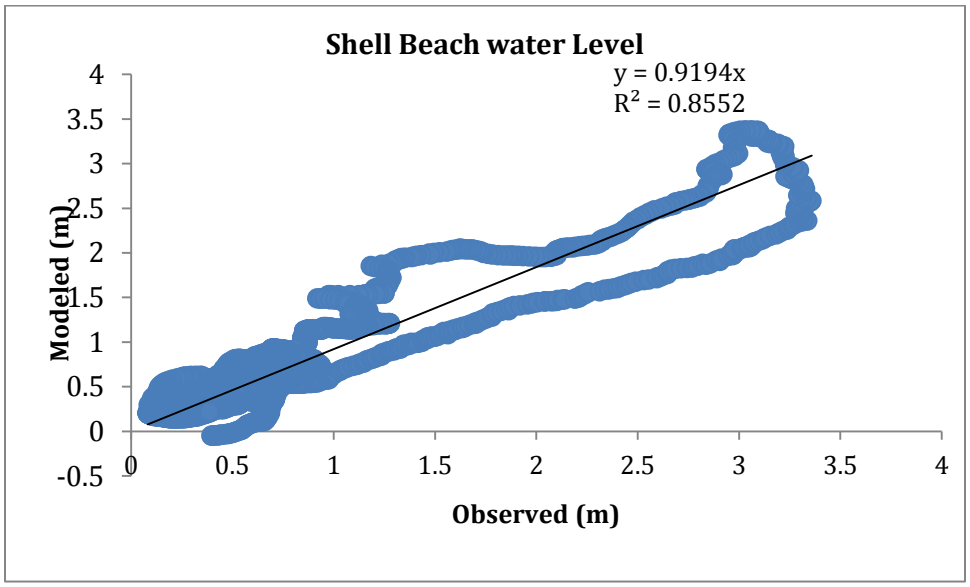


**Figure 4.23-Bias error calculation for Shell Beach water level during Isaac (Observed Source: NOAA, 2012)**

| Shell Beach 8/25/2012-9/25/2011 | | |
|---|---|---|
| Bias based on Slope | Surge Bias (m) | $R^2$ |
| 8.1% under predicting | -0.024 | 0.86 |

**Table 4.9-Calculated errors for Shell Beach water level during Isaac**

**New Canal**

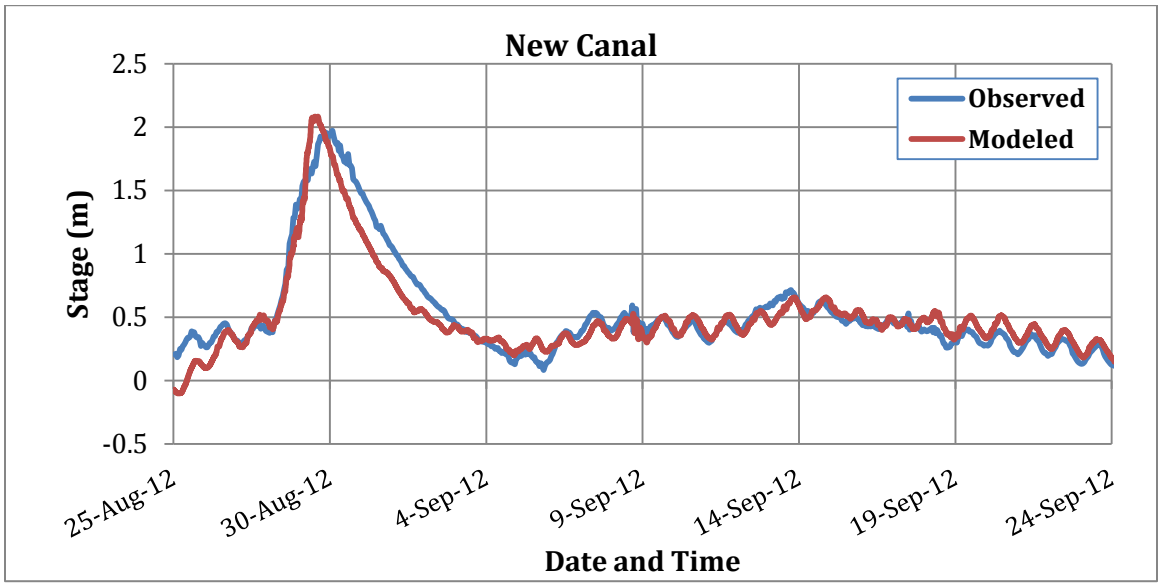


**Figure 4.24-Hurricane Isaac water level validation for New Canal (Observed Source: NOAA, 2012)**

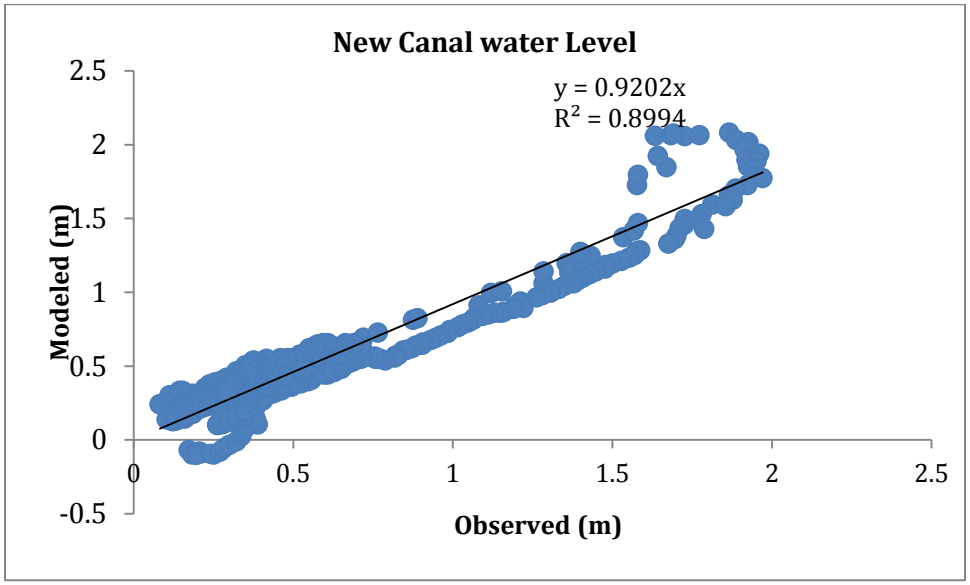


**Figure 4.25-Bias error calculation for New Canal water level during Isaac (Observed Source: NOAA, 2012)**

| New Canal 8/25/2012-9/25/2011 | | |
|---|---|---|
| Bias based on Slope | Surge Bias (m) | $R^2$ |
| 8% under predicting | -0.023 | 0.9 |

**Table 4.10-Calculated errors for New Canal water level during Isaac**

## Joseph Island

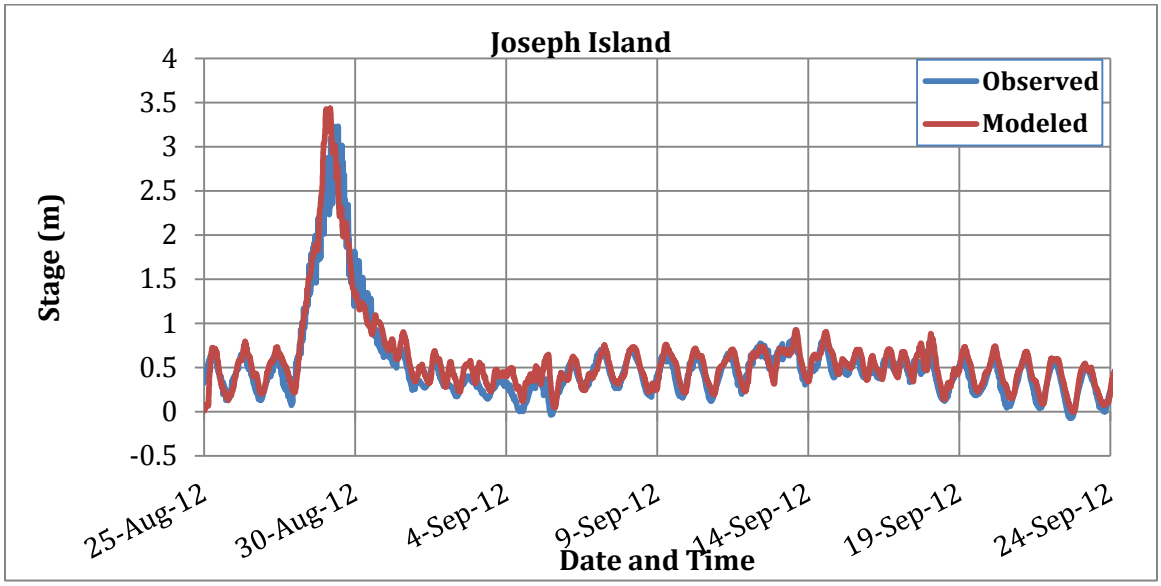


**Figure 4.26-Hurricane Isaac water level validation for Joseph Island (USGS, 2012)**

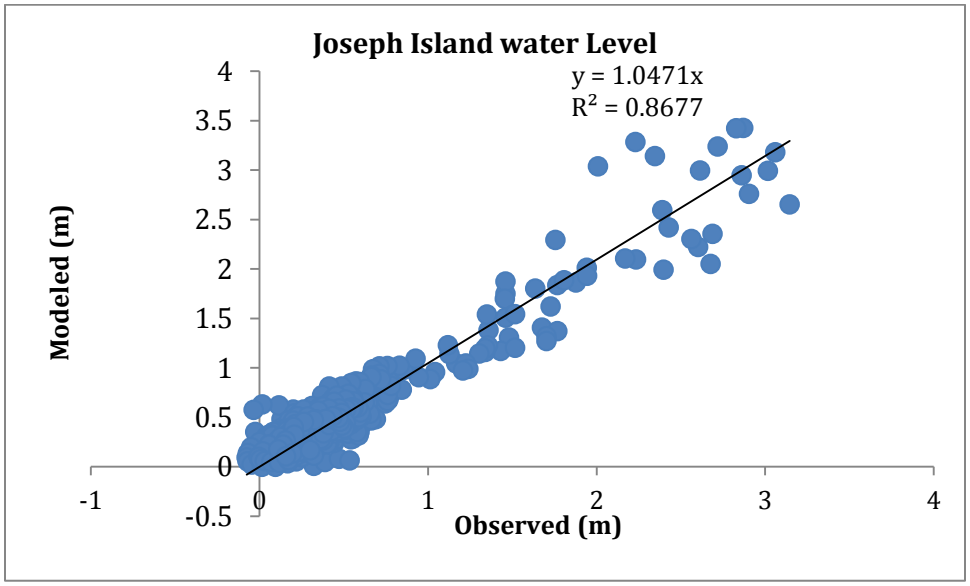


**Figure 4.27-Bias error calculation for Joseph Island water level during Isaac (Observed Source: USGS, 2012)**

| Joseph Island 8/25/2012-9/25/2011 | | |
|---|---|---|
| Bias based on Slope | Surge Bias (m) | $R^2$ |
| 4.7% over predicting | 0.065 | 0.87 |

**Table 4.11-Calculated errors for Joseph Island water level during Isaac**

Salinity validation and error calculation were done in the following Stations (see figures 4.29-4.31)

- Bayou St. John, LA (USGS, 30°01'28" N, 90°04'58" W )
- Rigolets, LA (USGS, 30°10'01" N, 89°44'26" W)
- East Pearl River, MS (USGS, 30°11'41" N, 89°32'03" W)

Surface Salinity map at August 30th 2012 9:00 AM is shown in Figure 4.28

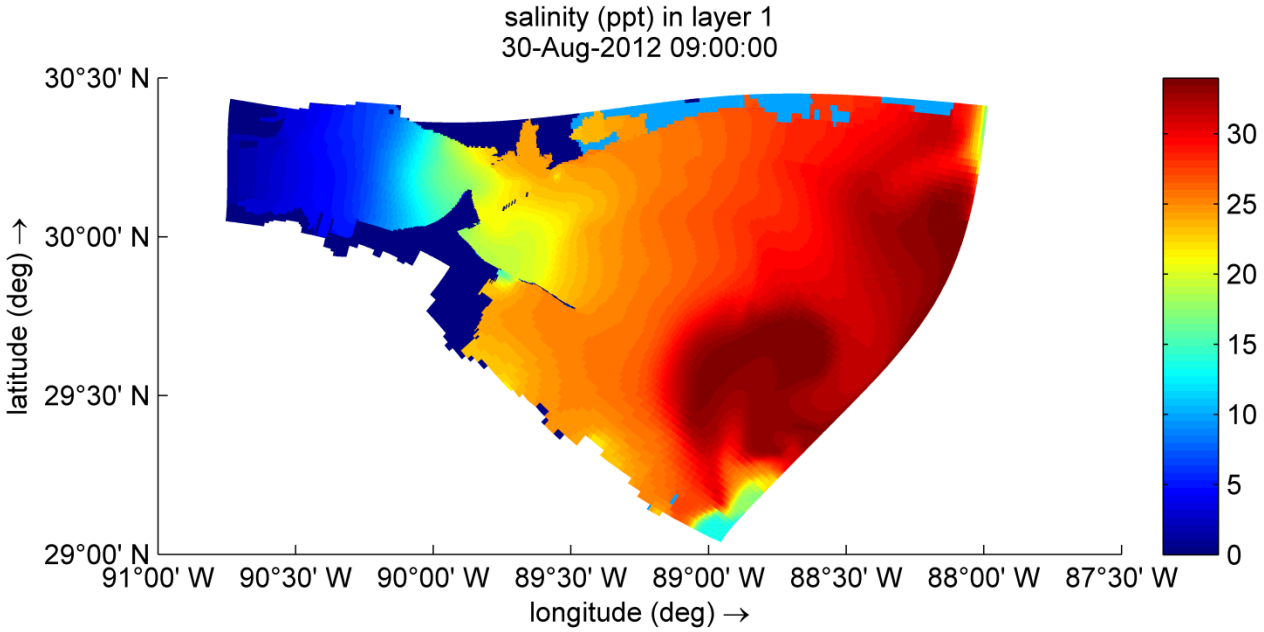


**Figure 4.28- Surface Salinity as of 8/25/2012 9:00AM**

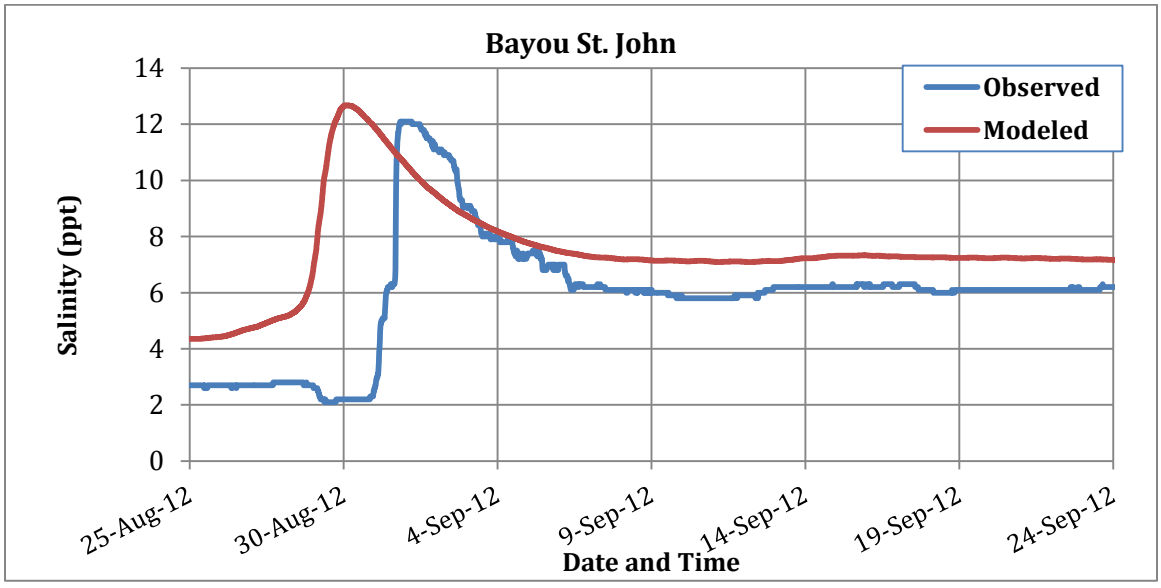


**Figure 4.29- Salinity Validation during Hurricane Isaac period in Bayou St. John (Observed Source: USGS, 2012)**

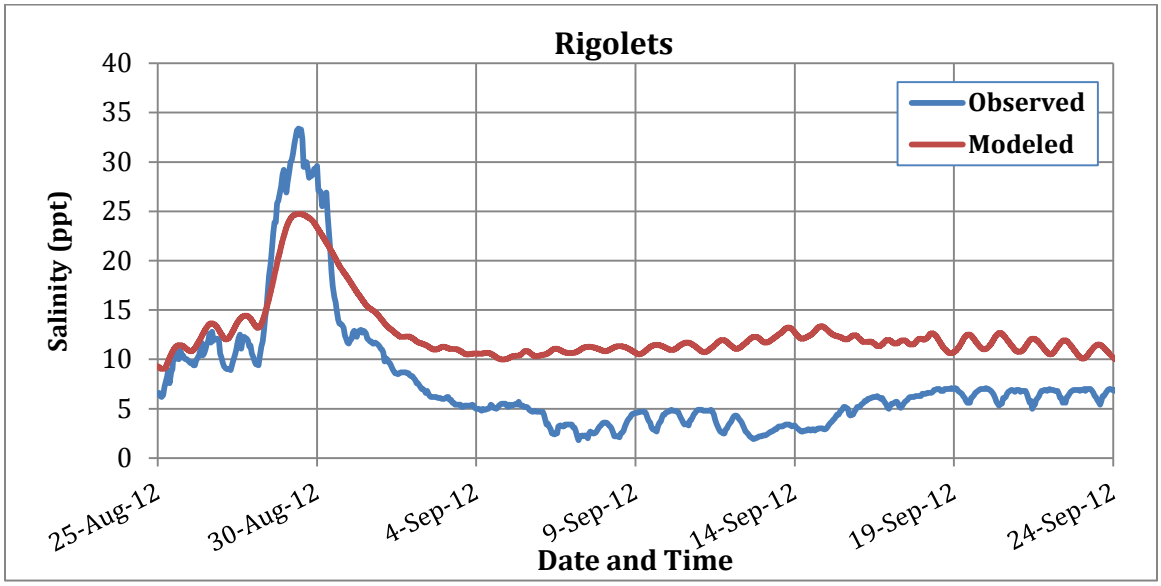


**Figure 4.30- Salinity Validation during Hurricane Isaac period in Rigolets (Observed Source: USGS, 2012)**

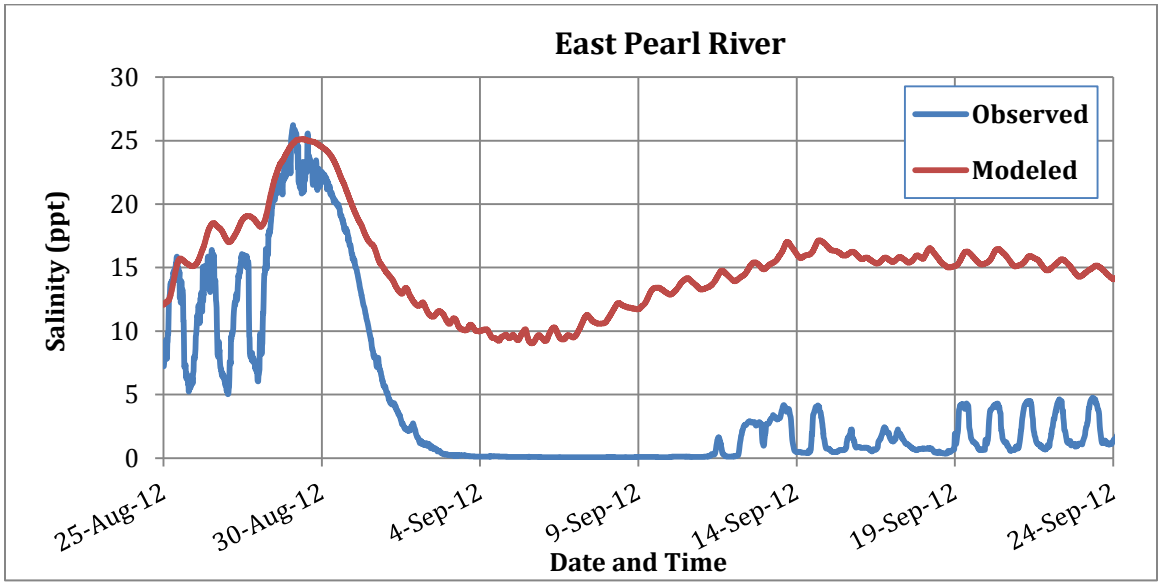


**Figure 4.31- Salinity Validation during Hurricane Isaac period in East Pearl River (Observed Source: USGS, 2012)**

# 5. APPLICATION

After the model was successfully calibrated, it was applied to several scenarios. The result of each scenario will give an approximate idea of what will happen if the system experiences such scenario. The main applications of interest was changing the forward speed of Isaac.

As a test, duration of Hurricane Isaac was changed and the maximum salinity and surge height was measured. Duration is inversely relevant forward speed. Table 5.1 contains all assumed scenarios for which the model was run.

| Run ID | Relative Duration to Isaac | Relative forward Speed to Isaac | Logical Description |
|---|---|---|---|
| DL21 | $2 \times T_{Isaac}$ | $\frac{1}{2} \times V_{Isaac}$ | 2×Slower |
| DL32 | $3/2 \times T_{Isaac}$ | $\frac{2}{3} \times V_{Isaac}$ | 1.5×Slower |
| DL11 | $T_{Isaac}$ | $V_{Isaac}$ | Same speed |
| DL23 | $\frac{2}{3} \times T_{Isaac}$ | $3/2 \times V_{Isaac}$ | 1.5×Faster |
| DL12 | $\frac{1}{2} \times T_{Isaac}$ | $2 \times V_{Isaac}$ | 2×Faster |
| DL13 | $\frac{1}{3} \times T_{Isaac}$ | $3 \times V_{Isaac}$ | 3×Faster |

**Table 5.1- Various senariou names for Hurricanes with different forward speeds from Isaac**

Hurricane Isaac was over the city of New Orleans more than a day. There have been some arguments indicating, the surge would be shorter if the storm was moving forward faster. The runs on Table 5.1 were conducted in order to provide some clarity to those arguments.

## 5.1. Run Setup

The water level at the open boundary has been prescribed in certain time increments. During the hurricane, the time interval was multiplied by the relative duration factor in order to represent faster or slower forward speeds (see Figures 5.1-5.3). Same procedure is applied to winds and river flows.

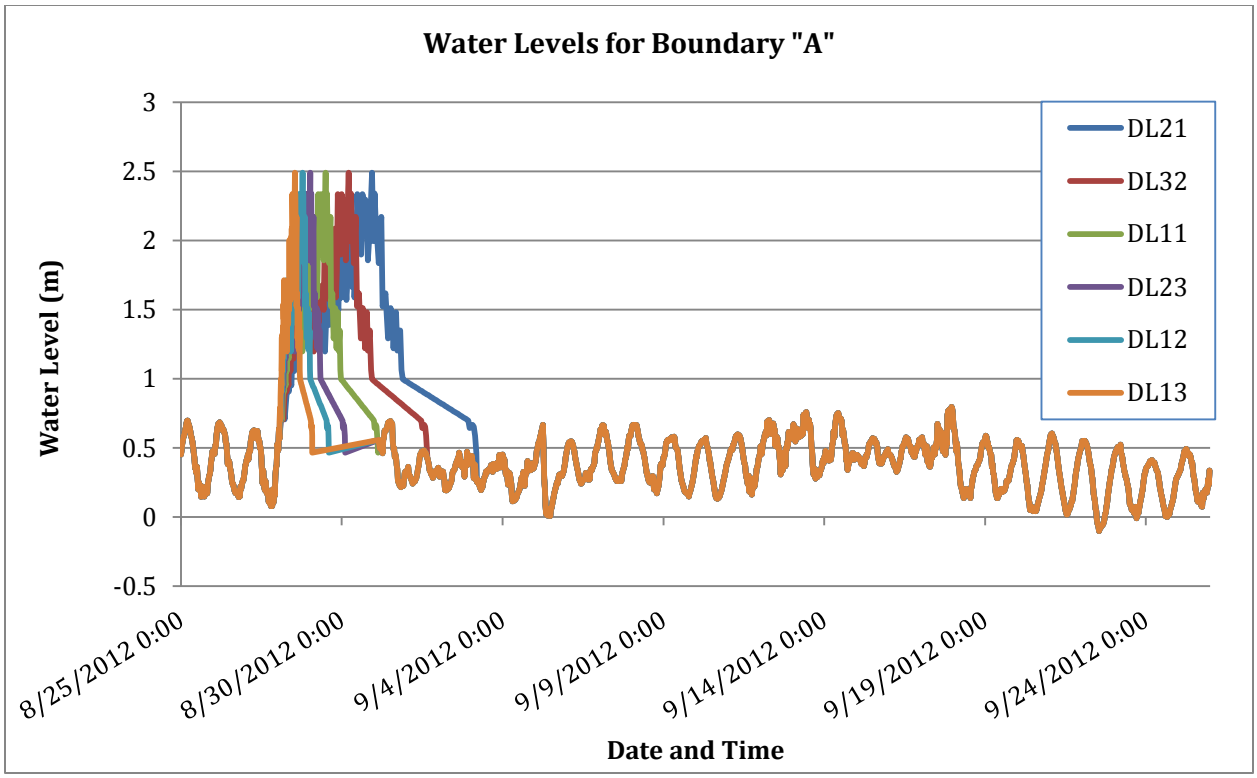


**Figure 5.1- Water Levels for Boundary "A"; Various forward speeds of Isaac**

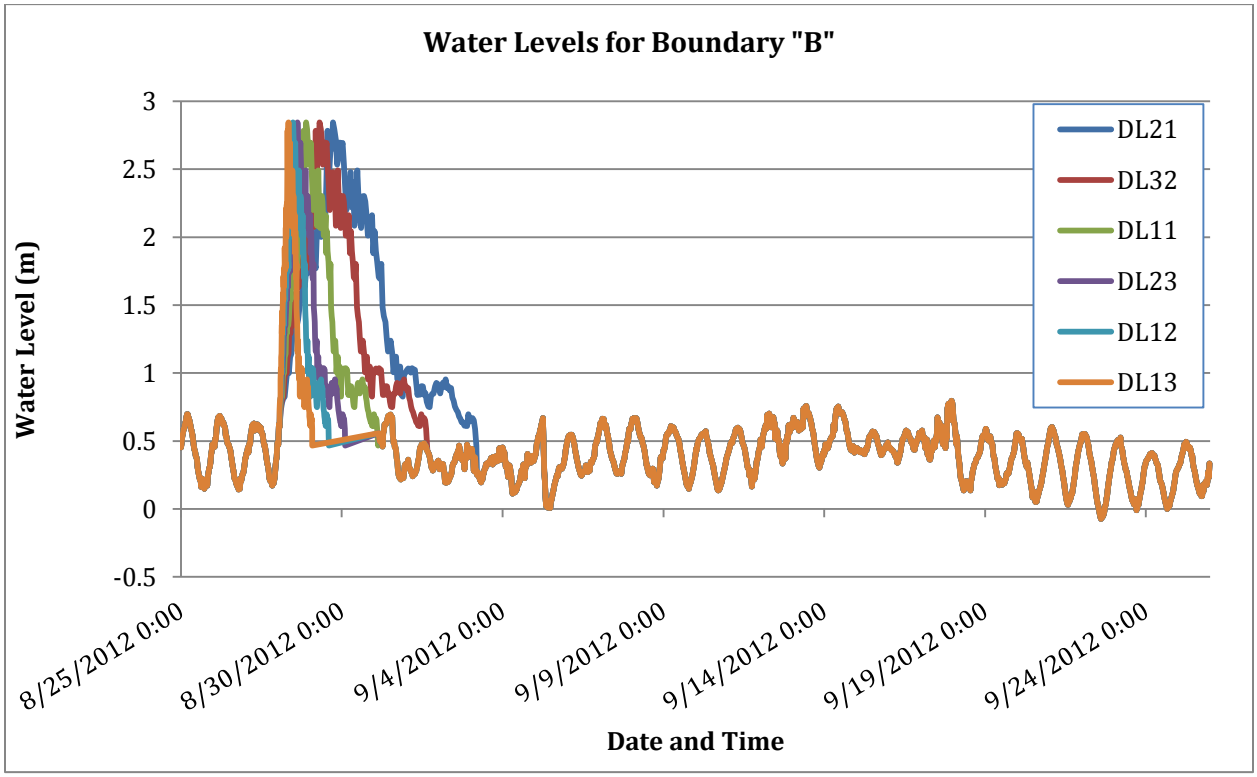


**Figure 5.2- Water Levels for Boundary "B"; Various forward speeds of Isaac**

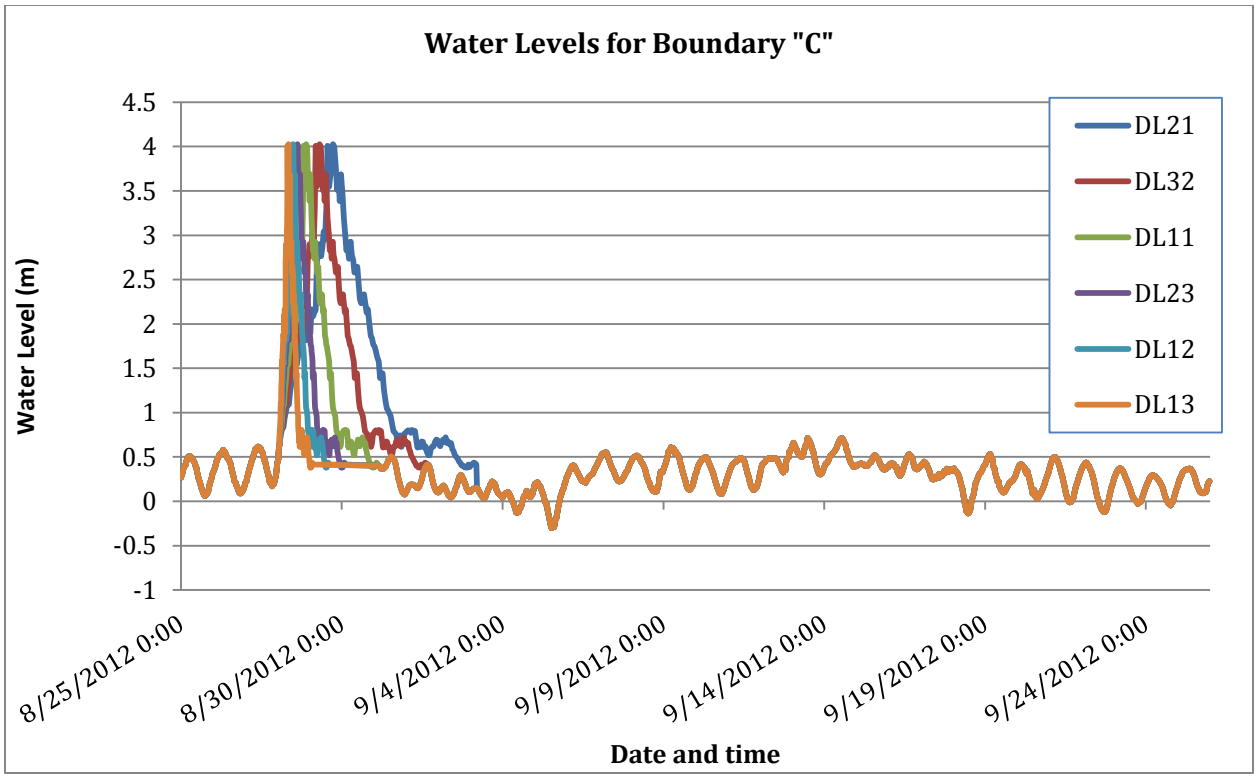


**Figure 5.3- Water Levels for Boundary "C"; Various forward speeds of Isaac**

### 5.2. Results

Water level results in Lakes Maurepas, Borgne and Pontchartrain are plotted in assuming various forward speeds of Isaac (Figures 5.4-5.6). Salinity results are plotted in Bayou St. John, Rigolets and East Pearl River (Figures 5.7 and 5.8).

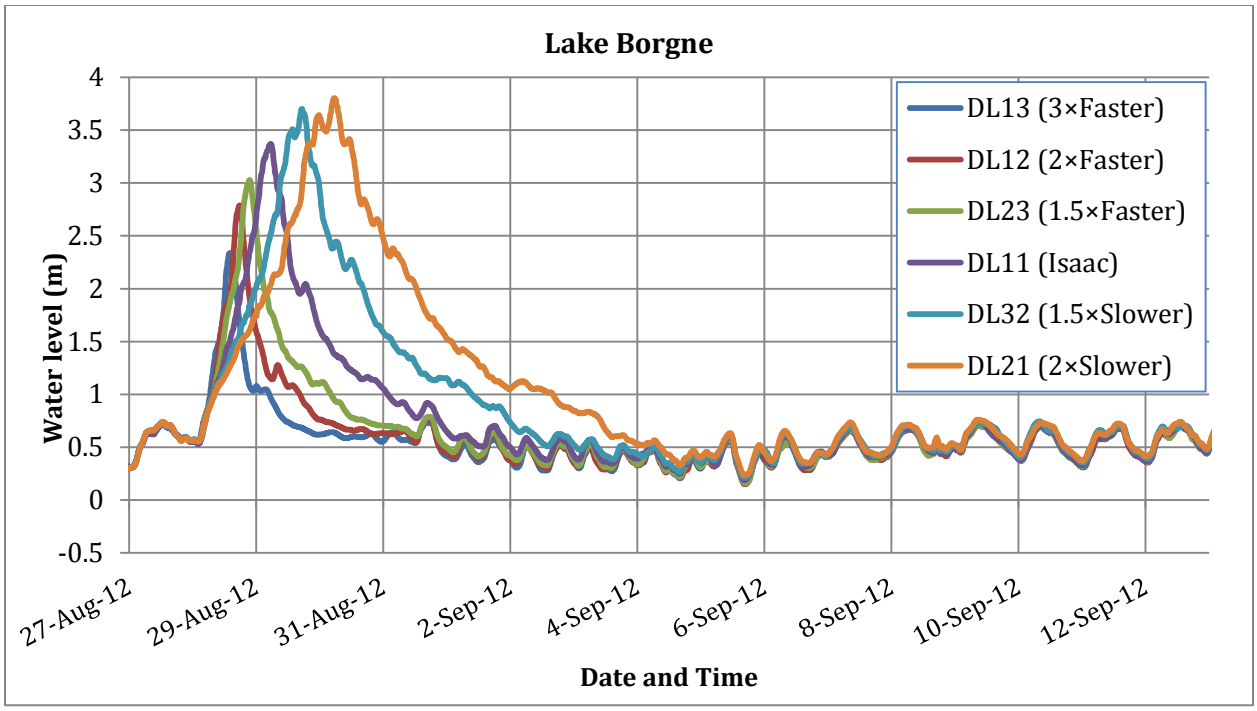


**Figure 5.4- Water Levels in Lake Borgne when the system experiences various forward speeds of Hurricane Isaac**

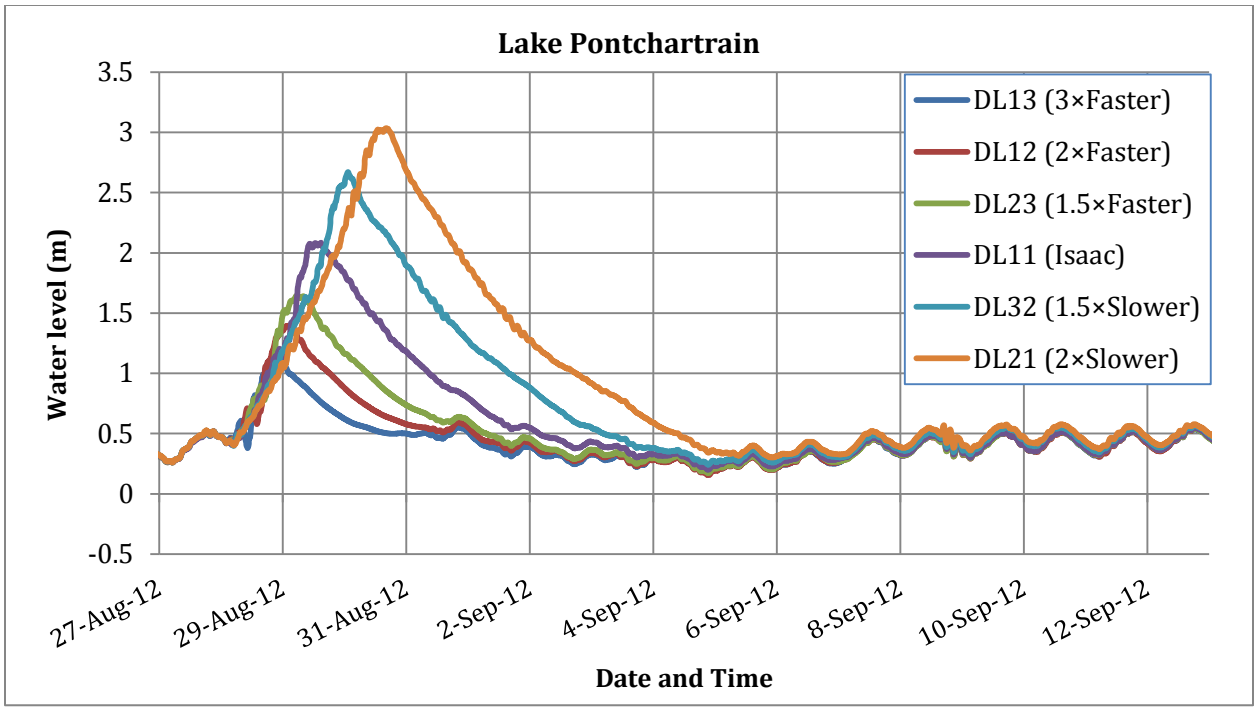


**Figure 5.5- Water Levels in Lake Pontchartrain when the system experiences various forward speeds of Hurricane Isaac**

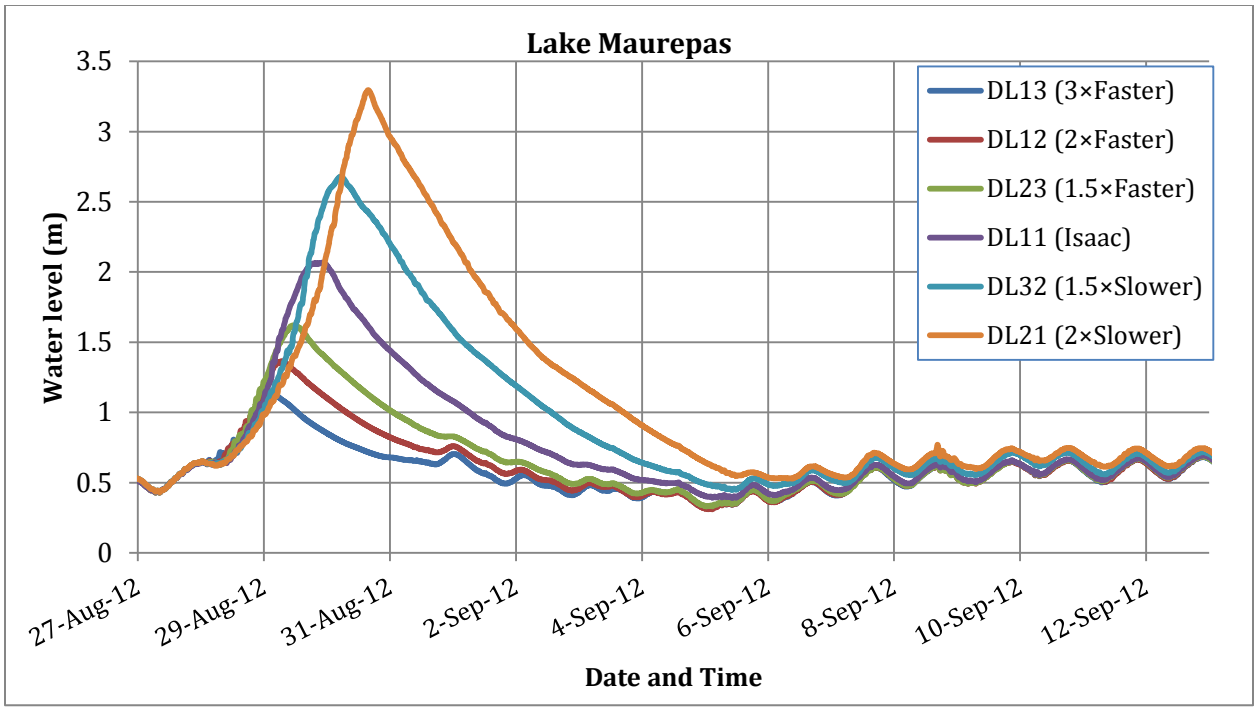


**Figure 5.6- Water Levels in Lake Maurepas when the system is applied to various forward speeds of Hurricane Isaac**

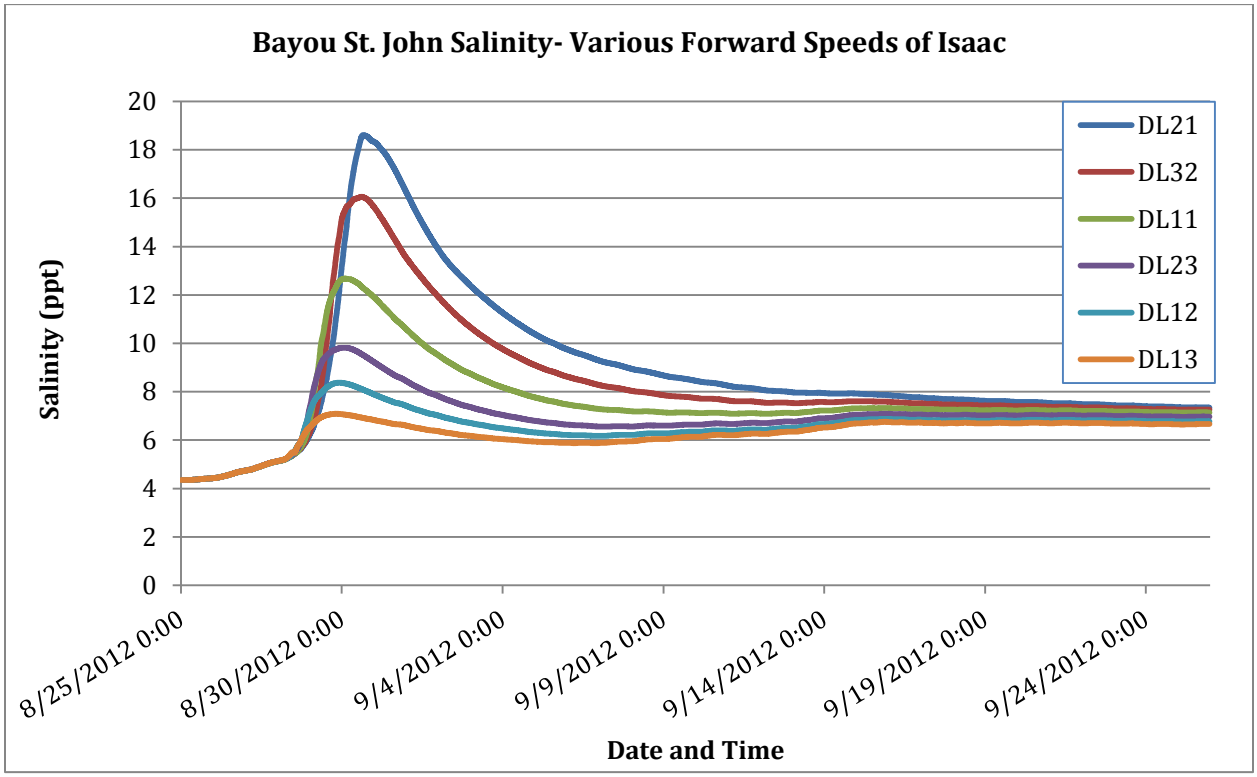


**Figure 5.7- Salinity in Bayou St. John when the system experiences various forward speeds of Hurricane Isaac**

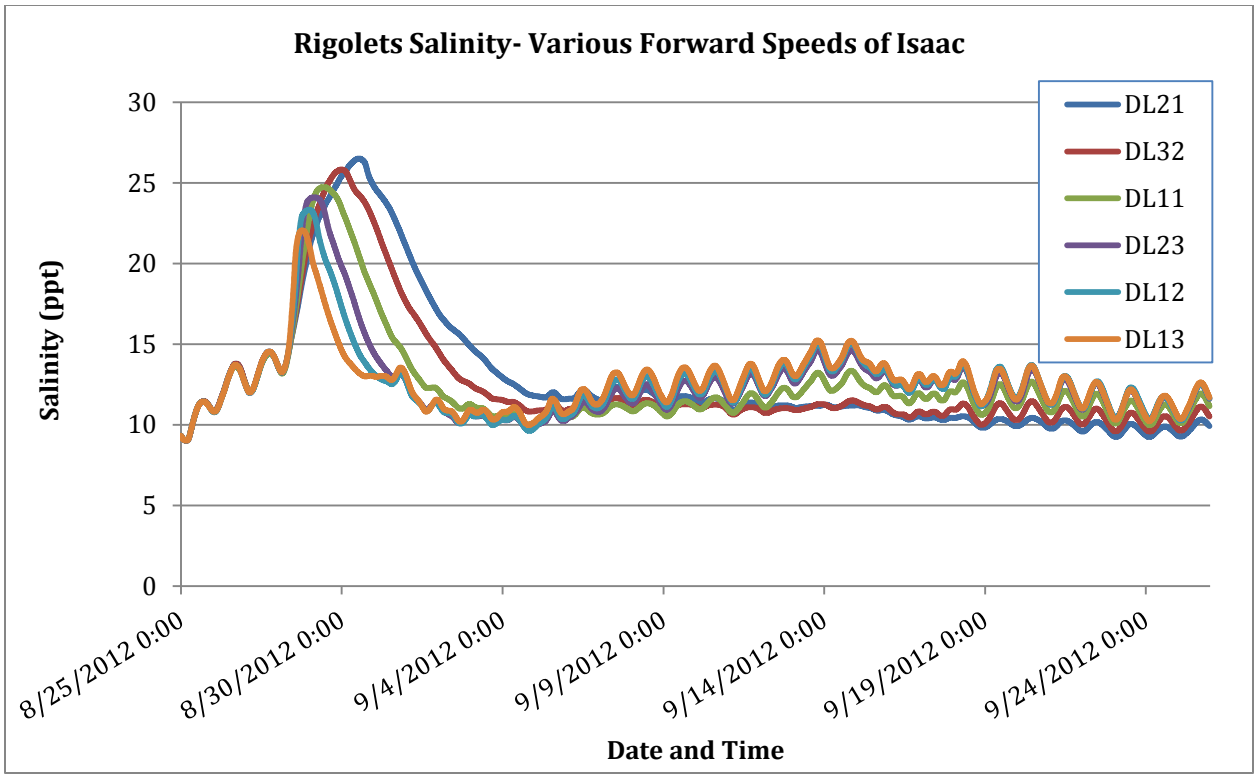


**Figure 5.8- Salinity in Rigolets when the system experiences various forward speeds of Hurricane Isaac**

# 6. DISCUSSIONS

It seems that the water level results are a bit out of phase. One possible explanation is that the wind field was simplified and may not have properly represented local wind setup effects. Another possible reason is that the open boundary water levels were derived from stations inside the domain. The model is showing very good agreement in water levels and fair agreement in the salinity. The peak salinities are generally close to the observed values but are sometimes out of phase; at the Rigolets and London Canal areas it is thought that the Pearl River and London Canal Pumping Station may have depressed the local salinities.

The Salinity at Bayou St John is a little out of phase compared to USGS measurements. This is identified as a possible cause of pumping effects at the London Canal or outflow from the Bayou itself. The sharp rise in salinity might be a result of the pumps being turned off.

The simulation of different hurricane durations which are inversely proportional to forward speeds, show that the hurricane duration plays a major role in the surge related flooding. However since the water level in the estuary cannot greatly exceed the maximum elevation at the open boundary, assuming insignificant winds it is seen that the maximum water level initially increases linearly with hurricane duration, then asymptotically reaches some value around the maximum water level at the open boundary. The further the point of interest is from the open boundary, the longer it takes for the maximum water level to reach the limiting height (asymptote value). As seen in Figures 6.1, 6.2 and 6.3 by exposing the estuary to some imaginary hurricanes with the same category and track as Isaac but moving half as fast compared to Isaac, water level in Lake Borgne reached an asymptotic value of 3.8 meters; however, the surge in Lake Pontchartrain and Lake Maurepas are still increasing more or less linearly. Assuming no density gradients, it is estimated that a water level of around 3.8 meters would occur at Lakes Pontchartrain and Maurepas if the system experiences a relatively slow moving (e.g. 4 times slower) Isaac.

The relation of water level to relative forward speed can be represented using the following exponential equation:

$$\zeta = \zeta_{max}(1 - e^{-k/VF}) \tag{6.1}$$

where,

$\zeta$ water level [m]

| | |
|---|---|
| $\zeta_{max}$ | maximum water level for the specific hurricane category and track [m] |
| k | constant |
| VF | relative forward speed VF = $V/V_{Isaac}$ |

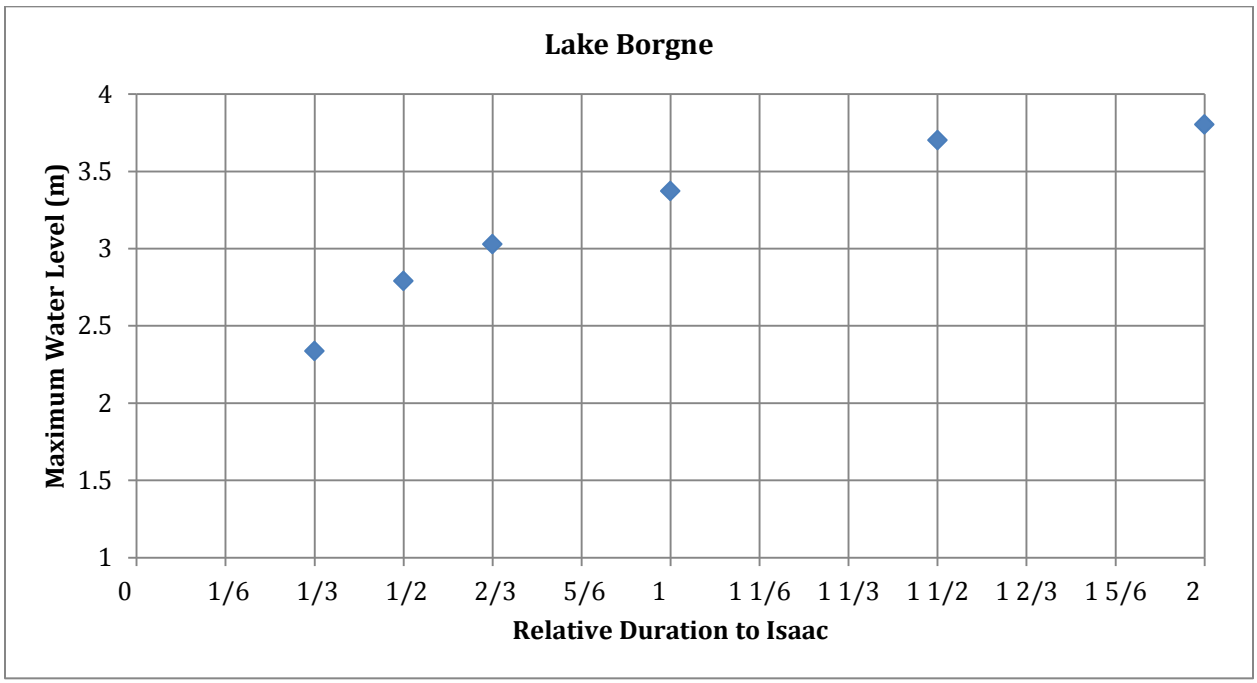


**Figure 6.1- Plot of maximum water level versus hurricane duration in Lake Borgne**

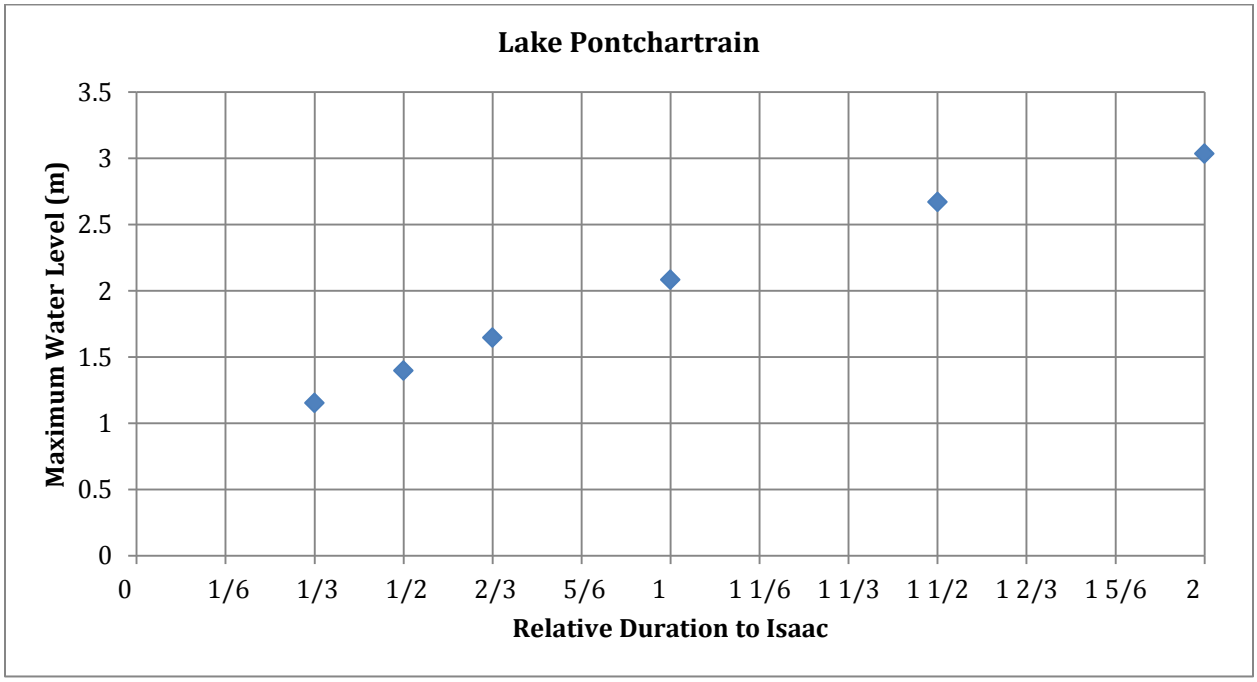


**Figure 6.2-Plot of maximum water level versus hurricane duration in Lake Pontchartrain**

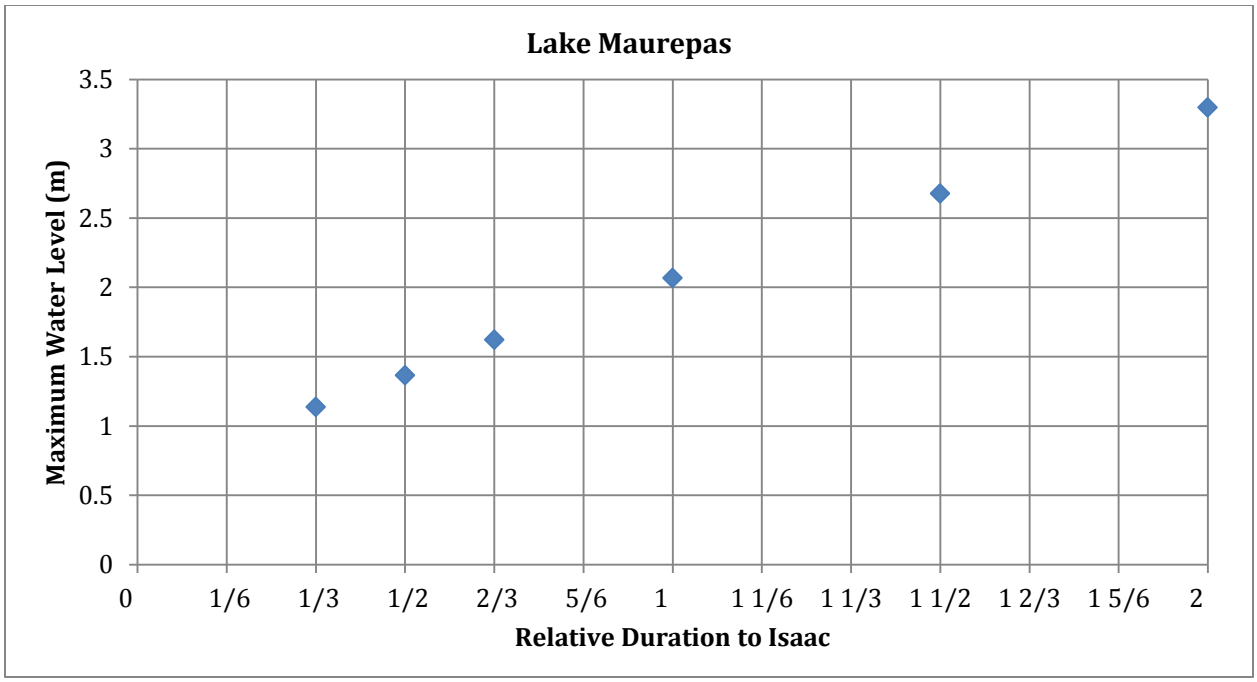


**Figure 6.3-Plot of maximum water level versus hurricane duration in Lake Maurepas**

Comparing Figure 6.3 with 6.2, it is seen that the water levels in Lake Maurepas is slightly higher than Lake Pontchartrain for relatively long duration hurricanes. A possible reason for this is that there is east to west setup in the Estuary due the dominantly East winds imposed on the system.

After doing several trial and error attempts, the values of $\zeta_{max}$ and K for each lake were found for hurricane Isaac's category and track. Table 6.1 contains best-fit values.

| Area | Lake Borgne | Lake Pontchartrain | Lake Maurepas |
|---|---|---|---|
| k | 2.4 | 0.8 | 0.7 |
| $\zeta_{max}$ (m) | 3.8 | 3.8 | 4.25* |

**Table 6.1- Best-fit coeeficcients for Equation 6.1**

*As seen in table 6.1, just like the modeled DL21 values, the $\zeta_{max}$ in Lake Maurepas is greater than values in Lakes Pontchartrain and Borgne as a possible effect of East major winds.

Figures 6.4 through 6.6 contain plots modeled water levels versus estimated water levels in Lakes Borgne, Pontchartrain and Maurepas respectively. As seen in the figures, the exponential approximation is giving plausible results.

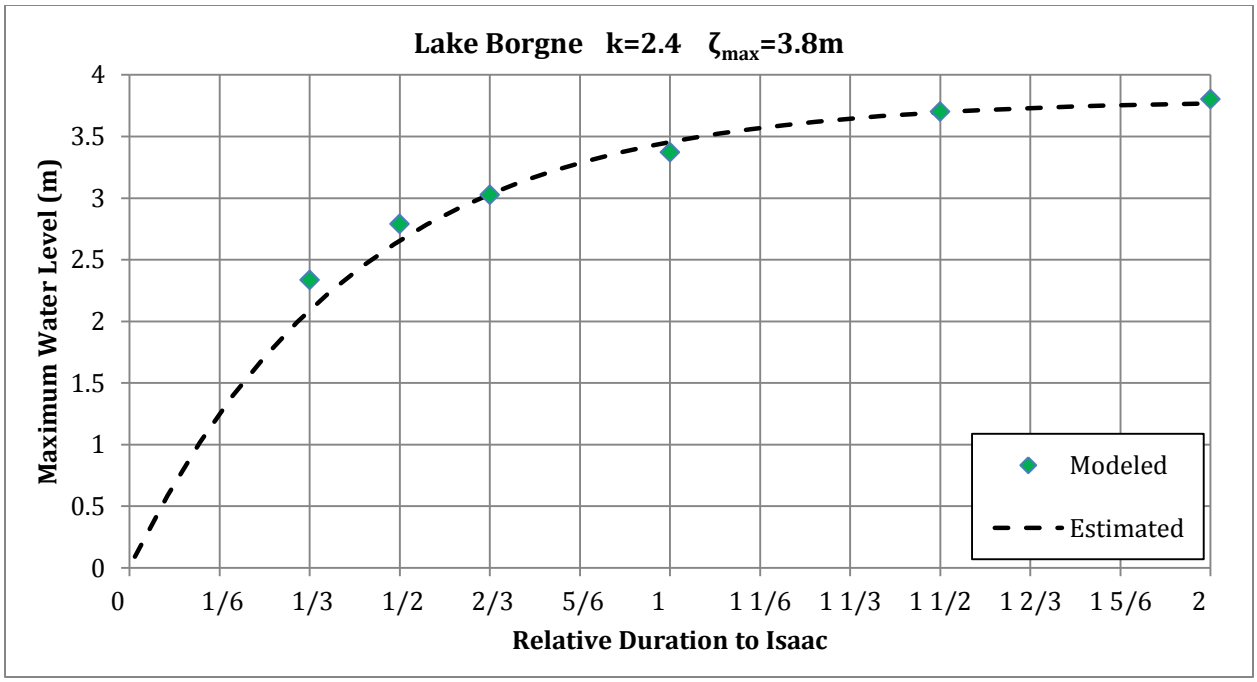


**Figure 6.4- Comparison of Modeled versus Estimated maximum water level in Lake Borgne**

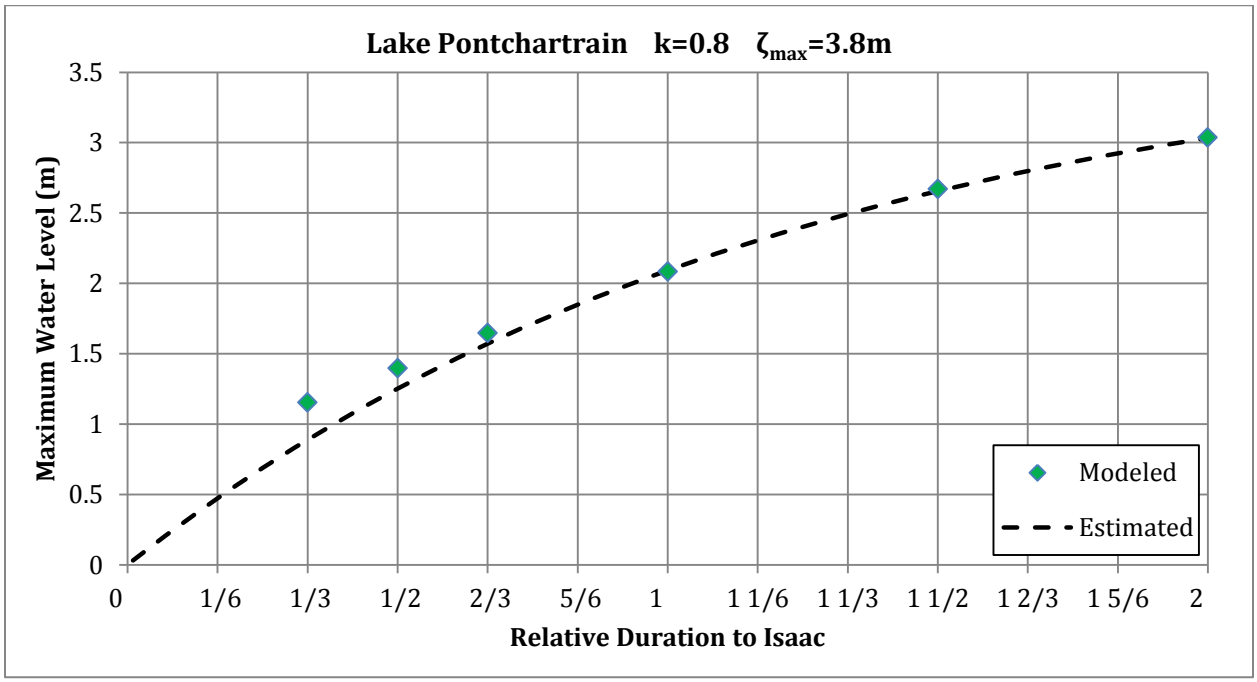


**Figure 6.5-Comparison of Modeled versus Estimated maximum water level in Lake Pontchartrain**

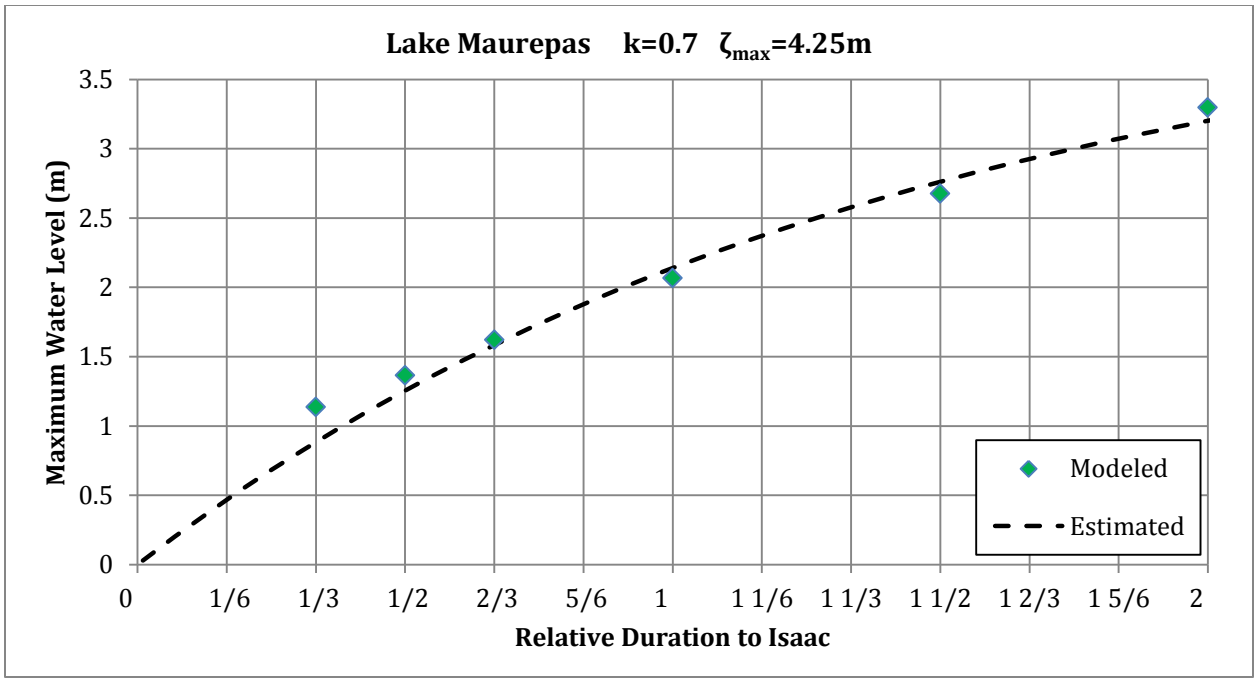


**Figure 6.6-Comparison of Modeled versus Estimated maximum water level in Lake Maurepas**

It should be mentioned that besides open boundary conditions, Rainfall and wind, the tidal cycle has an effect. Spring tide occurs when full moon or new moon is in the sky. Moreover, throughput the year, there would be differences in tidal amplitudes. Figure 6.7 shows tide predictions throughout 2012 hurricane season in Lake Pontchartrain.

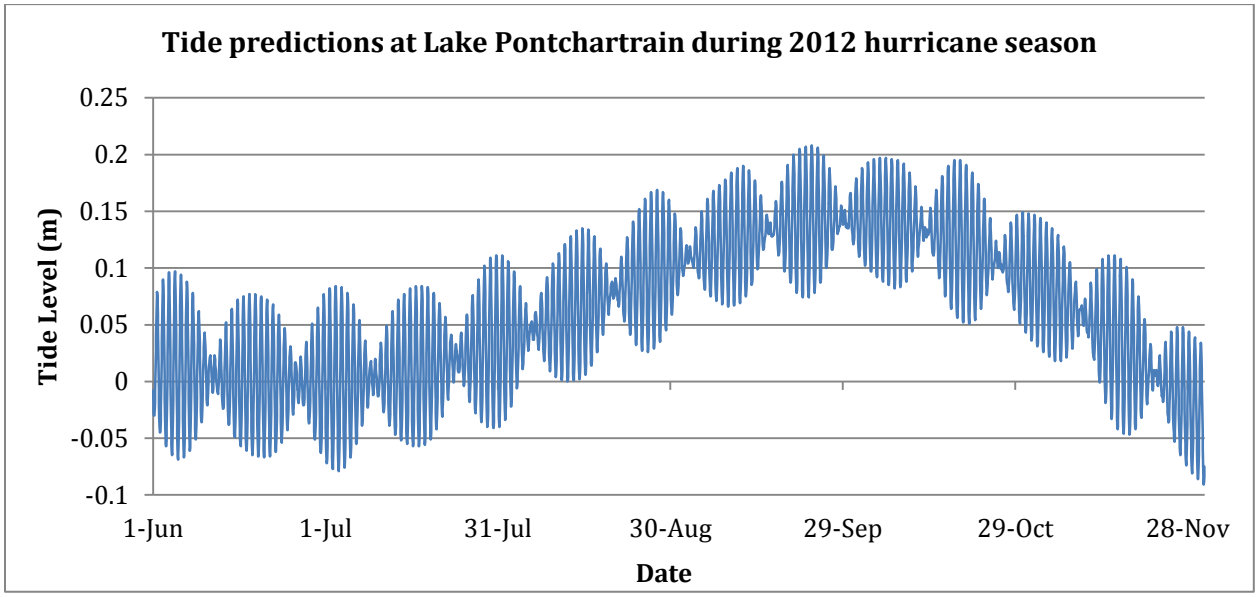


**Figure 6.7-Tide Predictions in Lake Pontchartrain during 2012 hurricane season**

Figure 6.7 shows although there is a small difference in tidal amplitudes during each lunar cycle in Lake Pontchartrain (Barely ±0.07 m), there is a significant seasonal variation of mean stage of the order of ±0.1m. For instance Isaac would have had lowest surge if occurred in November 2012 and highest surge if occurred in mid-September 2012.

Similar to maximum water level, peak salinity is also dependent on the storm forward speed (duration). As seen in Figures 6.8, 6.9 and 6.10, the; maximum salinities are also behaving similarly to the initial linear response that was noted for surges; these peak values also tended to reach some asymptotic value. Unlike water level, salinity heavily relies on initial conditions and local freshwater input from pumping station, tributaries and rainfall.

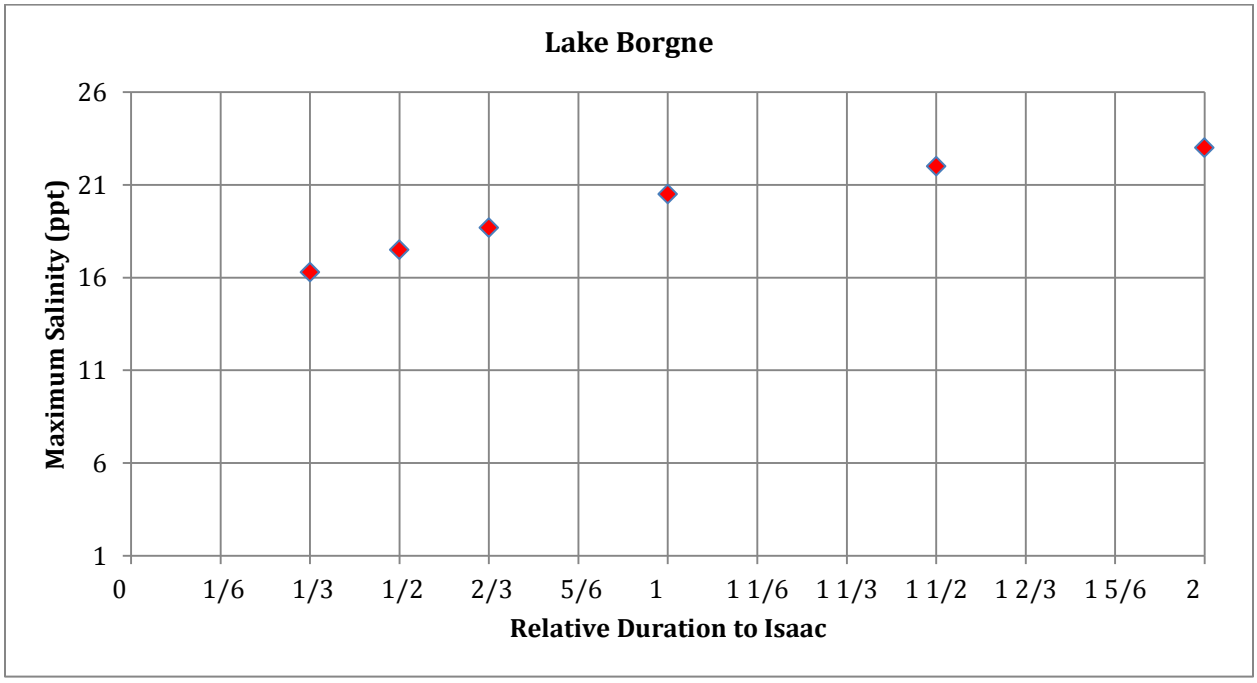


**Figure 6.8-Plot of maximum water level versus hurricane duration in Lake Borgne**

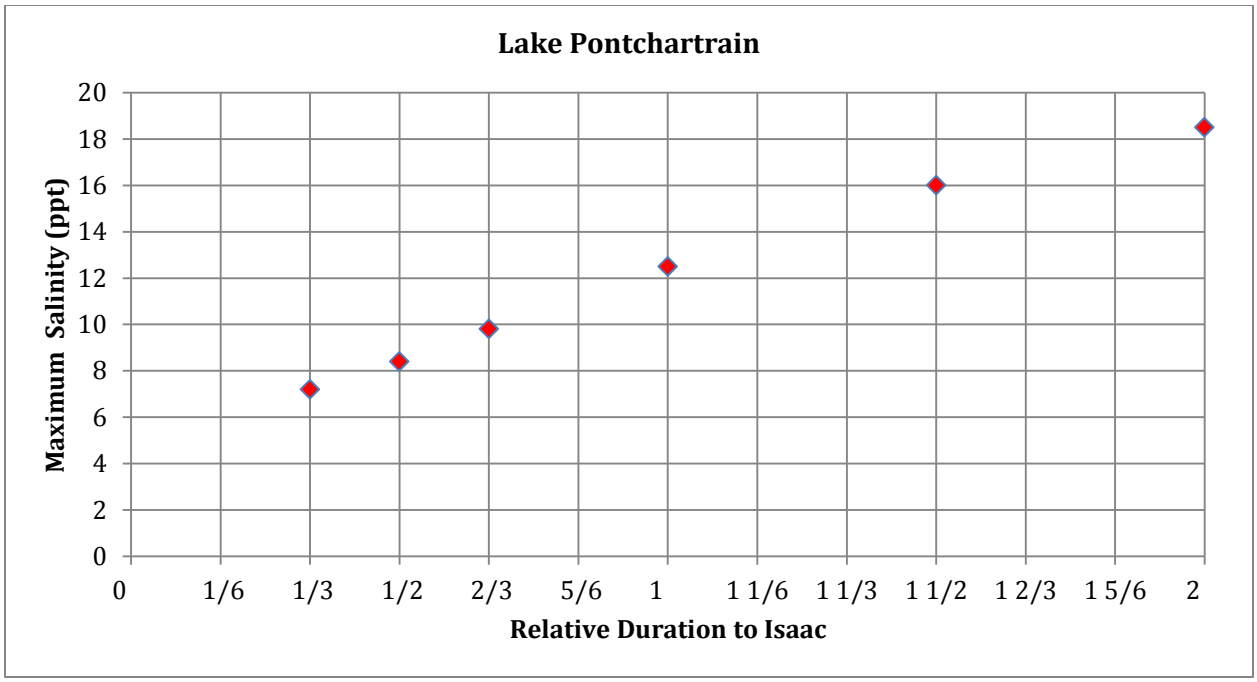


**Figure 6.9-Plot of maximum water level versus hurricane duration in Lake Pontchartrain**

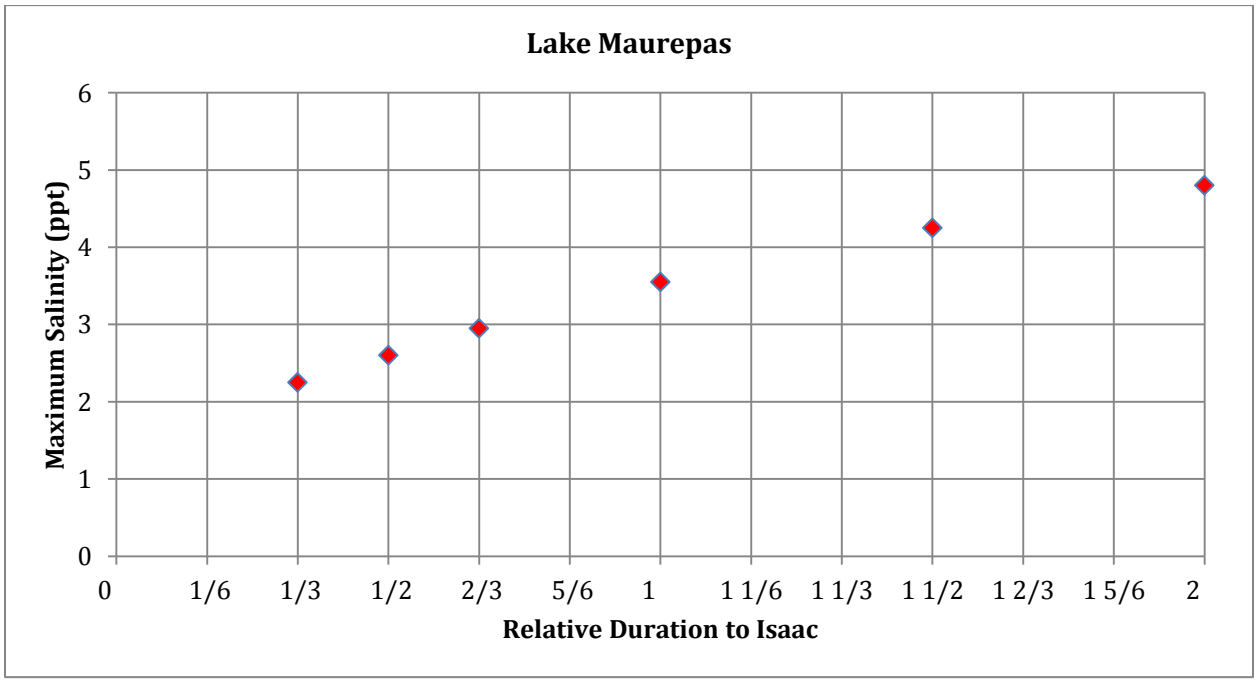


**Figure 6.10-Plot of maximum water level versus hurricane duration in Lake Maurepas**

Same methodology was conducted in FVCOM (the finite volume coastal ocean model) to find the relation of storm duration to maximum water level. An inter-model comparison of model features is presented in Table 6.2.

| Model | UNO Delft3D Model | UNO FVCOM Model |
|---|---|---|
| Number of Layers | 9 sigma layers | 9 sigma Layers |
| Time step | 1 minute | 0.2 seconds |
| Calibration for flooding effects | Model has flooding areas included (wet-dry) | Flooding/ebbing was treated as outflow/inflow |
| Execution time | 14 hours for a real month | 50 hours for a real month |
| Wind data | NOAA New Canal Station | Spatially Varied COAMP model |
| Eastern Boundary Covered | Mobile Bay | Biloxi Bay |

**Table 6.2- Intermodel comparison**

The forward speed of the Hurricane Isaac was also varied in FVCOM. Table 6.3 contains details of the FVCOM runs. The results show certain agreement with Delft3D with some differences that are probably due to dissimilarity in calibration methodology. Figures 6.11 and 6.12 show water levels in Lakes Maurepas and Pontchartrain if the system had experienced faster moving hurricanes but same wind field pattern as Isaac with an altered time coordinates.

| Run ID | Relative Duration to Isaac | Relative forward Speed to Isaac | Logical Description |
|---|---|---|---|
| Modeled x1 | $T_{Isaac}$ | $V_{Isaac}$ | Isaac |
| Modeledx1.5 | $\frac{2}{3} \times T_{Isaac}$ | $3/2 \times V_{Isaac}$ | $1.5 \times$ Faster |
| Modeled x2 | $\frac{1}{2} \times T_{Isaac}$ | $2 \times V_{Isaac}$ | $2 \times$ Faster |
| Modeled x3 | $\frac{1}{3} \times T_{Isaac}$ | $3 \times V_{Isaac}$ | $3 \times$ Faster |

**Table 6.3- FVCOM Runs on Isaac**

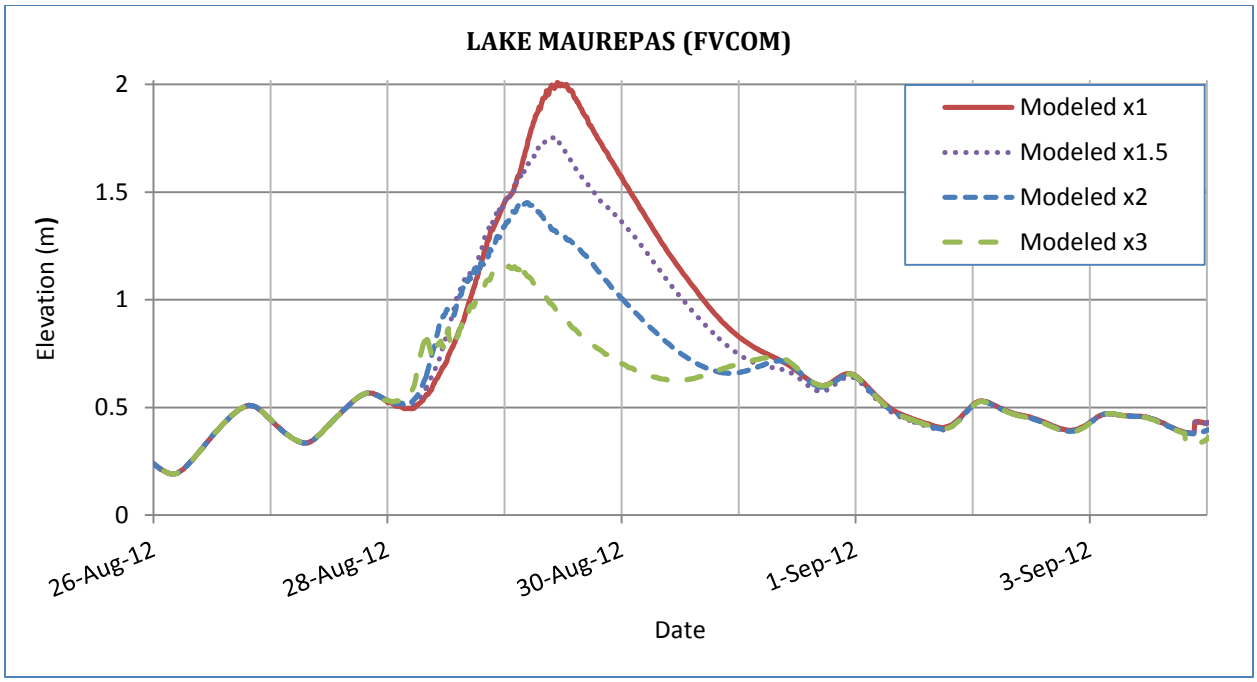


**Figure 6.11- Response of Lake Maurepas under various Hurricane forward speeds modeled in FVCOM**

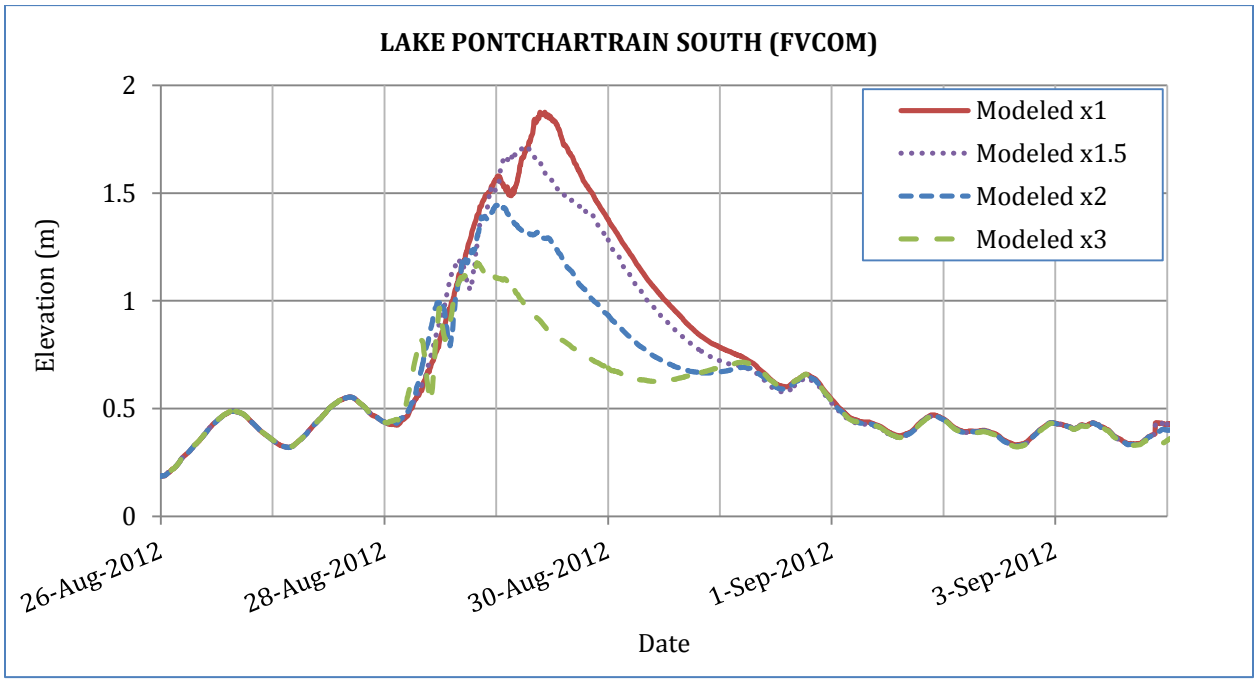


**Figure 6.12-Response of Lake Pontchartrain under various Hurricane forward speeds modeled in FVCOM**

# 7. CONCLUSIONS

The following conclusions are derived from this study:

- The hydraulics and salinity of the Pontchartrain Estuary has been successfully modeled. The model has been calibrated and validated for the periods of September 2013 and August-September 2012 which included Hurricane Isaac. It was necessary to represent Chef Menteur Pass with an equivalent channel to avoid stair stepping. The model effectively responded to wetting and drying conditions which occurred during hurricane period.

- The model showed the longer a storm stays over the area, the higher surge it will develop; however, there is an asymptotic limit.

- The maximum water level for a long duration hurricane with same track and category as Isaac is estimated to be 3.8 meters in Lakes Borgne and Pontchartrain, and 4.2 meters in Lake Maurepas

- During Hurricane Isaac, the gauge height in Lakes Borgne, Pontchartrain and Maurepas reached approximately 90%, 55% and 48% of the maximum of each lake respectively.

- It is assumed that higher predicted water level in Lake Maurepas is the effect wind setup due to the dominant East winds during hurricane Isaac.

- The estuary is expected to develop 90% of maximum estimated surge if experienced a hurricane with the same category and track of Isaac but with forward speeds that are: 34% of Isaac's forward speed for Lake Borgne; 30% of Isaac's forward speed for Lake Pontchartrain, and Lake Maurepas.

- The model showed that salinity in Lake Pontchartrain was influenced by the initial salinity in and near the Lake Borgne area and the duration of the storm. The salinity in the Lake Maurepas area was also a function of the storm duration and the salinity in initial Lake Pontchartrain.

- It was found that the peak salinity along the Estuary increase with the storm duration; however, it also tended to reach asymptotic values for along durations.

- It is seen that if Isaac would have been moving 20% faster, then the City of Laplace would not have been flooded since.

# 8. RECOMMENDATIONS

When hurricane Isaac reached Southeast Louisiana, the estuary was not experiencing a drought situation. There has been some drought time in 1999-2000 that the salinity in lake Maurepas was around 4 parts per thousand (Georgiou, 2002). Even without a hurricane, that caused a high damage to the wetlands. Figure 9.1 contains 5 years of salinity variations. The Author recommends running the model under normal tides with all the rivers having minimum flow to develop a drought hot start, then applying hurricane Isaac and looking at the maximum salinity.

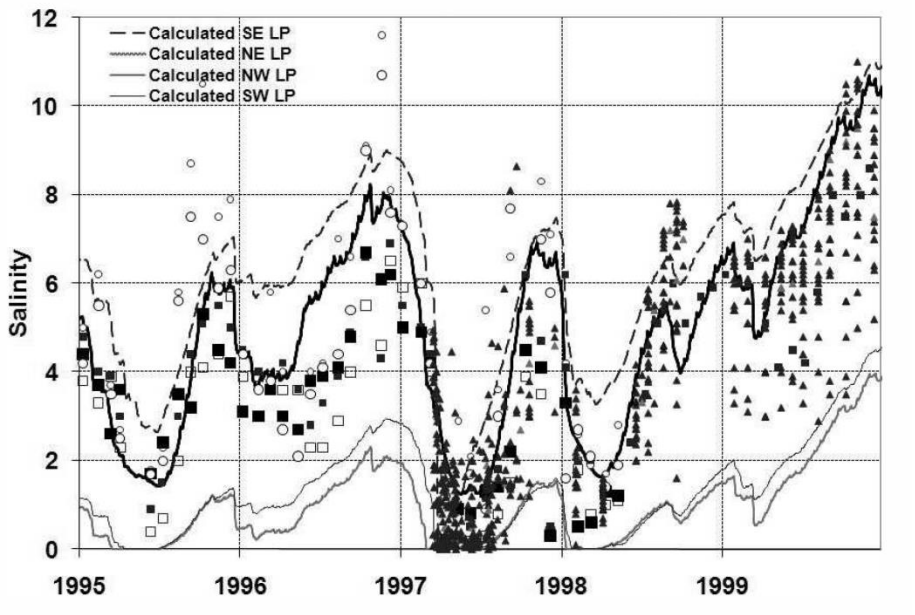


**Figure 8.1- Five years of salinity validation. (McCorquodale et al, 2009)**

It is recommended to have the sediment module on, and run the model under all scenarios for sediment. There has been a lot of discussion about the impact of hurricanes on sediment transport and morphology of the estuary. A good advantage of this model is the ability of Delft3D to run sediment and morphology at the same time of hydraulics. There may be some bed composition information needed from geotechnical coring.

Another recommendation coming out of this research is running water quality. Delft3D is capable of water quality simulations. After occurrence of hurricane Isaac, the state of Mississippi department of environmental quality announced a closure of all beaches in the State because of possible water quality hazards made by hurricane Isaac (MSDEQ, 2012).

The other recommendation is running the model with waves. Hurricanes develop severely tall waves which cause most of the transport and morphology changes. Adding waves to the model will also be useful for seawall designs.

Over the past months there have been some arguments stating the Laplace area would not have been flooded if St. Bernard Parish was allowed to flood. As a recommendation, it is worthwhile to run the model without the St. Bernard Parish levee to see whether or not the Laplace area would flood.

Finally, since there was flooding in Laplace, Louisiana; it is suggested to run the model with possible levee options for Laplace protection. According to Schleifstein (2013) the US Army Corps of Engineers has approved 881 Million dollars to be spent on a levee to protect some areas in St. James Parish. It is recommended to test the effect of each levee choice in Delft3D.

# 9. APPENDIX I: Measurement stations information

**Bay St. Louis:**

| | |
|---|---|
| Station name | Bay Waveland Yacht Club, MS |
| Latitude | 30° 19.5' N |
| Longitude | 89° 19.5' W |
| Operating Agency | National Oceanic and Atmospheric Administration |
| Station Homepage | http://tidesandcurrents.noaa.gov/stationhome.html?id=8747437 |

**Table 9.1- Station Information for Bay St. Louis**

**Shell Beach:**

| | |
|---|---|
| Station name | Shell Beach, LA |
| Latitude | 29° 52.0' N |
| Longitude | 89° 40.3' W |
| Operating Agency | National Oceanic and Atmospheric Administration |
| Station Homepage | http://tidesandcurrents.noaa.gov/stationhome.html?id=8761305 |

**Table 9.2- Station Information for Shell Beach**

**New Canal:**

| | |
|---|---|
| Station name | New Canal Station, LA |
| Latitude | 30° 1.6' N |
| Longitude | 90° 6.8' W |
| Operating Agency | National Oceanic and Atmospheric Administration |
| Station Homepage | http://tidesandcurrents.noaa.gov/stationhome.html?id=8761927 |

**Table 9.3-Station Information for New Canal**

**Joseph Island:**

| | |
|---|---|
| Station name | Mississippi Sound at USGS St Joseph Island Light |
| Latitude | 30°11'27" N |
| Longitude | 89°25'20" W |
| Operating Agency | United States Geological Survey |
| Station Homepage | http://waterdata.usgs.gov/nwis/uv?agency_code=USGS&site_no=301104089253400 |

**Table 9.4-Station Information for Joseph Island**

**Rigolets:**

| | |
|---|---|
| Station name | Rigolets at Hwy 90 near Slidell, LA |
| Latitude | 30°10'01" N |
| Longitude | 89°44'26" W |
| Operating Agency | United States Geological Survey |
| Station Homepage | http://waterdata.usgs.gov/nwis/uv?agency_code=USGS&site_no=301001089442600 |

**Table 9.5-Station Information for Rigolets**

**Bayou St. John:**

| | |
|---|---|
| Station name | Bayou Saint John outside gate at New Orleans, LA |
| Latitude | 30°01'28" N |
| Longitude | 90°04'58" W |
| Operating Agency | United States Geological Survey |
| Station Homepage | http://waterdata.usgs.gov/nwis/uv?agency_code=USGS&site_no=300128090045800 |

**Table 9.6-Station Information for Bayou St. John**

**East Pearl River:**

| | |
|---|---|
| Station name | East Pearl River at CSX Railroad Near Claiborne, MS |
| Latitude | 30°11'41" N |
| Longitude | 89°32'03" W |
| Operating Agency | United States Geological Survey |
| Station Homepage | http://waterdata.usgs.gov/nwis/uv?agency_code=USGS&site_no=301141089320300 |

**Table 9.7-Station Information for East Pearl River**

# 10. APPENDIX II: List of Tributaries

Amite River

Tickfaw River

Blind River

Tangipahoa River

Tchefuncta River

Pearl River

Jordan and Wolf Rivers

Pascagoula River

Biloxi River

# 11. References


Chen, C., Chen , C., Beardsley, R. C., & Cowles, G. (2006). *An Unstructured Grid, Finite-Volume Coastal Ocean Model FVCOM User Manual.* Dartmouth: University of Massachusetts-Dartmouth.

Chilmakuri, C. S. (2005, December). *Sediment Transport and Pathogen Indicator Modeling in Lake Pontchartrain.* New Orleans: University of New Orleans.

Deltares. (2011, January 12). Delft3D-FLOW Simulation of multi-dimensional hydrodynamic flows and transport phenomena, including sediments, User Manual. Delft, Netherlands.

Deltares. (2011, January). Delft3D-QUICKIN Generation and Manipulation of grid-related Parameters such as Bathymetry, Initial Conditions and Roughness. Delft, Netherlands.

Doyle, T. W., Conner , W. H., Day, H. R., Ken, K. W., & Swarzenski, C. M. (2005). *Wind Damage and Salinity Effects of Hurricanes Katrina and Rita on Coastal Baldcypress Forests of Louisiana.* USGS.

Eckart, C. (1958). Properties of water, Part II. The equation of state of water and sea water at low temperatures and pressures. *American Journal of Science*, 225-240.

Ferziger, J. H. (2002). *Computational Method for Fluid Dynamics.* Springer.

Georgiou, I. Y. (2002, August). *Three-Dimensional Hydrodynamic Modeling of Saltwater Intrusion and Circulation in Lake Ponchartrain.* University of New Orleans.

Georgiou, I. Y., McCorquodale, J. A., Schindler, J., Retana, A. G., FitzGerald, D. M., Hughes, Z., et al. (2003). Impact of Multiple Freshwater Deiversions on the Salinity Distribution in the Pontchartrain Estuary under Tidal Forcing. *Journal of Coastal Reasearch*.

Guillot, M. (2013). Series of class lectures in Computational Fluid Dynamics. New Orleans, LA, USA.

Haralampides, K. (2000). *A Study of the Hydrodynamics and Salinity Regimes of the Lake Pontchartrain System.* University of New Orleans.

Li, C., Weeks, E., & Blanchard, B. W. (2010). Storm surge induced flux through multiple tidal passes of Lake Pontchartrain estuary during Hurricanes Gustav and Ike. *Estuarine, Coastal and Shelf Science*, 517-525.

Lopez, J. (2009). The Environmental History of Human-Induced Impacts to the Lake Pontchartrain Basin in Southeastern Louisiana since European Settlement- 1718 to 2002 . *Journal of Coastal Reasearch*, 1-11.

McCorquodale, J. A., Roblin, R. J., Georgiou, I. Y., & Haralampides, K. A. (2009). Salinity, Nutrient, and Sediment Dynamics in the Pontchartrain Estuary. *Journal of Coastal Research*.

MSDEQ. (2012, August 31). *Nola*. Retrieved March 10, 2014, from http://www.nola.com/hurricane/index.ssf/2012/08/hurricane_isaac_debris_and_wat.html

Needham, W. (2000). *A Hurricane Rating System Based on Flooding to a New Orleans Watershed.* University of New Orleans.

NOAA, N. H. (2013, May). *Saffir-Simpson Hurricane Wind Scale*. Retrieved March 15, 2014, from http://www.nhc.noaa.gov/aboutsshws.php

Pereira, J. (2011). *Numerical Modeling of River Diversions in the Lower Mississippi River.* University of New Orleans.

Rego, J. L. (2009). *Storm Surge Dynamics over Wide Continental Shelves: Numerical Experiments Using the Finite Volume Coastal Ocean Model.* Baton Rouge, LA: Louisiana State University.

Retana, A. G. (2008, December). Salinity Transport in a Finite-Volume Sigma-Layer. New Orleans, LA, USA.

Roblin, R. J. (2008). *Water Quality of Freshwater Diversions in the Pontchartrain Estuary.* University of New Orleans.

Schindler, J. (2010). *Estuarine Dynamics as a Function of Barrier Island Transgression.* University of New Orleans.

Stelling, G. S., & van Kester, J. (1994). On the approximation of horizontal gradients in sigma co-ordinates for bathymetry with steep bottom slopes. *International Journal of Numerical Methods In Fluids*.

USGS. (n.d.). *USGS Water Data for the Nation.* Retrieved from http://waterdata.usgs.gov

Versteeg, H., & Malalasekera, W. (2007). *An Introduction to Computational Fluid Dynamics: The Finite Volume Method (2nd Edition).*

Wagner, R. J., Boulger, R. W., Oblinger, C. J., & Smith, B. A. (2006). *Guidelines and standard procedures for continuous water-quality monitors—Station operation, record computation, and data reporting*. Retrieved March 26, 2014, from United States Geological Survey: http://pubs.water.usgs.gov/tm1d3

Williams, S. J. (2006). The Lake Pontchartrain Basin: Louisiana's Troubled Urban Estuary. Louisana: United States Geological Survey.

# VITA

Sina Amini was born 1988 in Shiraz Iran, the homeland of poets and flowers. As the third child of his family, he became interested in engineering as a kid. After completing high school in 2006, Sina moved to Bandarabbas, Iran, to pursue his undergraduate degree in civil engineering at Hormozgan University.

In 2012 he moved to the United States to study for his master's degree in civil and Environmental engineering at UNO. Sina was then offered an opportunity to work with Professor McCorquodale as a research assistant, specializing in numerical modeling. He has met all the degree requirements and is anticipated to graduate in May 2014.